

Aus dem Institut für Klinische Neuroimmunologie
Klinik der Ludwig-Maximilians-Universität München
Leiter: Prof. Dr. Reinhard Hohlfeld und Prof. Dr. Martin Kerschensteiner

**Features of the two isoforms of TACI/TNFRSF13B
in soluble and membrane-bound form**

Dissertation

zum Erwerb des Doktorgrades der Medizin
an der Medizinischen Fakultät der
Ludwig-Maximilians-Universität zu München



vorgelegt von

Miriam Franziska Laura Fichtner

aus

Augsburg

2018

Mit Genehmigung der Medizinischen Fakultät
der Universität München

Berichterstatter: Professor Edgar Meinel

Mitberichterstatter: Prof. Dr. Anne Krug
PD Dr. Anton Eberharter
PD Dr. Gurumoorthy Krishnamoorthy

Mitbetreuung durch den
promovierten Mitarbeiter: Dr. Franziska Thaler

Dekan: Prof. Dr. med. dent. Reinhard Hickel

Tag der mündlichen Prüfung: 08.11.2018

Eidesstattliche Versicherung

Fichtner Miriam Franziska Laura

Name, Vorname

Ich erkläre hiermit an Eides statt,
dass ich die vorliegende Dissertation mit dem Thema

Features of the two isoforms of TACI/TNFRSF13B in soluble and
membrane-bound form

selbständig verfasst, mich außer der angegebenen keiner weiteren Hilfsmittel bedient und alle Erkenntnisse, die aus dem Schrifttum ganz oder annähernd übernommen sind, als solche kenntlich gemacht und nach ihrer Herkunft unter Bezeichnung der Fundstelle einzeln nachgewiesen habe.

Ich erkläre des Weiteren, dass die hier vorgelegte Dissertation nicht in gleicher oder in ähnlicher Form bei einer anderen Stelle zur Erlangung eines akademischen Grades eingereicht wurde.

Aichach, den 12.11.2018

Ort, Datum

Miriam Franziska Laura Fichtner

Unterschrift Doktorandin/Doktorand

Meinen Eltern in Dankbarkeit

Danksagung

Mein großer Dank gilt Herrn Prof. Dr. Edgar Meinel und Dr.med. Franziska S. Thaler für die Überlassung des Themas. Im Besonderen möchte ich mich bei Edgar für die außerordentliche Unterstützung, kontinuierliche Betreuung, herausragende Anleitung und die Möglichkeit Kongresse zu besuchen bedanken. Danke, dass du mich in meiner Entwicklung zu einer selbstständigen Wissenschaftlerin unterstützt hast. Auch unseren Institutsleitern Herrn Prof. Dr. Reinhard Hohlfeld und Herrn Prof. Dr. Martin Kerschensteiner gilt mein großer Dank für ihre Unterstützung.

Frau Prof. Dr. Michaela Smolle gilt mein großer Dank für ihre Unterstützung und fachliche Beratung im Bereich der Proteinanalytik.

Ich möchte mich bei unserer PTA Heike Rübsamen sehr herzlich dafür bedanken, dass sie mir oft mit Rat und Tat innerhalb des Labors zu Seite stand. Joachim Malotka, unserem Klonierungsexperten, danke ich für seine Tipps und Angelika Rinderle für ihre Unterstützung. Atay Vural (Postdoc) und Iris Marti (PhD candidate) danke ich für ihre fachliche Beratung.

Vor allem bedanke ich mich bei meinen Eltern dafür, dass sie mich immer bei allen meinen Vorhaben unterstützen.

CONTENT

LIST OF ABBREVIATIONS.....	IV
LIST OF FIGURES	VI
SUMMARY	VII
ZUSAMMENFASSUNG.....	IX
1. INTRODUCTION.....	1
1.1. EPIDEMIOLOGY OF MULTIPLE SCLEROSIS	1
1.2. PATHOGENESIS AND IMMUNOPATHOGENESIS OF MULTIPLE SCLEROSIS	2
1.3. B-CELLS IN MULTIPLE SCLEROSIS	3
1.4. THE BAFF/APRIL-SYSTEM	7
1.5. THE AMBIVALENT ROLE OF THE RECEPTOR TAC1 IN IMMUNITY	11
2. OBJECTIVE AND STRATEGY	14
3. MATERIAL AND METHODS.....	15
3.1. MATERIAL.....	15
3.1.1. GENERAL MATERIAL AND MACHINES	15
3.1.2. CELL CULTURE MEDIA, BUFFER AND SOLUTIONS	17
3.1.3. PRIMERS, VECTORS AND INSERTS USED FOR CLONING.....	21
3.1.4. GELS, DYES AND BUFFERS FOR SDS-PAGE AND COOMASSIE STAINING ..	23
3.1.5. ANTIBODIES AND FLUOROCHROMES	24
3.2. METHODS.....	26
3.2.1. GENERAL METHODS	26
3.2.1.1. AGAROSE GEL ELECTROPHORESIS	26
3.2.1.2. SPECTROPHOTOMETER.....	26
3.2.1.3. SDS-PAGE AND COOMASSIE BRILLIANT BLUE STAINING.....	27
3.2.1.4. WESTERN BLOT	27
3.2.1.5. ENZYME-LINKED IMMUNOSORBENT ASSAY (ELISA).....	28
3.2.1.6. BICINCHONINIC ACID (BCA) ASSAY	30
3.2.1.7. TRANSFECTION.....	30
3.2.1.8. HARVEST OF SUPERNATANTS.....	31
3.2.1.9. CELL LYSIS.....	31
3.2.2. MOLECULAR CLONING.....	32

3.2.2.1.	AMPLIFICATION AND PURIFICATION OF THE INSERT	32
3.2.2.2.	DIGESTION OF INSERT AND VECTOR WITH RESTRICTION ENZYMES..	33
3.2.2.3.	LIGATION.....	33
3.2.2.4.	TRANSFORMATION OF E. COLI, BACTERIAL CULTURE AND PLASMID DNA PURIFICATION	34
3.2.2.5.	SEQUENCING.....	34
3.2.3.	EXPRESSION OF PROTEINS AND CONSECUTIVE AFFINITY PURIFICATION	35
3.2.3.1.	PROTOCOL FOR TRANSFECTION	35
3.2.3.2.	DIALYSIS AND FILTRATION OF SUPERNATANTS	35
3.2.3.3.	AFFINITY PURIFICATION WITH HISTRAP COLUMNS.....	35
3.2.4.	CHARACTERIZATION OF THE PROTEINS	36
3.2.4.1.	PNGASE F DIGESTION AND TEST FOR DIVALENT ION-HIS6-TAG INTERACTION.....	36
3.2.4.2.	MASS SPECTROMETRY AND N-TERMINAL SEQUENCING	37
3.2.4.3.	SIZE EXCLUSION CHROMATOGRAPHY	38
3.2.4.4.	STATIC LIGHT SCATTER COUPLED TO SIZE EXCLUSION CHROMATOGRAPHY	40
3.2.4.5.	CO-IMMUNOPRECIPITATION	42
3.2.5.	FUNCTIONAL TESTS.....	44
3.2.5.1.	BINDING ELISA.....	44
3.2.5.2.	TEST OF DECOY FUNCTION WITH NF κ B ASSAY.....	45
3.2.5.3.	FLOW CYTOMETRY ASSAYS.....	46
3.2.6.	STATISTICAL ANALYSIS	48
4.	RESULTS.....	49
4.1.	CHARACTERIZATION OF SOLUBLE TACI ISOFORMS	49
4.1.1.	CLONING AND RECOMBINANT PRODUCTION OF sTACI-LONG, sTACI-SHORT AND sTACI-SHORT (W-68-154)	49
4.1.2.	OLIGOMERIZATION OF sTACI	52
4.1.3.	N-LINKED GLYCOSYLATION OF sTACI-LONG AND sTACI-SHORT	54
4.1.4.	MASS SPECTROMETRY AND N-TERMINAL SEQUENCING OF sTACI-LONG AND sTACI-SHORT	55
4.1.5.	SIZE EXCLUSION CHROMATOGRAPHY OF sTACI-LONG AND sTACI-SHORT 57	
4.1.6.	DETERMINATION OF MOLECULAR WEIGHT OF sTACI-LONG AND sTACI- SHORT 59	

4.1.7.	STABILITY OF sTACI-LONG DIMER AND MONOMER.....	62
4.1.8.	SUMMARY OF PROTEIN CHARACTERIZATION	62
4.2.	FUNCTIONAL ANALYSIS.....	63
4.2.1.	EVALUATION OF THE AFFINITY BY BINDING ELISA	63
4.2.2.	EVALUATION OF DECOY FUNCTION BY LUCIFERASE ASSAY (NFκB ASSAY) 69	
4.2.3.	SUMMARY OF FUNCTIONAL TESTS.....	71
4.3.	MEMBRANE-BOUND TACI ISOFORMS	72
4.3.1.	ASSESSMENT OF THE EXPRESSION, SHEDDING AND LIGAND INTERACTION OF TACI-LONG AND TACI-SHORT FROM HEK293T CELLS	72
4.3.2.	CO-IMMUNOPRECIPITATION OF TACI-LONG AND TACI-SHORT IN SOLUBLE AND MEMBRANE-BOUND FORM.....	74
4.3.3.	SUMMARY OF THE ANALYSIS OF MEMBRANE-BOUND ISOFORMS OF TACI 77	
5.	DISCUSSION.....	78
5.1.	BASIC CHARACTERIZATION OF sTACI-LONG AND sTACI-SHORT.....	78
5.1.1.	PURITY.....	78
5.1.2.	DIFFERENT VARIANTS OF sTACI-LONG AND sTACI-SHORT OUTSIDE OF THE CYSTEINE RICH DOMAINS	79
5.1.3.	OLIGOMERIZATION OF sTACI ISOFORMS	79
5.1.4.	GLYCOLSYLATION OF TACI ISOFORMS	83
5.2.	LIGAND BINDING AND DECOY FUNCTION OF sTACI-LONG AND sTACI-SHORT .	84
5.3.	EXPRESSION, SHEDDING, LIGAND BINDING AND OLIGOMERIZATION OF MEMBRANE-BOUND TACI-LONG AND TACI-SHORT.....	89
5.3.1.	EXPRESSION, SHEDDING AND LIGAND BINDING	89
5.3.2.	HOMOTYPIC AND HETEROTYPIC INTERACTION	90
6.	CONCLUSION AND OUTLOOK.....	91
7.	REFERENCES	93

LIST OF ABBREVIATIONS

Ab	antibody
ADEM	Acute disseminated encephalomyelitis
AP-1	Activator protein 1
APRIL	a proliferation-inducing ligand
ATAMS	atacept in multiple sclerosis
ATP	Adenosine triphosphate
BAFF	B-cell activating factor
BAFF-R	B-cell activating factor receptor
BCA	bicinchoninic acid
BCMA	B-cell maturation antigen
Bim	Bcl-2-like protein 11
Blimp-1	PR domain zinc finger protein 1
Breg	B regulatory cells
BIS-TRIS	Bis(2-hydroxyethyl)amino-tris(hydroxymethyl)methane
BSA	bovine serum albumin
clAP-1	Cellular Inhibitor of Apoptosis Protein 1
CIAP	Calf Intestinal Alkaline Phosphatase
CMV	cytomegalovirus
CNS	central nervous system
CPM	central pontine myelinolysis
CO ₂	carbon dioxide
Co-IP	Co-Immunoprecipitation
DMSO	dimethyl sulfoxide
DNA	deoxyribonucleic acid
dNTP	deoxynucleoside triphosphate
EAE	experimental autoimmune encephalomyelitis
ECL	enzymatic chemiluminescence
<i>E. Coli</i>	<i>Escherichia coli</i>
EDTA	ethylenediaminetetraacetic acid
ELISA	enzyme-linked immunosorbent assay
FACS	fluorescence-activated cell sorting
Fas	first apoptosis signal receptor
FasL	first apoptosis signal ligand
FBS	fetal bovine serum
Fc	fragment crystallizable
FCS	fetal calf serum
HCl	hydrochloric acid
HEK293T	human embryonic kidney cell line
HEK.EBNA	human embryonic kidney cell line
His6-tag	polyhistidine tag
HRP	horseradish peroxidase
ICOSL	inducible T-cell co-stimulator ligand
IP	immunoprecipitation

LB media	Luria-Bertani media
mAb	monoclonal antibody
MAG	myelin-associated glycoprotein
MFI	mean fluorescence intensity
MBP	myelin basic protein
MgCl ₂	magnesium chloride
MOG	myelin oligodendrocyte glycoprotein
MS	multiple sclerosis
MYD88	Myeloid differentiation primary response 88
Na ₂ HPO ₄	disodium hydrogen phosphate
NaCl	sodium chloride
NaN ₃	sodium azide
NaOH	sodium hydroxide
NF-AT	nuclear factor of activated T-cells
NFκB	nuclear factor 'kappa-light-chain-enhancer' of activated B cells
Nik	Nuclear factor κB-inducing kinase
Ni-NTA	nickel-nitrilotriacetic acid
NMO	neuromyelitis optica
OCBs	oligoclonal bands
PBS	phosphate buffered saline
PBST	phosphate buffered saline with Tween-20
PCR	polymerase chain reaction
PE	phycoerythrin
PLP	myelin proteolipid protein
PML	progressive multifocal leukoencephalopathy
PP-MS	primary progressive multiple sclerosis
PR-MS	progressive-relapsing multiple sclerosis
PVDF	polyvinylidene fluoride
RNA	ribonucleic acid
RPMI	Roswell Park Memorial Institute medium
RR-MS	relapse-remitting multiple sclerosis
SDS-PAGE	sodium dodecyl sulfate polyacrylamide gel electrophoresis
SEC	size exclusion chromatography
SIAP	shrimp alkaline phosphatase
SOC	super optimal broth with catabolite repression (glucose)
SP-MS	secondary progressive multiple sclerosis
SPR	surface plasmon resonance
SLS	static light scatter
TACI	transmembrane activator and CAML interactor
TAE	Tris-acetate-EDTA
TLR	Toll-like receptors
TRE	transcriptional response element
Treg	T regulatory cell
TBE	tris/borate/EDTA
UV	ultraviolet

LIST OF FIGURES

FIGURE 1: REGULATORY AND INFLAMMATORY ROLES OF B-CELLS.....	4
FIGURE 2: CELL SURFACE MARKER EXPRESSION DURING B-CELL DEVELOPMENT.....	6
FIGURE 3: THE BAFF/APRIL-SYSTEM	7
FIGURE 4: TACI CAN ONLY BE ACTIVATED BY OLIGOMERIC FORMS OF BAFF AND APRIL	9
FIGURE 5: DIFFERENT EFFECTS OF TACI	12
FIGURE 6: STRUCTURE OF STACI ISOFORMS.....	13
FIGURE 7: PRINCIPLE OF ELISA	29
FIGURE 8: PRINCIPLE OF SIZE EXCLUSION CHROMATOGRAPHY.....	38
FIGURE 9: PRINCIPLE OF STATIC LIGHT SCATTER DETECTION	40
FIGURE 10: PRINCIPLE OF CO-IMMUNOPRECIPITATION.....	43
FIGURE 11: PRINCIPLE OF BINDING ELISA	44
FIGURE 12: PRINCIPLE OF NFKB ASSAY.....	45
FIGURE 13: PRINCIPLE OF BINDING FLOW CYTOMETRY.....	47
FIGURE 14: ILLUSTRATION OF DIFFERENT TACI CONSTRUCTS.....	49
FIGURE 15: PLASMIDS OF STACI-LONG (A) AND STACI-SHORT (B).....	50
FIGURE 16: AFFINITY PURIFICATION OF STACI VARIANTS	51
FIGURE 17: ANALYSIS OF STABILITY OF OLIGOMERIZATION OF STACI-LONG AND STACI-SHORT.....	52
FIGURE 18: ANALYSIS FOR POSSIBLE ARTIFICIAL OLIGOMERIZATION OF STACI-SHORT (W-68-154).....	53
FIGURE 19: ANALYSIS OF GLYCOSYLATION OF STACI-LONG, STACI-SHORT AND HMOG	54
FIGURE 20: ANALYSIS OF RECOMBINANT STACI-LONG AND STACI-SHORT BY WESTERN BLOT, COOMASSIE STAINING, N-TERMINAL SEQUENCING AND MASS SPECTROMETRY	56
FIGURE 21: ANALYSIS OF OLIGOMERIZATION OF STACI-LONG AND STACI-SHORT BY SEC	57
FIGURE 22: ANALYSIS OF SMALL SEC PEAKS (S1-S4) OF STACI-SHORT	58
FIGURE 23: MOLECULAR WEIGHT DETERMINATION USING SEC STANDARD CURVE.....	59
FIGURE 24: MOLECULAR WEIGHT DETERMINATION USING SLS/SEC	60
FIGURE 25: STABILITY TEST OF STACI-LONG DIMER AND MONOMER.....	62
FIGURE 26 : BINDING OF VARIOUS TACI CONSTRUCTS TO BAFF AND APRIL MEASURED BY ELISA	65
FIGURE 27: BINDING OF SEC-SEPARATED FRACTIONS OF STACI-LONG AND STACI-SHORT TO BAFF AND APRIL MEASURED BY ELISA	67
FIGURE 28: DECOY ACTIVITY OF TACI CONSTRUCTS FOR BAFF AND APRIL MEASURED BY NFKB ASSAY NFKB ASSAY	70
FIGURE 29: EXPRESSION AND SHEDDING OF TACI-LONG AND TACI-SHORT BY TRANSFECTED HEK293T CELLS	72
FIGURE 30: ANALYSIS OF MEMBRANE-BOUND TACI-LONG AND TACI-SHORT BAFF AND APRIL INTERACTION	73
FIGURE 31: TEST OF EFFICIENCY OF IP	75
FIGURE 32: ANALYSIS OF HOMO- AND HETEROTYPIC INTERACTION OF TACI ISOFORMS IN SOLUBLE AND MEMBRANE-BOUND FORM.....	76
FIGURE 33: SEQUENCE ALIGNMENT OF THE CRD1 (TACI_D1), CRD2 (TACI_D2), BAFF-R (BR3) AND BCMA...81	
FIGURE 34: SEQUENCE OF THE TACI CONSTRUCTS FROM HYMOWITZ ET AL (FIGURE TAKEN FROM (140))86	

SUMMARY

The survival of B-cells is regulated by the two cytokines B-cell activating factor (BAFF) and a proliferation-inducing ligand (APRIL), which bind to the receptors transmembrane activator and CAML interactor (TACI), B-cell activating factor receptor (BAFF-R), and B-cell maturation antigen (BCMA). Due to the importance of B-cell regulation for immunopathological diseases, the BAFF/APRIL system is a potent therapeutic target. While an antibody to BAFF is approved in systemic lupus erythematoses, the soluble receptor TACI-Fc (atacept) unexpectedly worsened multiple sclerosis. Our lab has recently found that the receptor TACI is shed from activated B-cells by the protease ADAM10 releasing endogenous soluble TACI (sTACI) that shares essential features with the pharmacological atacept. TACI exists in two isoforms differing in the length of their extracellular domain by covering one or two cysteine rich domains (CRDs) (TACI-short (CRD2) and TACI-long (CRD1+CRD2)). The aim of this project is to elucidate properties of the two TACI isoforms in their soluble and membrane-bound form.

First, both soluble isoforms of TACI were recombinantly expressed in serum-free cultured HEK.293 cells as secreted proteins. The purified isoforms were analyzed by Coomassie stained SDS-PAGE, Western blot, N-terminal sequencing, and mass-spectrometry. This showed that sTACI-long and sTACI-short appeared in different N-terminal variants, largely due to Furin-cleavage. sTACI-short existed additionally in a C-terminal truncated version (sTACI-short (16-20-W-68-135)). Analysis and separation by size exclusion chromatography (SEC) revealed that the two major sTACI-short forms (1-20-W-68-154 and 16-20-W-68-135) appeared as monomers and to a small extent as higher oligomers. Static light scatter coupled to SEC showed that the majority of sTACI-long formed homodimers and only a minority appeared in the monomeric state. Both recombinant isoforms had no N-linked glycosylation, although they contain one predicted N-glycosylation site.

Next, the ability of the sTACI variants to bind to BAFF and APRIL was analyzed in a binding ELISA and their decoy function in a NF κ B reporter assay. Both isoforms of sTACI showed similar affinities for BAFF, while sTACI-long showed a significantly higher affinity to APRIL than sTACI-short. Similar results were obtained by the NF κ B reporter assay. The comparison of three N-terminal variants of sTACI-short, namely sTACI-short

(1-20-W-68-154), sTACI-short (16-20-W-68-135), and the recombinantly expressed sTACI-short (W-68-154) showed no difference in BAFF binding. In contrast, sTACI-short (1-20-W-68-154) bound to APRIL with significantly higher affinity when compared with sTACI-short (16-20-W-68-135) and sTACI-short (W-68-154). Thus, the N-terminal part outside of the CRD2 seems to contribute to APRIL binding. The dimer of sTACI-long bound to BAFF and APRIL significantly better than its monomer as seen by both binding ELISA and NF κ B reporter assay. Finally, CRD1-Fc, CRD2-Fc, CRD1+CRD2-Fc, and the related CRD1+CRD2-Fc-a obtained from Pascal Schneider (University of Lausanne, Switzerland) as Fc-fused homodimers were analyzed in comparison. CRD1-Fc showed only weak ligand interaction, whereas CRD1+CRD2-Fc, CRD1+CRD2-Fc-a, and CRD2-Fc bound to BAFF and APRIL in a similar manner. This result confirmed a previous publication.

Beside the soluble sTACI variants, the features of the two membrane-bound TACI isoforms (TACI-long and TACI-short) were analyzed. TACI-short was expressed and constitutively shed in significantly higher amount from transiently transfected HEK293T cells than TACI-long. Both membrane-bound isoforms bound to BAFF and APRIL. TACI-long and TACI-short interacted homotypically and heterotypically with each other in both the soluble and membrane-bound form as shown by Co-Immunoprecipitation. Neither of the TACI isoforms interacted in any way with BCMA.

In conclusion, the observed differences in the binding affinity, decoy function and oligomerization between both sTACI isoforms provide deeper insight into the interactions of TACI with its ligands BAFF and APRIL. These findings could be relevant for the understanding of B-cell biology and for future drugs targeting the BAFF/APRIL system.

ZUSAMMENFASSUNG

Die zwei Zytokine BAFF (B-cell activating factor) und APRIL (A proliferation-inducing ligand) regulieren das Überleben der B-Zellen durch die Bindung an die drei Rezeptoren TACI (transmembrane activator and CAML interactor), BAFF-R (B-cell activating factor receptor) und BCMA (B-cell maturation antigen). Dieses sogenannte BAFF/APRIL-System ist aufgrund seiner großen Bedeutung im Rahmen autoimmuner Erkrankungen ein wichtiger Angriffspunkt für Therapien. Im Gegensatz zu einem in systemischen Lupus erythematodes zugelassenen Antikörper gegen BAFF, führte der lösliche Rezeptor TACI-Fc (Atacicept) unerwartet zu einer Verschlechterung im Krankheitsverlauf von Patienten mit Multipler Sklerose. Unser Labor hat vor kurzem entdeckt, dass der Rezeptor TACI auf aktivierten B-Zellen von der Protease ADAM10 geschnitten wird und so auch als endogener löslicher Rezeptor vorkommt. Dieser lösliche Rezeptor weist erhebliche Ähnlichkeiten zum pharmazeutisch hergestellten Atacicept auf. TACI existiert in zwei verschiedenen Isoformen, welche sich in der Länge ihrer extrazellulären Domäne vor allem durch die Anzahl Cystein-reicher Domänen (CRD) unterscheiden (TACI-long (CRD1+CRD2) und TACI-short (CRD2)). Die Zielsetzung dieser Arbeit war es, die Eigenschaften beider TACI Isoformen in löslicher und membran-gebundener Form zu untersuchen und zu vergleichen.

Zunächst wurden beide löslichen Isoformen rekombinant in HEK.EBNA Zellen hergestellt, wobei diese in serum-freies Medium sezerniert wurden. Anschließend wurden beide TACI Isoformen durch SDS-PAGE in Verbindung mit Coomassie Färbung, Western Blot, N-terminales Sequenzieren sowie Massenspektrometrie analysiert und charakterisiert. Hierbei zeigte sich, dass sowohl sTACI-long als auch sTACI-short in verschiedenen N-terminalen Varianten vorkamen, die hauptsächlich durch Furin Spaltung erklärt werden konnten. In den sTACI-short Präparationen kam zusätzlich eine C-terminal verkürzte Variante (sTACI-short (16-20-W-68-135)) vor. Gelfiltration zeigte, dass die beiden Hauptvarianten von sTACI-short (1-20-W-68-154 und 16-20-W-68-135) überwiegend Monomere darstellten, wobei kleine Mengen höherer Oligomere nachgewiesen werden konnten. Die Charakterisierung von sTACI-long über Gelfiltration gekoppelt an statische Lichtstreuungsanalyse offenbarte, dass sTACI-long hauptsächlich

als Dimer und nur geringfügig als Monomer vorlag. Die unterschiedlichen Fraktionen von sTACI-long (Dimer und Monomer) und sTACI-short (1-20-W-68-154 und 16-20-W-68-135) konnten mittels Gelfiltration voneinander getrennt werden. Beide rekombinant hergestellten Isoformen wiesen keine N-verknüpften Glykosylierungen auf, obwohl beide eine vorhergesagte Glykosylierungsstelle besitzen.

In der Folge wurde das BAFF- und APRIL-Bindevermögen der sTACI Varianten mit einem Binde-ELISA (enzyme linked immunosorbant assay) und einem NFκB (nuclear factor kappa-light-chain-enhancer of activated B-cells) Reporter System untersucht: Im Binde-ELISA zeigten beide Isoformen eine ähnliche Affinität für BAFF, wobei sTACI-long APRIL signifikant besser band. Diese Ergebnisse wurden mit dem NFκB Reporter System bestätigt. Der Vergleich der drei N-terminalen Varianten von sTACI-short (sTACI-short (1-20-W-68-154), sTACI-short (16-20-W-68-135)) und das rekombinant exprimierte sTACI-short (W-68-154)) ergab, dass alle drei Varianten keinen Unterschied bezüglich ihrer Bindeeigenschaft zu BAFF aufwiesen. sTACI-short (1-20-W-68-154) band jedoch signifikant besser an APRIL als die anderen beiden Varianten. Der N-terminale Teil, welcher außerhalb der CRD2 gelegen ist, scheint somit Einfluss auf die Bindefähigkeit zu APRIL zu haben. Das Dimer von sTACI-long, welches durch Gelfiltration vom Monomer getrennt werden konnte, band BAFF und APRIL signifikant besser als das Monomer im Binde-ELISA und NFκB Reporter System. Die von Pascal Schneider (Universität von Lausanne, Schweiz) zur Verfügung gestellten TACI-Fc-fusions Homodimere CRD1-Fc, CRD2-Fc, CRD1+CRD2-Fc und CRD1+CRD2-Fc-a wurden vergleichend untersucht. Dabei zeigte CRD1-Fc kaum Interaktionen mit BAFF und APRIL. CRD1+CRD2-Fc, CRD2-Fc und CRD1+CRD2-Fc-a wiesen hingegen ähnliche Affinitäten für BAFF und APRIL auf. Diese Ergebnisse bestätigten eine frühere Veröffentlichung.

Abschließend, untersuchten wir beide Isoformen in ihrer Membran-gebundenen Form. TACI-short wurde signifikant mehr auf transient transfizierten Hek293T Zellen exprimiert und von der Zellmembran geschnitten als TACI-long. Sowohl TACI-long als auch TACI-short waren in der Lage BAFF und APRIL zu binden. Beide Isoformen interagierten in Membran-gebundener und löslicher Form miteinander auf homo- und heterotypische Art, was wir mit unserer Co-Immunopräzipitation Bestimmung nachweisen konnten. Keine der beiden Isoformen zeigte eine Interaktion mit BCMA.

Zusammenfassend konnten in dieser Arbeit Unterschiede in der Affinität, Decoy-Rezeptor Funktionalität und Oligomerisierung zwischen den beiden sTACI Isoformen aufgezeigt werden, wodurch das Verständnis für die Regulation des BAFF/APRIL-Systems erweitert wurde. Dies könnte relevant für die Interpretation verschiedener Vorgänge in der B-Zell Biologie sein. Des Weiteren könnten die Erkenntnisse dieser Studie von Bedeutung für die Entwicklung neuer direkt das BAFF/APRIL-System beeinflussender Medikamente sein.

1. INTRODUCTION

1.1. EPIDEMIOLOGY OF MULTIPLE SCLEROSIS

Multiple sclerosis (MS) is a demyelinating and inflammatory disease of the central nervous system (CNS). There are estimated to be approximately 2.5 million cases of MS worldwide (1). The male:female ratio is approximately 1:2-3 (2). This ratio seems to increase over time. In 1955, the ratio was around 1:1.5 and increased to 1:2.3 by 2000 (3). The general prevalence of MS in Europe is estimated to be 83 cases per 100.000 persons with an incidence of 4.3 cases per 100.000 persons (4). The disease onset is primarily around the ages of 20-40 (2, 5). A Danish study found that MS decreases life expectancy approximately 10 years and increases the risk of death roughly threefold in comparison to an age-matched control group from the general population (6).

The diagnosis of MS is based on the McDonald diagnostic criteria (7, 8). The basis for this criteria builds the dissemination of lesions in the CNS in time and place (7). Before 2010 MS could only be diagnosed when manifestations of two clinical symptoms were at least 30 days apart and affecting different sites of the CNS. Since 2010 one episode together with the proof of earlier events that are in concordance with the dissemination in time and place validated through magnetic resonance imaging (MRI) is enough. This is an improvement for patients who can now get the therapy they need at an earlier stage of disease (8). MS is clinically characterized by four different courses. Primary-progressive (PP), relapsing-remitting (RR), secondary-progressive (SP) and progressive-relapsing (PR) (9). In 2013 the progressive-relapsing course of disease was revised and it has since been considered as a primary-progressive course of disease which is either active or not active (10). 85% of patients start with RRMS and develop PPMS within 10 years of disease onset. 15% of patients have PPMS from the start (9, 11, 12).

1.2. PATHOGENESIS AND IMMUNOPATHOGENESIS OF MULTIPLE SCLEROSIS

A combination of genetic susceptibility together with environmental factors that promote disease onset seems like the most probable explanation for disease outbreak (13-15). Several studies found elevated prevalence of certain MHC (HLA) antigens in MS patients (16-18). In addition to these MHC connected variations, several non-MHC risk genes have been identified (19). The geographical distribution exhibits clusters of disease incidence with higher prevalence in the northern hemisphere and with increasing distance to the equator (20). Thus, migration studies give interesting insights. On the one side, immigrants who come to their new residency before reaching adulthood exhibit a risk of MS onset equivalent to the population of their new location (21). On the other side, immigrants older than 15 years maintain the same MS risk of their original area of upbringing. Whether this distribution in MS risk is attributed to exposition to infections, living conditions, diet or environmental influences remains unknown (22, 23). Additionally, Vitamin D exposition is discussed to contribute to the pathogenesis of MS which could explain to some extent the findings observed by the geographical distribution (24, 25). (26)

MS is a chronic CNS disease with detectable lesions that show demyelination, inflammation, axonal loss and reactive gliosis (27-32). Only a few other diseases like neuromyelitis optica (NMO), central pontine myelinolysis (CPM), acute disseminated encephalomyelitis (ADEM) or progressive multifocal leukoencephalopathy (PML) show demyelination in the CNS. (26)

The primary causes of this heterogeneity in MS is not known and believed to be quite diverse. An immunologic cause of the disease is suspected (33). Nevertheless, other theories suggest, that in some (33), or maybe in all cases (34), the disease onset could be attributed to a primary degenerative process. Additionally, viral or bacterial infections are proposed to be involved in the primary pathogenesis. Until now no case could be attributed to a primary infectious cause (35). Intrathecal IgG synthesis against pathogens like chlamydia, HHV 6 and EBV are part of the typical polyspecific reaction of the immune

system inside the MS CNS (36-39). Also, an implication of EBV has been hypothesized (40), however this remains controversial (41-43). (26)

Nevertheless, the immunological contribution during early and later phases of disease is indisputable. Immunologically, MS was previously believed to be a mainly T-cell driven disease. Autoreactive T-cells get activated in the periphery, for example as a consequence of viral infections. These T-cells manage to cross the blood brain barrier into the CNS, where they clonally expand. The invasion into the CNS by immunologic cells can be visualized and is characterized by vasogenic edemas (44). Local microglia and astrocytes present autoantigens to T-cells. T-cells misjudge these autoantigens (45-49), like myelin basic protein (MBP), myelin oligodendrocyte glycoprotein (MOG), myelin-associated glycoprotein (MAG) and myelin proteolipid protein (PLP), and become stimulated. T-cells then produce pro-inflammatory cytokines like TNF and Interferon gamma. This leads to the recruitment of other cellular parts of the immune system like macrophages and B-cells. The destruction of the myelin is then caused by a cooperation between T- and B-cells through the production of cytokines, inflammatory mediators, cytotoxic cells and autoantibodies. This leads to demyelination and axonal loss that can be detected by MRI (50). (29)

1.3. B-CELLS IN MULTIPLE SCLEROSIS

The role of B-cells in MS is still not fully understood, however, lately a prominent role is suspected. B-cells exert on the one hand pro-inflammatory and on the other hand anti-inflammatory effects (**Figure 1**). On the anti-inflammatory side, B-cells produce anti-inflammatory cytokines, stimulate the expansion of Treg cells, reduce the differentiation of Th1 and Th17 cells, hinder the activity of macrophages and dendritic cells and produce regulatory antibodies as well as neurotrophic factors. On the Pro-inflammatory side, B-cells lead to the generation of pro-inflammatory cytokines, complement activation, autoantibody production and antibody dependent cellular cytotoxicity (ADCC). Additionally, B-cells take part in antigen-transport and in antigen-presentation. Thus, B-cells seem to possess regulatory functions within the immune system (11).

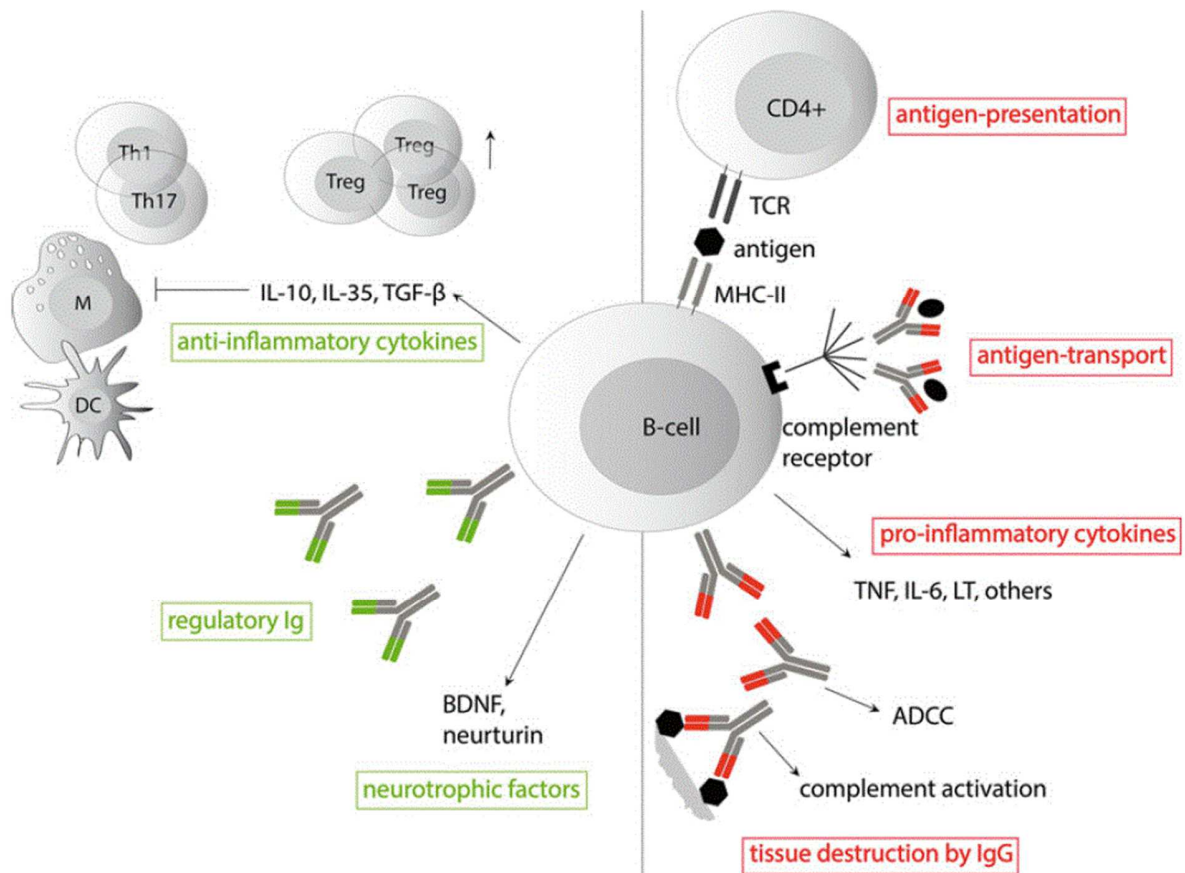


Figure 1: Regulatory and inflammatory roles of B-cells

B-cells are regulators of the immune system. On the one hand, B-cells have anti-inflammatory effects as indicated in green as well as pro-inflammatory effects as indicated in red. B-cells produce anti-inflammatory cytokines such as IL-10, IL-35 or TGF- β . These cytokines lead to the expansion of Treg cells. The differentiation of Th1 and Th17 cells is reduced and the activity of macrophages and dendritic cells is hindered. Additionally, B-cells produce regulatory antibodies as well as neurotrophic factors. Pro-inflammatory effects include the production of autoantibodies. These autoreactive antibodies can lead to complement activation and antibody dependent cellular cytotoxicity (ADCC). B-cells are responsible for producing the pro-inflammatory cytokines TNF, IL-6 and LT, and take part in antigen-transport and in antigen-presentation. (11) Figure taken from (11).

The prominent role of B-cells in MS can be concluded due to several findings (11, 51, 52):

B-cells are found in lesions, the leptomeningeal space of MS patients, where they form follicle-like aggregates (53), and in early MS lesions as part of the inflammatory environment (54). These findings have been linked to SPMS (53) and have also been shown at early stages of RRMS (55).

Oligoclonal bands (OCBs) are part of the diagnostic criteria of MS (8). OCBs are immunoglobulins -mostly IgG- that are intrathecally produced and that can be detected in the cerebrospinal fluid (CSF) of MS patients (56). The typical pattern of bands is not yet attributable to specific autoantigens. Proteomics revealed that OCBs originate from local B-cells in the CSF and brain tissue (57). Ubiquitous self-proteins (58) or myelin obtained lipid complexes and lipids (58) were suggested as possible autoantigens (59). Although the production of autoantibodies in MS has been well delineated at a descriptive level, the mechanism underlying the production of MS autoantibodies and the target antigens remain widely unknown. More specific than the OCBs for MS is the 'MRZ reaction' inside the CNS. It is an immune reaction targeted against viral antigens such as measles, rubella and varicella zoster virus (MRZ) which can be detected in 80-100% of MS patients (60, 61).

The persistence and stability of the OCBs over an extended time in the CNS of MS patients (62) despite immunosuppressive therapies (52) suggests B-cell nurturing conditions in MS brains. Astrocytes express a B-cell survival factor (BAFF) and thus could play a part in the long-term survival and clonal expansion of B-cells in the CNS (63). BAFF expression on astrocytes is upregulated during inflammation (63). Additional mediators of B-cell survival like CXCL12 and CXCL13 are found on astrocytes and blood vessels (CXCL12) or perivascular in CNS parenchyma (CXCL13) (64). B-cells of the CNS are not sequestered in the CNS. B-cells are connected to the periphery through cervical draining lymph nodes (65). Moreover, B-cells seem to mature in the draining cervical lymph nodes before invading the CNS tissue (66).

Different transgenic mouse models were used to investigate the function of B-cells in autoimmune encephalitis (67-69). These animal models facilitate the analysis of the contribution of B-cells to autoimmune diseases. These studies found that B-cells contribute to pathogenesis by producing autoantibodies (69) and by presenting antigens to T-cells (67).

Different cell surface markers can be detected during B-cell maturation (**Figure 2**). These cell surface markers (**Figure 2**) are the target of several B-cell directed therapies (52).

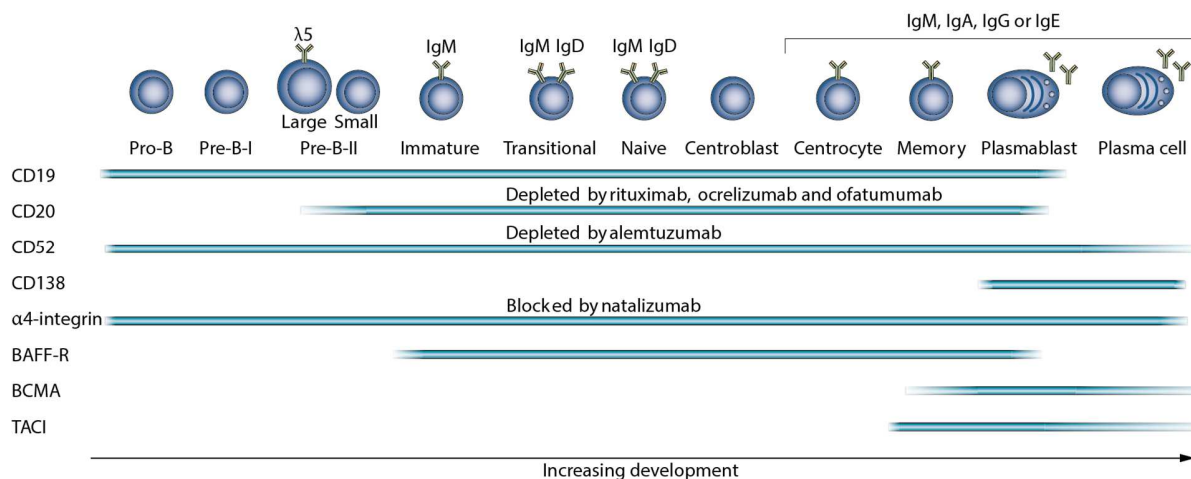


Figure 2: Cell surface marker expression during B-cell development

The blue lines indicate cell surface marker expression during different developmental states of B-cells. These markers can be the target of mAb therapies (written in black letters above blue lines). (52) General expression opinion is not uniform as indicated with the fading blue lines. Figure taken from (52).

B-cell depleting drugs like rituximab (anti-CD20 mAb), are highly effective in MS patients. CD20 is expressed on B-cells at almost every step of B-cell differentiation. Only, Pro-B-cells, Pre-B-I and plasma cells do not express CD20 (**Figure 2**) (52). After one application rituximab reduced clinical relapses and MS brain lesions for 48 weeks (70). Rituximab is not approved for MS. However, another anti-CD20 mAb (Ocrelizumab) showed similar results and is promising for the treatment of MS (71) and is already approved for the treatment of MS (72, 73).

1.4. THE BAFF/APRIL-SYSTEM

The survival of B-cells is regulated by the BAFF/APRIL system. The BAFF/APRIL system consists of the two ligands B-cell activating factor (BAFF/BLyS/TALL-1) and a proliferation-inducing ligand (APRIL) and the three receptors B-cell activating factor receptor (BAFF-R), B-cell maturation Ag (BCMA) and transmembrane activator and CAML interactor (TACI) (**Figure 3**) (74). The ligands and receptors of the BAFF/APRIL belong to the tumor necrosis factor (TNF) superfamily system. (75)

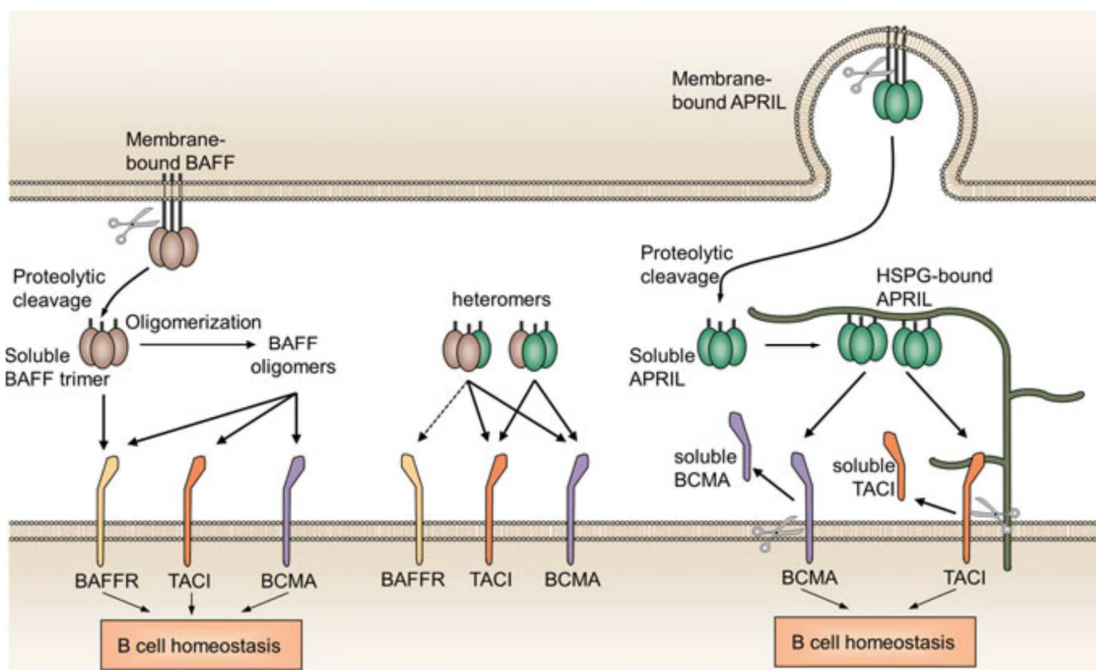


Figure 3: The BAFF/APRIL-System

The BAFF/APRIL-system consists of the two ligands BAFF and APRIL and the receptors BAFF-R, BCMA and TACI. BAFF can bind to all three receptors, while APRIL can only bind to BCMA and TACI. BAFF exists as a soluble form that can build trimers and oligomers. APRIL is processed intracellularly and forms trimers that bind to proteoglycans (HSPGs). HSPGs are presumed to increase the biological activity of APRIL. In addition, to these homotypic formations both BAFF and APRIL form heterotrimers that show similar features. BAFF2APRIL1 is comparable to BAFF, while BAFF1APRIL2 is comparable to APRIL. Two of the receptors, namely BCMA and TACI, get shed from the cell surface and act as decoy receptors. (74) Figure taken from (74).

BAFF and APRIL assemble as homotrimers (76-78), just like TNF and other TNF ligand superfamily members (79). BAFF exists in membrane-bound and soluble form (80,

81), while APRIL is cut intracellularly in the Golgi apparatus without any as yet observed cell surface expression (82). Both ligands exist in diverse variants. BAFF can form a homotrimer and a virus-cluster-like 60mer (83). The function and existence of the 60mer is controversial and has not yet been endogenously confirmed in humans. The 60mer expression could be a consequence of experimental set ups (pH dependency of the construct, recombinant protein production) (84, 85). APRIL exists as a homotrimer that can be concentrated through its interactions with proteoglycans on the cell surface of B-cells (86, 87). Additionally, newly found heterotrimeric hybrid versions of BAFF and APRIL have been described that share similar features with BAFF- and APRIL homotrimers. BAFF2APRIL1 is comparable to BAFF, while BAFF1APRIL2 is comparable to APRIL (88, 89). The existence of active soluble heterotrimers has already been proven in patients with rheumatoid conditions (90). The complexity within the ligands indicates distinct roles and functions of these diverse ligand variations in B-cell biology. The existence and functions of all constructs in vivo, however, must be shown and further characterized to further understand this system. (75) BAFF and APRIL are different in their functional and binding qualities:

BAFF can bind to all three receptors BAFF-R, TACI and BCMA. All variations of BAFF can interact and induce downstream pathways after binding to BAFF-R, while only oligomeric forms of BAFF (BAFF-60mer) can induce intracellular pathways in TACI (91, 92) (**Figure 4**). APRIL can bind to TACI and BCMA, not to BAFF-R. Several findings suggest that APRIL needs to be bound to proteoglycans to exert its biological functions. Soluble APRIL alone was shown to interact only weakly with BCMA (91). Similar observations had been made for TACI (86, 91). APRIL that was crosslinked by proteoglycans, however, was able to activate TACI dependent intracellular pathways in contrast to the soluble variant (86, 91) (**Figure 4**). (75)

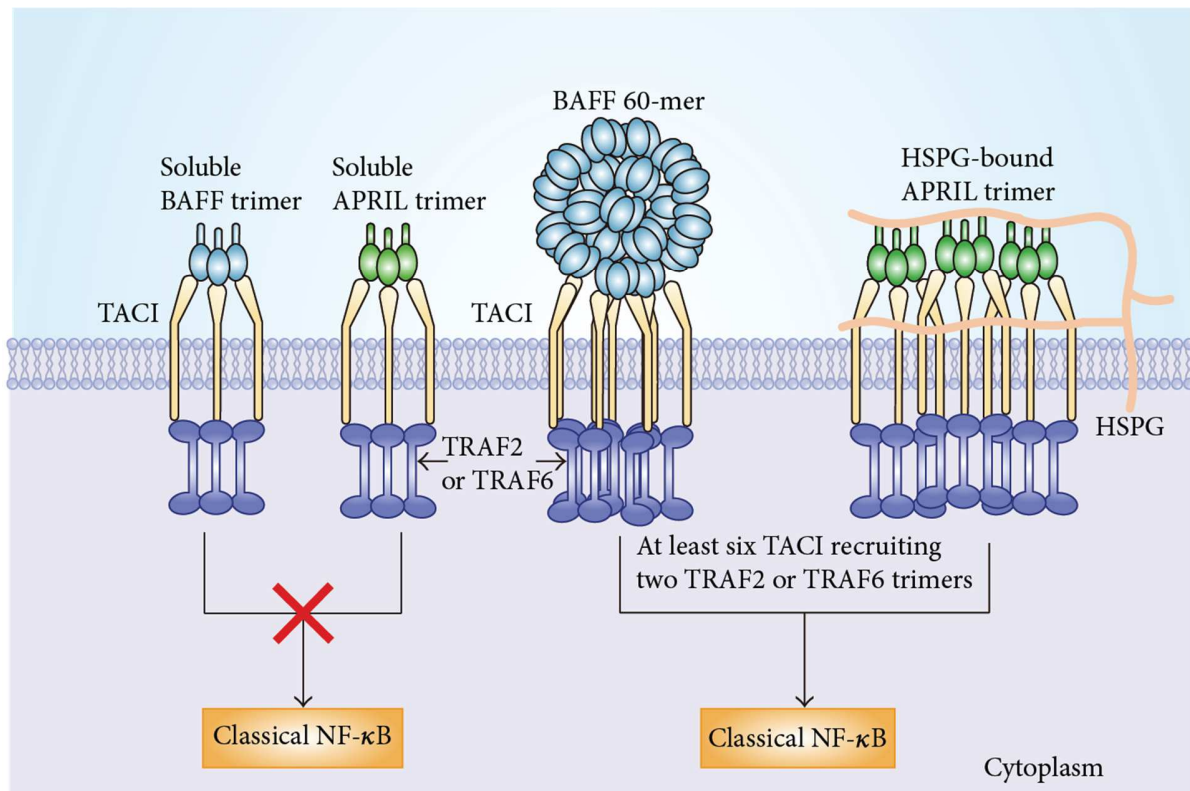


Figure 4: TACI can only be activated by oligomeric forms of BAFF and APRIL

Trimers of BAFF and APRIL can bind to TACI assembled as a trimer on the cell surface. For intracellular NF κ B activation six TACI receptors need to be connected to recruit TRAF2 or TRAF6 trimers. Only BAFF60mer and HSPG-bound trimers are able to connect TACI receptors and activate the classical NF κ B pathway through the TRAF trimers. (92) Figure taken from (92).

BCMA and TACI exist as soluble receptors in vivo (91, 93, 94). The protease gamma-secretase is responsible for BCMA cleavage (94) and the metalloproteinase ADAM10 causes extracellular shedding of TACI followed by intracellular processing of the resulting stump by gamma-secretase (93). Soluble BCMA (sBCMA) is able to act as a decoy receptor for APRIL (94), while soluble TACI (sTACI) can act as a decoy receptor for BAFF and APRIL (93). sBCMA and sTACI could be used as possible biomarkers to improve patient care, since both soluble receptors are elevated in B-cell driven pathologies (95, 96).

High levels of BAFF are linked to autoimmunity (97). In concordance with this, a BAFF variant that led to BAFF overexpression in a population of Sardinians was connected to MS and systemic lupus erythematodes (SLE) (98). SLE is a generalized

autoimmune disease associated with high levels of BAFF (99). An Anti-BAFF mAb (belimumab) is beneficial and already approved for the treatment of SLE (100-103).

Another attempt to target the BAFF/APRIL system was the mAb atacicept (TACI-Ig). In principle, atacicept was developed as soluble TACI fused to the Fc domain of human IgG1 (104, 105) to capture BAFF and APRIL (104). The Fc part of atacicept exhibited mutations to inhibit FcγR interaction and complement binding (106-108). Atacicept showed positive effects in rheumatoid arthritis (RA) and, in high doses, in SLE (109-113). Unfortunately, atacicept worsened MS. The atacicept in multiple sclerosis (ATAMS) trial was terminated due to elevated disease activity in treated patients. The group treated with atacicept showed an increase in annual relapse rate in comparison to a placebo controlled group (significant results for the application of 25 and 150 mg of atacicept) (114-116).

Several reasons could be responsible for the unexpected effect of atacicept on MS, while Rituximab was beneficial (11):

1. Rituximab and atacicept target different subpools of B-cells with atacicept affecting Breg cells (regulatory B-cells).
2. Atacicept treatment leads to an increase of memory B-cells that could enhance inflammatory processes.
3. In EAE atacicept increased the proinflammatory cytokine IL15 that could attribute to the inflammatory process during atacicept treatment.
4. Atacicept leads to a decrease of Fc-receptor blockage due to decreased levels of serum Igs. Fc-receptor blockage is beneficial and obligatory for the effect of IVIG treatment in MS patients.
5. Receptors of the BAFF/APRIL system are expressed on neurons and could affect neuronal modulation after inflammation like axonal growth. Atacicept inhibits this beneficial process by blocking BAFF and APRIL.

1.5. THE AMBIVALENT ROLE OF THE RECEPTOR TAC1 IN IMMUNITY

The ambivalent role of the receptor TAC1 within the immune system could be a possible cause for the unexpected failure of atacicept (TAC1-Fc/TAC1-Ig) in MS (116). Earlier studies in TAC1 (-/-) deficient mice revealed an interesting role of TAC1 as on the one hand a positive and on the other hand a negative regulator of immunity (117-119). One study described that mice with TAC1 deficient B-cells developed splenomegaly, B-cell aggregates due to increased levels of B-cells and elevated antibody levels (118). Another study found that TAC1 deficient mice had increased levels of autoantibodies, developed autoimmune glomerulonephritis and that in vitro inhibition of TAC1 on B-cells decreased B-cell proliferation and a recombinant receptor containing the internal sequencing signal of TAC1 lead to apoptosis of B-cells (117). Another group investigated the immune response of TAC1 deficient mice and showed that these mice were not capable to generate a response to specific antigens (T-independent type II antigens) (119). In addition, the diseases common variable immunodeficiency (CVID) and IgA deficiency are both associated with mutations of TAC1 (120-123). Some of these patients showed signs of lymphoproliferation and autoimmunity together with immunodeficiency (122). These findings justify a closer look at the receptor TAC1.

TAC1 is expressed on memory B-cells, plasmablasts, plasma cells and a subpopulation of activated (CD 27⁺) B-cells (**Figure 2**) (52, 124). TAC1 was firstly described as interactor with the protein calcium-modulator and cyclophilin ligand (CAML), which leads to induction of NF-AT, AP-1 and the classical NFκB pathway (125). TAC1 was found to be important for Ig class switch (126, 127). MyD88 binding to TAC1 initiates the class-switch recombination (92, 128). Additional functions and intracellular pathways have been described for TAC1 (92) (**Figure 5**). TAC1 induces plasma cell differentiation and decreases B-cell proliferation through mediation of Blimp-1 expression (129). Inhibition of the ICOSL receptor through TAC1 blocks germinal center reactions and B-cell proliferation (130). It was found that TAC1 stops the noncanonical NFκB pathway (NFκB 2) by mediating the degradation of NIK through cIAP-1 (131, 132). Moreover, TAC1 promotes together with TLR4 apoptosis in marginal zone B-cells through induction of FasL and Fas

(133). In contrast to TACI's effect on marginal zone B-cells, TACI decreases apoptosis of plasma cells by suppression of Bim (130). Concerning the BAFF/APRIL system, TACI decreases BAFF concentration and is a direct competitor with BAFF-R for BAFF (91, 92, 134, 135).

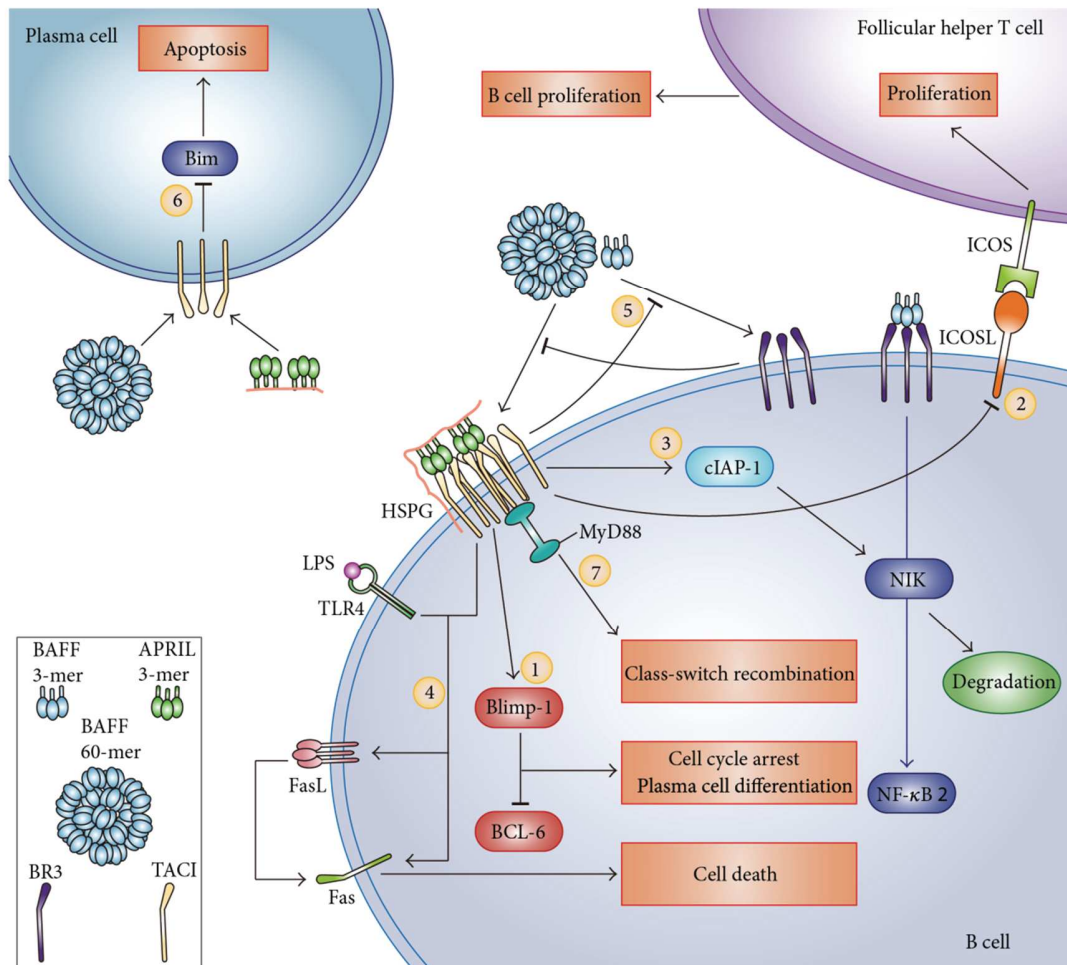


Figure 5: Different effects of TACI

1. TACI mediated Blimp-1 expression leads to plasma cell differentiation and decreased B-cell proliferation. 2. TACI hinders germinal center reactions and B-cell proliferation through ICOSL receptor inhibition. 3. TACI leads to degradation of NIK through cIAP-1 and thus stops the noncanonical NF κ B pathway (NF κ B 2). 4. Together with TLR4 TACI promotes apoptosis through induction of FasL and Fas in marginal zone B-cells. 5. TACI decreases BAFF concentration and is a direct competitor with BAFF-R for BAFF (and BCMA for APRIL (not shown)). 6. Plasma cell apoptosis is decreased by suppression of Bim. 7. MyD88 binding to TACI initiates the class-switch recombination. (92) Figure taken from (92).

TACI interacts with high affinity with the ligands BAFF and APRIL (136-139). TACI expresses two CRDs - CRD1 and CRD2. The CRD2 of TACI is responsible for high affinity binding (140). The CRDs of TACI share 50% of their sequence and both exhibit the DXL motif ((Phe/Tyr/Trp)-Asp-Xaa-Leu-(Val/Thr)-(Arg/Gly)) (140). The DXL motif is part of the binding module of TACI (140). The DXL motif binds directly to BAFF and APRIL (140-144). The role of the CRD1 is not known yet. It is proposed to be responsible for dimerization (145) or to be an evolutionary leftover without any function (140).

In humans, TACI appears in two isoforms with the shorter isoform being the product of alternative splicing (140). The splicing variant results from the loss of exon 2 which codes the CRD1 of TACI and its replacement with a tryptophan (W) residue (140, 146). This leads to changes on the extracellular domain. TACI-long expresses both CRDs, while TACI-short only CRD2 (**Figure 6**). A study examined both isoforms of TACI as full length receptors expressed on the cell surface (146). That study discovered that human B-cells express both isoforms with the shorter isoform predominating in CD27+ B-cells, splenic marginal zone B-cells and TLR9-activated peripheral B-cells and that the shorter isoform seems to be more potent in inducing plasma cell differentiation. (146) Both isoforms of TACI were able to bind to BAFF and APRIL in transduced murine B-cells (146).

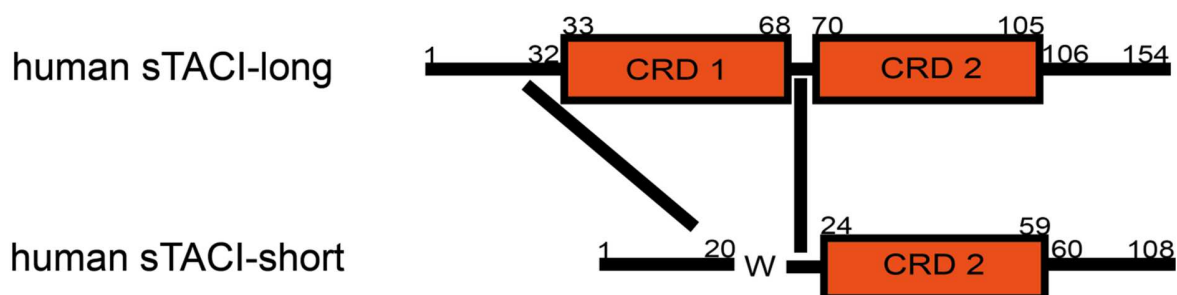


Figure 6: Structure of sTACI isoforms

Human sTACI long and short differ in the length of their extracellular domain. sTACI long expresses both CRD1 and CRD2. Alternative splicing in human TACI results in a short form only consisting of the CRD2. Illustration of the structure of both proteins was adapted from (146) supplementary material and the reported protein sequence for sTACI (93) and the TACI isoforms (140).

2. OBJECTIVE AND STRATEGY

The aim of this thesis was to get a deeper insight into details of the BAFF-APRIL system that regulates B-cell survival. Specifically, features of both isoforms of human soluble TACI were analyzed.

To this end, we produced the two soluble TACI isoforms recombinantly in HEK293T cells. These proteins were analyzed by mass spectrometry and N-terminal sequencing and characterized for posttranslational modifications (N-linked glycosylation) with PNGase F assay. We determined then the MW with size exclusion chromatography (SEC) and static light scatter (SLS) coupled to SEC. We assessed the oligomerization by SEC, SLS, Western blot and Coomassie stained SDS-PAGE. Next, we investigated both soluble isoforms for their functionality within the BAFF/APRIL system. We tested them for their binding affinity for BAFF and APRIL by binding ELISA and their decoy function by NF κ B assay. CRD1+CRD2-Fc, CRD1-Fc, CRD2-Fc, CRD1+CRD2-Fc-a, sTACI-short variants with differences in amino acid sequence N-terminal outside of CRD2, and SEC separated sTACI-long dimer and monomer were compared for binding affinity. Finally, we expressed both isoforms in their full-length form transiently in HEK293T cells and analyzed release of soluble receptors, ligand binding and homo- or heterotypic interactions.

3. MATERIAL AND METHODS

3.1. MATERIAL

3.1.1. GENERAL MATERIAL AND MACHINES

The following Kits were used for cloning, measurement of the concentration of proteins and determination of MW:

Table 1: Kits

Kit	Company
Human TACI/TNFRSF13B DuoSet ELISA	R&D Systems
Pierce™ BCA Protein Assay Kit	Thermo scientific
QIAquick™ Gel Extraction Kit	Qiagen GmbH
Hispeed® Plasmid Maxi Kit	Qiagen GmbH
Hispeed® Plasmid Midi Kit	Qiagen GmbH
QIAprep® Spin Miniprep Kit	Qiagen GmbH
MinElute® PCR Purification Kit	Qiagen GmbH
Human BCMA/TNFRSF17 DuoSet ELISA	R&D Systems
Gel Filtration LMW Calibration Kit	GE Healthcare Life Sciences

Different cell lines that were used:

Table 2: Cell lines

Cell line	Medium
HEK293T	DMEM-medium
HEK293.EBNA	Freestyle™293 + Glutamin medium

Different pipettes (**Table 3**) and consumables (**Table 4**) and general machines (**Table 5**) used in this thesis:

Table 3: Pipettes

Device	Company
Accu-jet® pro	Brand® GmbH & Co. KG
Eppendorf®Reference 2	Eppendorf AG

Table 4: List of consumables

Product	Company
pipet tips with/without filter	Kisker Biotech GmbH & Co. KG
Eppendorf tubes	Eppendorf AG
Serological pipets	Corning-Costar Corporation
Cryotubes	Kisker Biotech GmbH & Co. KG
Cell culture plates	Nunc®
Nunc® 96-Well Polystyrene Conical Bottom MicroWell™Plates	Thermo scientific
Costar® Assay plate	Corning-Costar Corporation
Corning® 96 well plates	Corning-Costar Corporation
Gloves	B. Braun AG
Steritop filter	Merck Millipore

Table 5: General Machines

Machine	Model	Company
Incubator	Galaxy 170 S	Eppendorf AG
Hood	B-(MxPro)^2-160	BERNER INTERNATIONAL GMBH
Gel-electrophoreses	XCell SureLock Mini-Cell	Thermo scientific
Centrifuge for small volumes	Cetrifuge 5417R	Eppendorf AG
Centrifuge for big volumes and flow cytometry	MULTIFUGE X3R centrifuge	Thermo scientific
Vortex	Vortex-Genie 2	Scientific Industries

The ingredients of the Gel Filtration LMW Calibration Kit (**Table 1**):

Table 6: Content of Gel Filtration LMW (low molecular weight) Calibration Kit

Protein	Molecular weight (M _r)	Stoke`s Radius ¹ (Å)	Source
Aprotinin	6500	NA	Bovine lung
Ribonuclease A	13700	16.4	Bovine pancreas
Carbonic Anhydrase	29000	NA	Bovine erythrocytes
Ovalbumin	44000	30.5	Hen egg
Conalbumin	75000	NA	Chicken egg white
Blue Dextran 2000	Void volume		

Columns that were used for size exclusion chromatography (SEC) and static light scatter analysis (SLS):

Table 7: Columns for size exclusion chromatography

Column	Geometric column volume (VC (ml))	Recommended sample volume (µl) during calibration	Application	Company
HiLoad 16/60 Superdex 75 pg	120	500	SEC	GE Healthcare Life Sciences
Superdex 200 Increase 10/300 GL	24	25–500	SLS	GE Healthcare Life Sciences

3.1.2. CELL CULTURE MEDIA, BUFFER AND SOLUTIONS

All buffers were filtered with 0.22 µm MILLIPORE Stericup® Vacuum filters (Merck Millipore) before usage. The buffers for protein production were additionally degassed. The pH was adjusted to 7.4 with NaOH and HCl if not stated otherwise. Double deionized water (dH₂O) was generated with a Milli-Q System (Merck Millipore) and used for all buffers.

The following buffers and media were used for cell and bacteria culture:

Table 8: Buffers for cell and bacteria culture

Reagent	Amount/concentration	Company
<u>DMEM-medium</u>		
DMEM	500 ml	SIGMA-Aldrich® Co.LLC.
FCS	10%	
P/S	1%	GIBCO®
<u>RPMI-medium</u>		
RPMI (1640)	500 ml	SIGMA-Aldrich® Co.LLC
FCS	10%	
P/S	1%	GIBCO®
Sodium pyruvate	1%	GIBCO®
L-Glutamine	1%	GIBCO®
Nonessential Amino acids	1%	GIBCO®
<u>Freestyle™293 + Glutamin medium</u>		
Freestyle™293+Glutamin	1 l	GIBCO®
G418/Geneticin	500 µl	GIBCO®
10%Pluronic® F-68	1%	GIBCO®
<u>Kryo-medium</u>		
FBS Superior	90%	Merck Millipore
DMSO	10%	New England BioLabs, Inc.
<u>LB-Medium (1L)</u>		
Bacto-tryptone	10 g	BD Biosciences
Yeast extract	5 g	BD Biosciences
NaCl	10 g	Merck Millipore
<u>LB-agar (dissolved in 1L LB-medium)</u>		
Agar	15 g	Thermo Scientific
Ampicillin	100 µg/ml	SIGMA-Aldrich® Co.LLC.

The following buffers were used for protein expression:

Table 9: Buffers for protein production

Reagent	Amount/concentration	Company
<u>Elution Buffer 1M Imidazol</u>		
Imidazol	1 M	Merck Millipore
Nacl	0.5 M	SIGMA-Aldrich® Co.LLC.
Na ₂ HPO ₄	20 mM	Merck Millipore
<u>Elution Buffer without Imidazol</u>		
Nacl	0.5 M	SIGMA-Aldrich® Co.LLC.
Na ₂ HPO ₄	20 mM	Merck Millipore
<u>5x Dialysis Buffer</u>		
Na ₂ HPO ₄	0.1 M	Merck Millipore
Nacl	2.5 M	SIGMA-Aldrich® Co.LLC.
Imidazol	50 mM	Merck Millipore
<u>Cleaning Buffer</u>		
NaOH	1 or 0.5 M	SIGMA-Aldrich® Co.LLC.
<u>System Storage Buffer 1</u>		
Ethanol	20%	SIGMA-Aldrich® Co.LLC.
<u>System Storage Buffer 2</u>		
NaN ₃	0.01%	SIGMA-Aldrich® Co.LLC.
<u>Storage Buffer</u>		
Na ₂ HPO ₄	20 mM	Merck Millipore
Nacl	0.3 M	SIGMA-Aldrich® Co.LLC.

The following buffers were used for Enzyme Linked Immunosorbent Assay (ELISA), flow cytometry, and Co-Immunoprecipitation (Co-IP):

Table 10: Buffers for ELISA, flow cytometry and Co-IP

Reagent	Amount/concentration	Company
<u>ELISA</u>		
<u>Reagent Diluent</u>		
PBS	500 ml	GIBCO®
BSA	1%	SIGMA-Aldrich® Co.LLC.
<u>Stop Solution</u>		
H ₂ SO ₄	1 M	Carl Roth®GMBH + CO.KG
<u>FLOW CYTOMETRY</u>		
<u>Wash Buffer</u>		
PBS	500 ml	GIBCO®
BSA	1%	SIGMA-Aldrich® Co.LLC.
<u>CO-IP</u>		
<u>Lysis Buffer</u>		
NP-40	0.5%	SIGMA-Aldrich® Co.LLC.
HEPES Buffer (1M)	50 mM	SIGMA-Aldrich® Co.LLC.
Nacl	250 mM	SIGMA-Aldrich® Co.LLC.
EDTA	5 mM	SIGMA-Aldrich® Co.LLC.
Complete protease inhibitor mixture	1 Tablet for 50 ml	SIGMA-Aldrich® Co.LLC.
<u>TBS Buffer</u>		
Tris Hcl (Trizma)	50 mM	SIGMA-Aldrich® Co.LLC.
Nacl	150 mM	SIGMA-Aldrich® Co.LLC.
<u>Elution Buffer</u>		
Glycine	1 M (pH = 3)	SIGMA-Aldrich® Co.LLC.
<u>Neutralization Buffer</u>		
Trizma base/Hcl	1 M (pH= 9)	SIGMA-Aldrich® Co.LLC.

3.1.3. PRIMERS, VECTORS AND INSERTS USED FOR CLONING

The following oligonucleotides were synthesized by Metabion (**Table 11**). The vectors used for cloning are shown in **Table 12**.

Table 11: Primers for cloning

Primer	Sequence 5'→3'	Application
TACI Nhe 1 secretion-tag forward	ATTAGCTAGCATGGAGACCGACACCCTGCT GCTGTGGGTGCTGCTGCTGTGGGTGCCCG GCAGCACCGGCGACGCCGCCATGAGTGG CCTGGGCCGG	soluble TACI isoforms
TACI Xba 1 secretion-tag forward I	ATTATCTAGAATGGAGACCGACACCCTGCT GCTGTGGGTGCTGCTGCTGTGGGTGCCCG GCAGCACCGGCGACGCCGCCATGAGTGG CCTGGGCCGG	soluble TACI isoforms
TACI Not 1 His6-tag reverse	ATTAGCGGCCGCTCAGTGGTGGTGGTGGT GGTGCCCCCCTTCAGCCCCGGGAGAG	soluble TACI isoforms
TACI Xba 1 secretion-tag forward II	ATTATCTAGAATGGAGACCGACACCCTGCT GCTGTGGGTGCTGCTGCTGTGGGTGCCCG GCAGCACCGGCGACGCCGCCCTCACTCAGC TGCCGCAAG	soluble TACI isoforms
TACI Nhe 1 HA-tag forward	ATTAGCTAGCAATGTACCCATACGATGTTC CAGATTACGCTAGTGGCCTGGGCCGG	CO-IP
TACI Nhe 1 FLAG [®] -tag forward	ATTAGCTAGCAATGGATTACAAGGATGACG ATGACAAGAGTGGCCTGGGCCGG	CO-IP
TACI Not 1 reverse	ATTAGCGGCCGCTTATGCACCTGGGCCCC C	CO-IP
PTT5 forward	GGGGTGAGTACTCCCTCTCAAAGC	Sequencing
PTT5 reverse	GGGGCAGAGATGTTCGTAGTCAGG	Sequencing
CMV forward	CGCAAATGGGCGGTAGGCGTG	Sequencing
TACI forward	CAGACAACCTCGGGAAGG	Sequencing
TACI reverse	TGGCAGGAGCAGGGATC	Sequencing

Table 12: Vectors for cloning

Vector	Resistance	Origin
PTT5	Ampicillin	Judy King Man Ng
pcDNA3.1(+)	Ampicillin, Puromycin	AG Lichtenthaler

Several tags were added to the constructs during cloning:

Table 13: tag

Tag	DNA sequence
His6-tag	GGGGGGCACCACCACCACCACCACTGA
HA-tag	TACCCATACGATGTTCCAGATTACGCT
FLAG [®] -tag	GATTACAAGGATGACGATGACAAG
secretion-tag	ATGGAGACCGACACCCTGCTGCTGTGGGTGCTGCTGCTGT GGGTGCCCGGCAGCACCGGCGACGCCGCC

These restriction enzymes were used for all cloning processes:

Table 14: Restriction enzymes

Name of restriction enzyme	Target sequence 5' → 3'	Temperature and buffer	Company
Nhe 1 HF	GCTAGC	NE CUT SMART BUFFER 37 °C	New England BioLabs, Inc.
Not 1 HF	GCGGCCGC	NE CUT SMART BUFFER 37 °C	New England BioLabs, Inc.
Xba 1	TCTAGA	NE CUT SMART BUFFER 37 °C	New England BioLabs, Inc.

All plasmids that were used for the experiments are summarized in **Table 15** for TACI plasmids and **Table 16** for non-TACI plasmids.

Table 15: TACI plasmids

Plasmid	Resistance	Origin
TACI-long in pcDNA3.1(+)	Ampicillin, Puromycin	Franziska S. Thaler
TACI-short in pcDNA3.1(+)	Ampicillin, Puromycin	Franziska S. Thaler
sTACI-long in PTT5	Ampicillin	Miriam Fichtner

sTACI-short in PTT5	Ampicillin	Miriam Fichtner
sTACI-short (W-68-154) in PTT5	Ampicillin	Miriam Fichtner
TACI-long HA-tag in pcDNA3.1(+)	Ampicillin, Puromycin	Franziska S. Thaler
TACI-long FLAG-tag in pcDNA3.1(+)	Ampicillin, Puromycin	Franziska S. Thaler
TACI-short HA-tag in pcDNA3.1(+)	Ampicillin, Puromycin	Miriam Fichtner
TACI-short FLAG-tag in pcDNA3.1(+)	Ampicillin, Puromycin	Miriam Fichtner

Table 16: Non-TACI plasmids

Plasmid	Resistance	Origin
Renilla-Luciferase	Ampicillin	AG Rothenfusser
Firefly-Luciferase	Ampicillin	AG Rothenfusser
BCMA full length	Ampicillin	OriGene Technologies, Inc.
BCMA FLAG [®] -tag in pCMV	Ampicillin	Sarah Laurent

3.1.4. GELS, DYES AND BUFFERS FOR SDS-PAGE AND COOMASSIE STAINING

The following materials were used for SDS-PAGE applications:

Table 17: Material for SDS-PAGE

Gels	Company
Novex [®] Bis-Tris 6-12 %	Invitrogen [™]
Novex [®] Tricine 10-20 %	Invitrogen [™]
LOADING DYES	
NuPAGE [®] LDS Sample Buffer (4X)	Invitrogen [™]
Novex [®] Tricine SDS Sample Buffer (2X)	Invitrogen [™]
RUNNING BUFFERS	
Novex [®] Tricine SDS Running Buffer (10X)	Invitrogen [™]

Novex® Tricine SDS Running Buffer (10X)	Invitrogen™
MOPS SDS Running Buffer (20X)	Invitrogen™
SAMPLE REDUCING AGENT	
NuPAGE® Sample Reducing Agent (10X)	Invitrogen™

The following buffers were used for Coomassie staining:

Table 18: Buffers for Coomassie staining

Reagent	Concentration	Company
<u>Coomassie blue solution</u>		
(w/v) Coomassie brilliant-blue R-250	0.1%	SERVA Electrophoresis GmbH
Methanol	40%	SIGMA-Aldrich® Co.LLC.
Acetic acid	10%	SIGMA-Aldrich® Co.LLC.
<u>Destain solution</u>		
Methanol	50%	SIGMA-Aldrich® Co.LLC.
Acetic acid	7%	SIGMA-Aldrich® Co.LLC.
<u>Storage solution</u>		
Acetic acid	10%	SIGMA-Aldrich® Co.LLC.

3.1.5. ANTIBODIES AND FLUOROCHROMES

The following antibodies were used for Western blot (**Table 19**), Co-IP/Binding ELISA (**Table 20**) and flow cytometry (**Table 21**):

Table 19: Antibodies for Western Blot

Antibody	Company	Application	Clone
Monoclonal TACI/TNFRSF13B Anti-human produced in mouse (IgG1)	R&D Systems	primary antibody	165609
Anti-mouse IgG (H+L) HRP conjugated produced in goat	Promega GmbH	Western blot, secondary antibody	polyclonal

Table 20: Antibodies for Co-IP and Binding ELISA

Antibody	Company	Application	Clone
Monoclonal Anti-FLAG [®] M2 – Antibody produced in mouse (IgG1)	SIGMA-Aldrich [®] Co.LLC.	Co-IP (capture Ab), Binding ELISA (capture Ab)	M2, monoclonal
Monoclonal Anti-HA.11 Epitope Tag produced in mouse (IgG1)	BioLegend	Co-IP (capture Ab)	HA-7, monoclonal

Table 21: Antibodies for flow cytometry

Antibody	Company	Application	Clone
Monoclonal Anti-FLAG [®] M2 – Antibody produced in mouse (IgG1)	SIGMA- Aldrich [®] Co.LLC.	primary antibody for binding studies	M2, monoclonal
Monoclonal TACI/TNFRSF13B Anti- human produced in mouse (IgG1)	R&D Systems	primary antibody for expression	165609, monoclonal
Polyclonal Anti-mouse Immunoglobulins/RPE produced in goat	Dako	secondary antibody	polyclonal

The fluorochromes that were used for flow cytometry had the following excitation and emission values:

Table 22: Fluorochromes for flow cytometry

Fluorochrome	Excitation	Emission
Phycoerythrin (PE)	565 nm	575 nm
TO-PRO [®] -3 Iodide (Invitrogen [™])	642 nm	661 nm

3.2. METHODS

3.2.1. GENERAL METHODS

3.2.1.1. AGAROSE GEL ELECTROPHORESIS

Agarose gel electrophoresis was used to determine the size, yield and purity of PCR products and to scan for positive clones. DNA has a negative net charge and thus can be run in an electrical field. Agarose is used as matrix.

1% Agarose gels in TAE buffer were cast into a self-assembled mold with a comb suitable for the ongoing application. Peqgreen DNA/RNA Dye (PEQLAB Biotechnologie GmbH) was added in a ratio of 4-6 μl per 100 ml Agarose to the solved gel at 55 °C before decanting it to the mold to make DNA bands visible. 2-Log DNA Ladder (New England BioLabs, Inc.) was used as a size standard that spans a range from 0.1-10.0 kb. The bands consisting of the expected DNA fragments were cut after electrophoresis during UV light exposure ($\lambda = 254\text{-}366\text{ nm}$) in a UV light box and stored at -20 °C or purified immediately.

3.2.1.2. SPECTROPHOTOMETER

DNA and protein concentrations were measured with a UV-based spectroscopy named Nanodrop (Nanodrop 2000, Thermo scientific). Small volumes of sample (1-2 μl) were tested by spectrophotometry. The system measures the absorbance (**Equation 1**) of the sample with the blanking value as basis and uses the Beer-Lambert equation (**Equation 2**) to correlate the absorbance to the concentration:

$$Absorbance = -\log\left(\frac{intensity_{sample}}{intensity_{blank}}\right)$$

Equation 1: Absorbance

$$A = \epsilon bc$$

Equation 2: Beer-Lambert

(A = absorbance (A=absorbance units), ϵ = extinction coefficient, b = path length (cm), c = concentration (M))

The absorbance (optical density (OD)) was measured at 260 nm for DNA molecules and 280 nm for proteins.

3.2.1.3. SDS-PAGE AND COOMASSIE BRILLIANT BLUE STAINING

Sodium dodecyl sulfate (SDS)-PAGE gels were used to analyze proteins for their size, oligomerization, and purity. SDS, the matrix of the gel, lead in combination with sample reducing agent (50 mM DTT) and heat denaturation (95 °C for 5 min) to denaturation of proteins. Electrophoresis was performed at 70-100 V. Novex® sharp prestained Protein Standard (Thermo scientific) that spans a range of 3.5-260 kDa was used as size standard. Bis-Tris gels (6-12%) were used to check for protein fractions after affinity purification (**Table 17**). Tricine gels were used for analytical purposes such as Western blot (**Table 17**). After gel-electrophoresis the gel was incubated for 20-30 min in Coomassie blue solution (**Table 18**). Next, destain solution (**Table 18**) was applied and exchanged several times for at least 1 h. To decrease the amount of background staining the gel was then incubated in storage solution Table 18 overnight. Analysis was done by Odyssey Fc (LI-COR Biosciences) with 700 nm. All steps were carried out at room temperature.

3.2.1.4. WESTERN BLOT

Western blot was used to identify proteins after SDS-PAGE. 300-750 ng of Protein were loaded on a Tricine gel and run at 70-100 V. The gel was blotted semi dry (Amersham pharmacia biotech EPS 3501 XL; GE Healthcare Life Sciences) on a

polyvinylidene difluoride (PVDF) membrane (GE Healthcare Life Sciences) for 1.5 h at 60 mA to transfer the proteins. PBST (0.05% Tween[®] 20 (Bio-Rad Laboratories GmbH) in PBS, pH 7.2-7.4) with 5% milk powder (blocking solution) was used to block the membrane for 1 h at room temperature to prevent unspecific binding of the detection antibodies to areas where no proteins were transferred. The primary antibody (**Table 19**), diluted in PBST with 5% BSA Fraction V (SERVA Electrophoresis GmbH) to a concentration of 1 µg/ml) was added and the membrane was incubated over night at 4 °C. All incubation and washing steps were carried out on a shaker. 12-18 h later the primary antibody that was not specifically bound to the proteins on the membrane was removed by washing the membrane three times with PBST for 10 min at room temperature. Then, the membrane was incubated with the secondary antibody that was conjugated with horseradish peroxidase (HRP) (**Table 19**), diluted in PBST with 5% milk powder to a concentration of 0.4 µg/ml for 2 h. After incubation the unspecific bound secondary antibody was removed with the same washing steps that were used to remove the primary antibody. ECL Western Blotting Substrate (Merck Millipore or Pierce™) was applied and the membrane was analyzed by Odyssey Fc (LI-COR Biosciences) with 700 nm for the marker and the chemiluminescence channel for the light reaction (400-700 nm).

3.2.1.5. ENZYME-LINKED IMMUNOSORBENT ASSAY (ELISA)

Enzyme-linked immunosorbent assay (ELISA) is a quantitative immunoassay. The antigen concentration correlates to the substrate turnover caused by an enzyme (for example HRP). A dilution series with known concentrations of the measured antigen is used to generate a standard curve. The standard curve can be used to calculate concentrations of the applied sample.

An ELISA starts with coating a plate with a capture antibody (**Table 20**). After blocking the plate the antigen is incubated. A detection antibody is added. Either the enzyme for the later color reaction is directly bound to the detection antibody or added in an additional step (**Figure 7**).

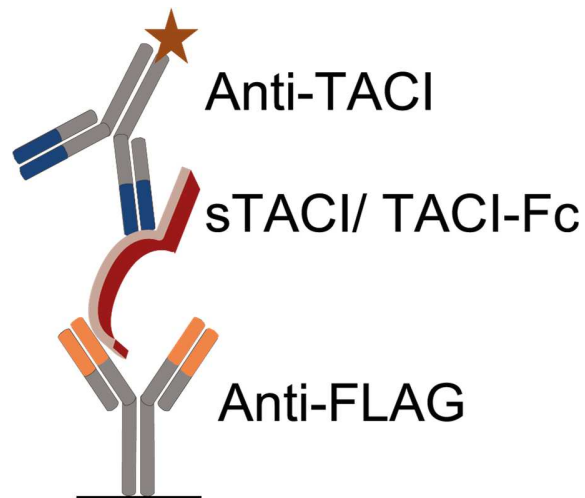


Figure 7: Principle of ELISA

After coating a plate with a capture antibody, an antigen is added. The antigen gets detected by a detection antibody. A color reaction is used to measure the reaction. Adapted from (93)

sTACI and sBCMA ELISA Kits from **Table 1** were used to determine the concentration of samples prior to consecutive experiments. In both ELISAs the secondary antibody was coupled with biotin. Horseradish peroxidase (HRP) conjugated to streptavidin was added in a next incubation step. Streptavidin and biotin are able to form a strong bond (147). Substrate solution (Mix A (H_2O_2) and Mix B (Tetramethylbenzidine) in a ratio of 1:1) was added and after 20 min incubation the reaction was stopped by the addition of stop solution (1 M H_2SO_4). The peroxidase reaction with tetramethylbenzidine and HRP was detected by photometry. Both ELISAs were read out with Victor2 1420 Multilabel Counter (Perkin Elmer) with 450 nm for the absorbance and 540 nm for the background from the plate.

3.2.1.6. BICINCHONINIC ACID (BCA) ASSAY

Bicinchoninic acid assay (BCA) was used to determine protein concentration after protein expression. Two chemical reactions comprise the basis for this method. First, the peptides of the protein lead to the reduction of Cu^{2+} to Cu^{+} ion of the substrate Copper(II) sulfate pentahydrate. This reaction correlates to the amount of protein that is measured. A second reaction detects the Cu^{+} ions. Bicinchoninic acid is added which is able to form a chelate with Cu^{+} ion which can be detected by a purple color reaction. The BCA assay was read out at 540 nm with Victor2 1420 Multilabel Counter (Perkin Elmer).

3.2.1.7. TRANSFECTION

Transfection of cells was performed using lipofection, which is a chemical transfection method. Lipofectamine 2000 (Thermo scientific) was used as transfection reagent. During the transfection process, first the DNA is enveloped in a lipid shell. This lipid shell interacts with the cell membrane which leads to an integration of the DNA into the cell.

For flow cytometry, HEK293T cells were plated at a concentration of 200.000 cells per ml in a 96 well Costar plate. The cells were transfected at a confluency of 70% with 5, 10, 25, 50 or 100 ng of TACI-short or TACI-long plasmid. For the NF κ B assay, HEK293T cells were plated at a concentration of 200.000 cells per ml in a 96 Costar plate and transfected at a confluency of 70% with Firefly-Luciferase (40 ng per well), Renilla-Luciferase (40 ng per well) and BCMA (2.5 ng per well). For Co-Immunoprecipitation (Co-IP) HEK293T cells were plated at a concentration of 300.000 cells per ml in a 10 cm dish. At a confluency of approximately 70% the cells were transfected with 10 μ g of TACI-long, TACI-short and BCMA plasmids containing an N-terminal FLAG- and/or HA-tag. 48-72 h after transfection supernatants were harvested and cell lysates were obtained.

3.2.1.8. HARVEST OF SUPERNATANTS

Different methods were applied to purify and separate proteins of interest from cell culture media. These methods were based on separation through centrifugation. For small volumes of up to 2 ml and supernatants from assays with HEK293T cells the proteins were harvested and centrifuged two times at 400 g at 4 °C for 7 min and one time for 20.000 g at 4 °C for 30 min. The supernatants were stored at -20 °C. For bigger volumes like for example during the Co-IP assay the last step of centrifugation was carried out at 4122 g for 30 min. During production of proteins with HEK293.EBNA cells the supernatants were harvested 72 h after transfection. The cell/supernatant mix was centrifuged once at 1200 rpm for 5 min at 4 °C. The supernatant was centrifuged a final time for 2500 rpm for 20 min at 4 °C followed by filtration with 0.22 µm MILLIPORE Stericup® Vacuum filter system (Merck Millipore). The supernatant was stored at 4 °C before application of the next steps.

3.2.1.9. CELL LYSIS

For NFκB assay the cells needed to be lysed to measure luciferase reaction. The cells were lysed with passive lysis buffer from Promega. The lysis buffer was diluted with distilled H₂O in a ratio of 1:5. The cell culture media was removed and 50 µl of the lysis buffer was added. Everything was incubated for 10 min on a shaker at room temperature. For Co-IP the cells were washed with PBS and centrifuged once for 7 min at 400 g to eliminate cell culture medium residues. The cells were then lysed in 1.8 ml lysis buffer (**Table 10**) and stored for 30 min on ice. After cell lysis the lysates were centrifuged one time for 10 min at 14.000 rpm. The lysate aliquots were stored at -80 °C.

3.2.2. MOLECULAR CLONING

3.2.2.1. AMPLIFICATION AND PURIFICATION OF THE INSERT

In general, plasmids, genomic DNA or cDNA can be used as templates for polymerase chain reaction (PCR) during cloning. For this thesis, the plasmids TACI-short and TACI-long in PCDNA3.1 vector were used as template and these DNA sequences were amplified by PCR. The different steps of the PCR protocol used for all experiments are described in **Table 24** and the different reagents of the PCR mixture in **Table 23**.

The following general PCR mixture (**Table 23**) and standard protocol (**Table 24**) was used for all constructs:

Table 23: PCR mixture

Amount in μ l	Reagents	Company
31	H ₂ O	Invitrogen™
10	5x GC Puffer	New England BioLabs, Inc.
1	dNTPs (10 mM)	Fermentas
2.5	Reverse primer (10 μ M)	Metabion
2.5	Forward primer (10 μ M)	Metabion
1	Template (10 ng)	-
1.5	DMSO 100 %	New England BioLabs, Inc.
0.5	Phusion HF DNA Polymerase	New England BioLabs, Inc.

Table 24: Polymerase chain reaction protocol

PCR step	Temperature	Time
Denaturation	95 °C	30 s
Primer Annealing	95 °C	15 s
Elongation	72 °C	2 min
	The first three steps were repeated 38 times	
Final Elongation	72 °C	7 min
Final hold	4 °C	Infinitely

Several tags and restriction sites were added to the DNA sequences during cloning (**Table 13**). For the creation of the sTACI-long and sTACI-short the signal peptide of the Ig kappa chain was added at the N-terminus of the proteins to ensure the secretion of the proteins. Moreover, a His6-tag consisting of the sequence for six consecutive histidines was added at the C-terminus for affinity purification with Nickel columns. The resulting DNA was inserted into vectors suitable for the destined application (**Table 12**). The plasmids for Co-IP were cloned with either a HA- or FLAG[®]-tag on the N-terminal side. The restriction enzymes (**Table 14**) and corresponding sites were chosen with the help of NEBcutter V2.0 and the sequences were added during PCR. After PCR the products were analyzed by agarose gel electrophoresis. After electrophoresis, the desired bands were cut. The DNA was purified with the QIAquick[™]Gel Extraction Kit (Qiagen GmbH) and stored at -20 °C. The concentration was measured with Nanodrop (Thermo scientific).

3.2.2.2. DIGESTION OF INSERT AND VECTOR WITH RESTRICTION ENZYMES

To generate sticky ends both the vector and insert DNA were incubated for 1-3 h with restriction enzymes at 37 °C (**Table 14**). In the last hour of digestion, the vector was dephosphorylated by adding calf intestine alkaline phosphatase (CIAP). The vector was loaded on a DNA gel and consecutively cut and purified using the QIAquick[™]Gel. MinElute columns (Qiagen GmbH) were used instead of the columns of the QIAquick Kit (Qiagen GmbH) to concentrate the sample to a smaller volume. The insert was purified using the MinElute[®] PCR Purification Kit (Qiagen GmbH). Both products were stored at – 20 °C before ligation.

3.2.2.3. LIGATION

Ligation was executed for 1 h at room temperature or overnight at 16 °C using the T4 DNA Ligase and the T4 DNA Ligase buffer containing ATP (New England BioLabs, Inc.). As a control one condition was comprised of only digested vector to test for self-ligation.

3.2.2.4. TRANSFORMATION OF *E. COLI*, BACTERIAL CULTURE AND PLASMID DNA PURIFICATION

After ligation the samples were transformed into *E. coli* (NEB® 5-alpha Competent *E. coli*) using heat shock transformation. The tube containing the frozen *E. coli* was thawed on ice for 10 min. Afterwards, around 100 ng of plasmid was added and mixed with the *E. coli* carefully. The *E. coli* and plasmid were then incubated for 30 min on ice, before heat shock was performed at 42 °C for 90 s. After Heat shock treatment the *E. coli* had a last cooling step on ice for 5 min. SOC medium was added to cooled down *E. coli* and the mixture was incubated for 1 h at 37 °C in a bacteria shaker at 250 rpm. Finally, the transformed bacteria were centrifuged at 4000 rpm for 5 min and dissolved in 100 µl Medium and then applied to preheated selection plates containing ampicillin. All vectors used contained ampicillin resistance. The plates were incubated overnight in a 37 °C bacteria incubator. The next day clones were picked and incubated for one day in 2 ml LB medium with addition of ampicillin in a ratio of 1:1000 to prevent unspecific growth of other bacteria. The following day DNA was purified using the QIAprep® Spin Miniprep Kit (Qiagen GmbH). 1 µg of DNA was digested with the identical restriction enzymes that were used to clone the construct for 1 h at 37 °C and then loaded on a DNA gel to check for positive clones.

3.2.2.5. SEQUENCING

After cloning the clones that were screened as positive, were analyzed and verified with Sanger sequencing by the LMU Sequencing Service. The method Big Dye v.3.1. cycle, clean and run was selected for the control of the sequence of the insert.

3.2.3. EXPRESSION OF PROTEINS AND CONSECUTIVE AFFINITY PURIFICATION

3.2.3.1. PROTOCOL FOR TRANSFECTION

HEK293.EBNA cells were transfected with Polyethyleneimine reagent (PEI, SIGMA-Aldrich® Co.LLC.) at a concentration of 1×10^6 cells/ml. First, the plasmid DNA-lipid complexes were prepared in Optipro Medium (GIBCO®). 1 µg of Plasmid was used per 10^6 cells. PEI was applied at a concentration of 2 µg per 10^6 cells. After an incubation period of 20-30 min at room temperature the plasmid DNA-lipid complexes were added to the cells and then everything was placed into the Pro incubation shaker (Multitron) at 5% CO₂ and 37 °C. 12-24 h later 5% Lactalbumin (SIGMA-Aldrich® Co.LLC.) was added to feed the cells.

3.2.3.2. DIALYSIS AND FILTRATION OF SUPERNATANTS

The supernatants were dialyzed with 8 kDa Spectra/Por®6 Dialysis Membrane (sTACI-long) or 3.5 kDa Spectra/Por®7 Dialysis Membrane (sTACI-short, sTACI-short (W-68-154)). The supernatants were dialyzed at 4 °C for 24 h in 1x dialysis buffer (**Table 9**) while rotating on a magnetic stirrer. The buffer was exchanged every 8 h and in total three times. Finally, the supernatant was filtered with 0.45 µm MILLIPORE Stericup® Vacuum filter system (Merck Millipore) and stored at 4 °C before application to the column.

3.2.3.3. AFFINITY PURIFICATION WITH HISTRAP COLUMNS

Affinity purification or affinity chromatography was used to extract the recombinant proteins from the supernatant. The His6-tag that was added C-terminally to the soluble TACI isoforms during cloning was used for purification with HisTrap nickel columns (HisTrap HP (1 ml), GE Healthcare) on the ÄKTA™ START (GE Healthcare). The His6-tag was added as it can form a chelate with the nickel ions of the used columns. Later Imidazole was used to elute the specifically bound proteins. Imidazole competes with

His6-tags for the binding to Nickel. Increasing amounts of Imidazole can remove the proteins and clean the column.

Firstly, the HisTrap column was washed with Millipore H₂O to remove the storage buffer from the column (20% ethanol). Then 1x dialysis buffer (**Table 9**) was added to equilibrate the column to the sample milieu. Depending on the volume of the supernatant, the column was either directly loaded with the ÄKTA START™ for small volumes or overnight with the LKB Pump P-1 Peristaltic Pump (Pharmacia) in the cold room at 4 °C for high volumes. After sample application one last washing step was carried out with 1x dialysis buffer to get rid of unspecifically bound proteins. The elution step was performed with an Imidazole gradient ranging from 0.01–1 M. Eluted proteins were dialyzed against the storage buffer (**Table 9**) with 3,500 MWCO Slide-A-Lyzer Dialysis cassettes (Thermo scientific) to avoid protein aggregation upon freezing.

3.2.4. CHARACTERIZATION OF THE PROTEINS

3.2.4.1. PNGase F DIGESTION AND TEST FOR DIVALENT ION-HIS6-TAG INTERACTION

Glycosylation of the proteins was tested with the enzyme PNGase F (New England BioLabs, Inc.). PNGase F is an amidase able to cleave N-linked sugars from glycoproteins and glycopeptides when Asn-oligosaccharides are present (148). The sTACI isoforms were incubated with glycoprotein denaturation buffer and then denatured for 10 min at 100 °C. The mixture was chilled on ice and then centrifuged for 10 s. Next, Glycobuffer, 10% NP-40 and distilled water were added. In the final step PNGase F was added and incubated for 1 h at 37 °C. Controls consisted of several conditions with and without PNGase F and non-treated protein that only followed the temperature regime. hMOG which is known to be N-linked glycosylated was used as a positive control. Western blot was used to analyze the results.

His6-tagged proteins are susceptible to aggregation caused by divalent metals such as nickel and cobalt. During purification this mechanism is used to purify the recombinant proteins from other proteins that are co-produced during protein synthesis. Divalent Nickel ions sometimes can be washed of the purification column and lead to protein aggregation through building chelates with His6-tag purified proteins. To exclude

an artificial interaction of the His6-tags of the recombinant proteins` with eluted nickel ions 100 mM EDTA with a pH of 7.5 was added to the proteins and incubated for 1-2 h at room temperature in order to sequester possible nickel ions. Several conditions with or without DTT and with or without EDTA were tested.

3.2.4.2. MASS SPECTROMETRY AND N-TERMINAL SEQUENCING

Mass spectrometry can be used to identify and to provide sequence information of different protein bands after gel-electrophoresis. Therefore, the bands of interest were accurately cut from the gel, stored in distilled water and then processed by Reinhard Mentele (Institute of Clinical Neuroimmunology, LMU) at the MPI and the Biomedical Center (BMC) of the LMU. Trypsin digestion was used for all affinity purified proteins. The N-terminal part of the proteins can be analyzed by N-terminal sequencing. After running the proteins through gel electrophoresis to separate the different fractions by size the proteins were transferred semidry to a polyvinylidene difluoride (PVDF) membrane. The membrane was consecutively stained for 3-4 min with Coomassie brilliant blue, destained for 10 min with destain buffer and washed 10 min with distilled water. After cutting the bands of interest, the bands were air dried. The analysis was carried out by Reinhard Mentele at the MPI and the BMC of the LMU.

3.2.4.3. SIZE EXCLUSION CHROMATOGRAPHY

Size Exclusion Chromatography (SEC/Gel-filtration) was used to determine the molecular weight of both sTAC1 isoforms and to figure out whether the proteins form oligomers. Additionally, it was used to obtain the different fractions of the sTAC1 isoforms by size exclusion. SEC was carried out in collaboration with Prof. Michaela Smolle (Department of Physiological Chemistry, LMU). The columns for gel-filtration are filled with gel beads that are characterized by holes and an internal gel matrix. Big proteins cannot enter the beads and thus run through the column with high velocity. This fraction represents the void volume. Consequently, proteins can be separated by size as small proteins need longer to run through the column than bigger proteins (**Figure 8**).

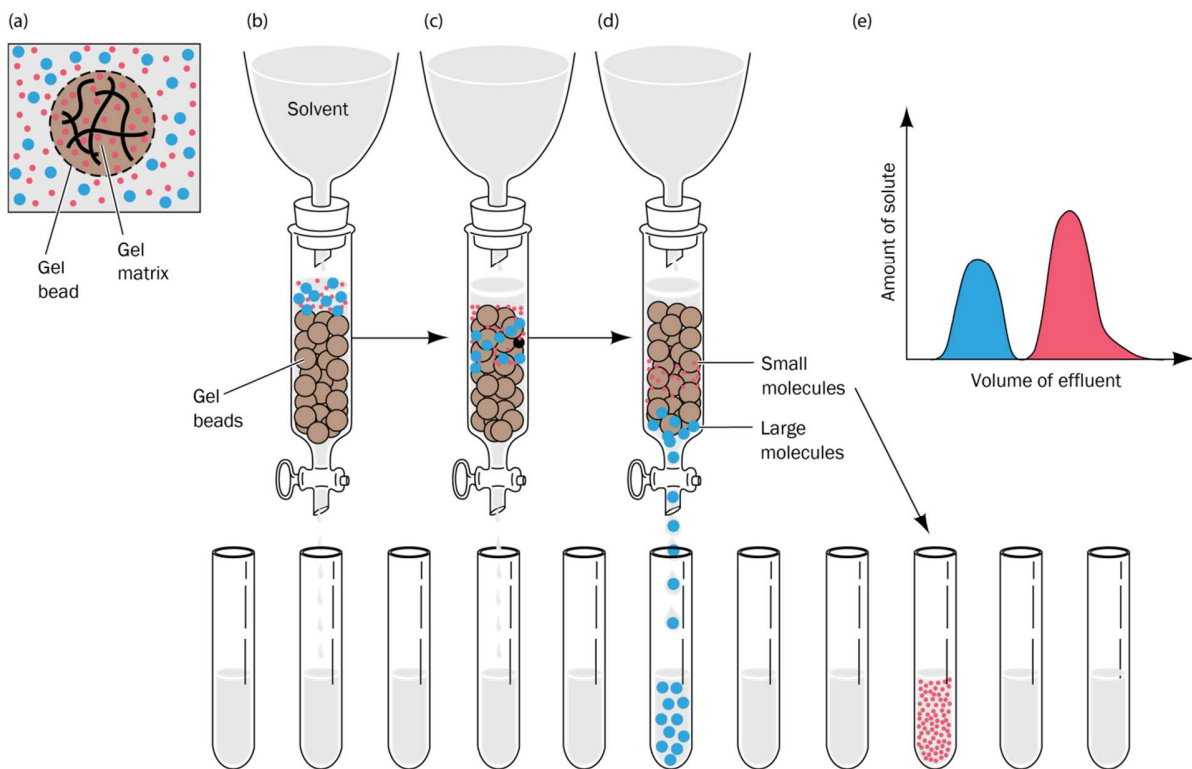


Figure 8: Principle of size exclusion chromatography

Proteins run through a column filled with Gel beads (a-d). Holes and an internal Gel matrix characterize these Gel beads. While running through the column bigger proteins (blue) which cannot enter the Gel matrix run through the column without delay and are eluted earlier than smaller proteins (red) who have to go through the holes of the Gel beads and Gel matrix. (b-e) Proteins can be divided by size and separated in different fractions through SEC as indicated in the tubes below. (b-e) A chromatogram shows the different fractions. (e) Picture taken from (149) page 139.

First, the proteins were concentrated to approximately 3-10 mg/ml with Amicon® Ultra centrifugal filters (Ultracel® - 3K). Before application to the column the concentrated proteins were centrifuged at 14 000 rpm for 5 min at 4 °C to decrease the amount of aggregated protein. The column (**Table 7**) was equilibrated with exchange buffer over night with the ÄKTA™ PURE (GE Healthcare) at 4 °C before loading approximately 500 µl of concentrated protein. During the run, the equilibrated machine measured the volume of buffer that went through its system together with data concerning the UV-absorbance of the fluid. The volume was important for later calculations of the MW. For this calculation the elution volume of each fraction was needed. Finally, the separated fractions were collected and then further analyzed by SDS-PAGE. After the run the column was cleaned with 0.5 M NaOH and the ÄKTA™ PURE system and columns were stored in H₂O with 0.01% sodium azide.

Additionally, a series of standard proteins was run under the identical conditions. The elution volume of each protein was used to calculate the partition coefficient (K_{av}) with the following equation (**Equation 3**).

$$K_{av} = \frac{V_e - V_o}{V_c - V_o}$$

Equation 3 : Partition coefficient

(V_o = column void volume, V_e = elution volume, V_c = geometric column volume, K_{av} = partition coefficient)

The calibration curve was then determined by the K_{av} of the standard proteins on the x-axis and the given logarithm of MW of the standard proteins on the y-axis. Size standard and Void volume were compiled using the Low Molecular Weight (LMW) Gel-filtration Calibration Kit (**Table 6**). Blue Dextran was used to determine the void volume.

3.2.4.4. STATIC LIGHT SCATTER COUPLED TO SIZE EXCLUSION CHROMATOGRAPHY

Another method to determine the molecular weight of proteins is static light scatter (SLS) coupled to SEC. Molecules and Particles can be characterized by the properties they show when they are hit with light. Molecules absorb the energy from the light and then reemit the energy in all directions (**Figure 9**). All SEC and SLS/SEC experiments were carried out in collaboration with Prof. Michaela Smolle (Department of Physiological Chemistry, Ludwig-Maximilian University) at the LMU BioPhysics Core Facility.

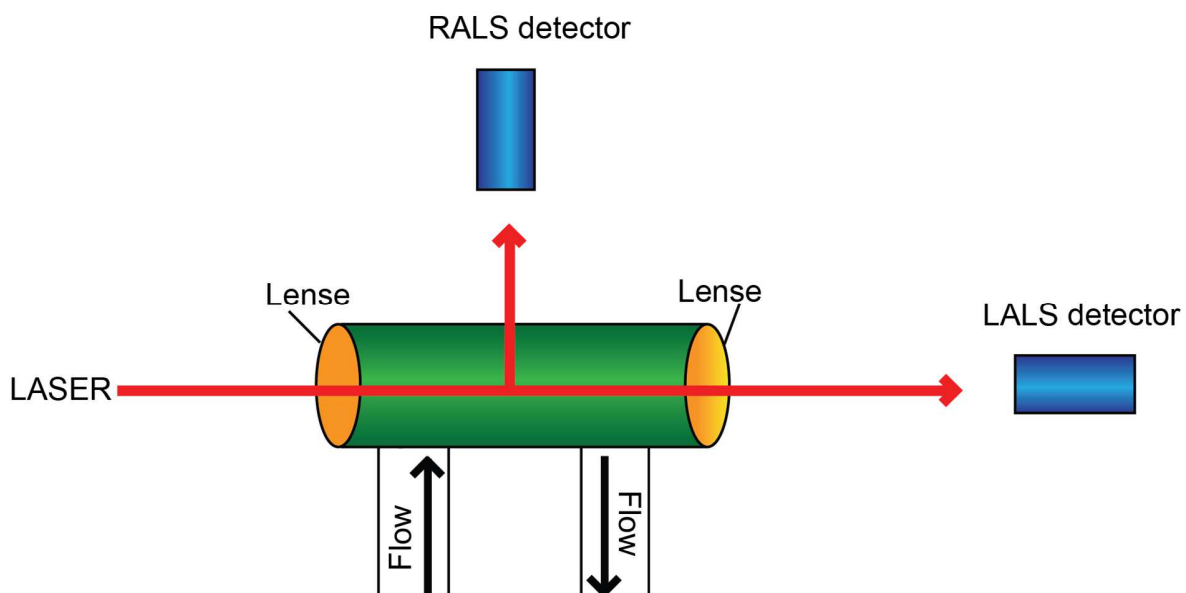


Figure 9: Principle of static light scatter detection

Directly after gel-filtration proteins run through the flow cell. Light from the laser enters the cell and is detected at 90° (RALS = Right-angle light scattering) and at a low angle for example 7° (LALS = low-angle light scattering). Figure adapted from (150).

The Rayleigh equation combines the size, MW and intensity of the scattered light and is the foundation of static light scatter analysis (**Equation 4**). The refractive index detector (RI) measures the concentration of proteins.

The Rayleigh equation is defined as:

$$\frac{KC}{R_{\theta}} = \left(\frac{1}{M} + 2A_2C \right) \frac{1}{P_{\theta}}$$

Equation 4: Equation of Rayleigh

(K = Optical constant, C = Concentration, M = Molecular weight, R_{θ} = Rayleigh ratio, A_2 = 2nd Virial coefficient, $P(\theta)$ = Shape (or form) factor)

With Optical constant K defined as:

$$K = \frac{4\pi^2}{\lambda_0^4 N_A} \left(n_0 \frac{dn}{dc} \right)^2$$

Equation 5: Optical constant K

(λ_0 = laser wavelength, N_A = Avogadro's number, n_0 = Solvent RI, dn/dc = differential RI increment)

With Rayleigh ratio R_{θ} defined as:

$$R_{\theta} = \frac{I_A n_0^2}{I_T n_T^2} R_T$$

Equation 6: Rayleigh ratio R_{θ}

(I_A = intensity of analyte (sample I – solvent I), n_0 = solvent RI, I_T = intensity of standard (toluene), n_T = standard (toluene) RI, R_T = Rayleigh ratio of standard (toluene))

With Shape factor P_{θ} defined as:

$$\frac{1}{P_{\theta}} = 1 + \frac{16\pi^2 n_0^2 R_g^2}{3\lambda_0^2} \sin^2 \left(\frac{\theta}{2} \right)$$

Equation 7: Shape factor P_{θ}

(n_0 = refractive index of the solvent, λ_0 = laser wavelength in a vacuum, R_g = Radius of gyration, θ = Measurement angle)

After acquiring all data - including the intensity of the scattered light- the MW of the sample can be calculated. The sTACI-long and sTACI-short proteins were applied to a Superdex 200 Increase 10/300 GL column and run through the ÄKTA PURE® to separate the different fractions by SEC. The same concentration that had been used previously for

SEC was added to the column, after determining and verifying the optimal amount for SLS analysis with a dilution series of bovine serum albumin fraction V (SIGMA-Aldrich® Co.LLC.). The range was about 1-3 mg/ml. The separated fractions were directly run through the OMNISEC REVEAL (Malvern) instead of being eluted in contrast to SEC. The whole OMNISEC REVEAL system was equilibrated prior with 1x storage buffer to the sample milieu. BSA was used to equilibrate the static light scatter system as standard protein for the later MW calculations. Some of the proteins from the Low Molecular Weight (LMW) Gel-filtration Calibration Kit were used as a positive control (**Table 6**).

3.2.4.5. CO-IMMUNOPRECIPITATION

Immunoprecipitation (IP) is used to concentrate and isolate antigens from a solution with the help of antibodies. Co-Immunoprecipitation (Co-IP) is an advancement of this method. Co-IP is used to analyze protein-protein interactions with the use of a target protein. The target protein is isolated and concentrated through IP. Proteins that interact with the target protein and form complexes can be detected after IP.

FLAG®-tagged beads (ANTI-FLAG® M2 Magnetic Beads, Sigma Aldrich) were resuspended and separated into 1.5 ml tubes. To remove the storage buffer the beads were washed five times with TBS Buffer using a magnetic separator (**Table 10**). The cell-lysates and supernatants were added sequentially in 1 ml steps and each time incubated for 1.5 h or overnight at 4 °C while rotating and shaking. Different amounts of protein were loaded between the supernatant and cell-lysates. Within the group of supernatants and the group of cell-lysates every condition had the same amount of protein applied. The supernatants were separated from the beads with a magnetic separator at the end of every incubation period and discarded. After application of the sample, the beads were washed five times with TBS Buffer to eliminate proteins that were not directly bound to the beads. The elution was done under acidic conditions by incubation with glycine (1 M pH 3) for 20 min at 56 °C. To preserve activity of the proteins the eluates were neutralized with Tris Buffer (1 M Ph 9) (**Table 10**). (**Figure 10**)

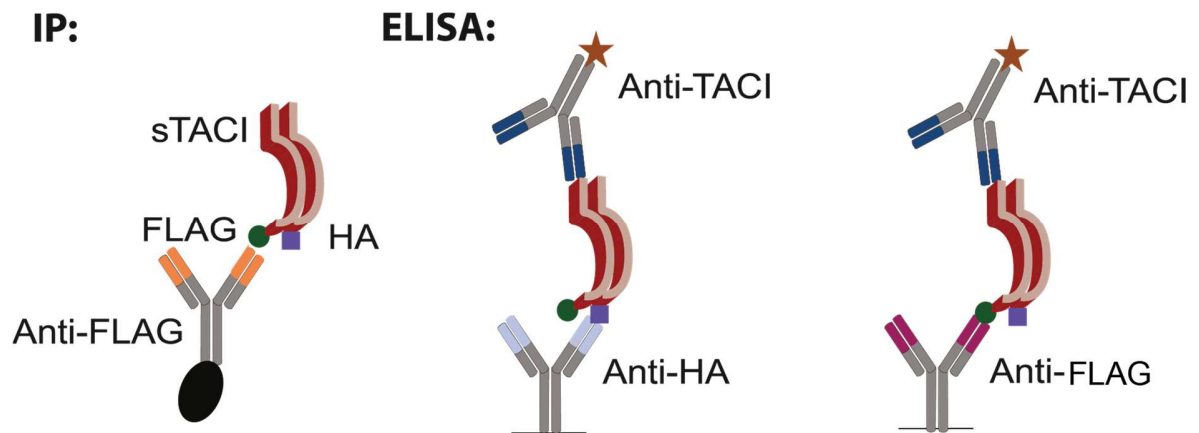


Figure 10: Principle of Co-Immunoprecipitation

FLAG[®]-coated beads are used to capture FLAG[®]-tagged target proteins. The TACI isoforms either have a FLAG[®]- (green dot) or HA-tag (blue square) added to the N-terminal side. The Anti-HA ELISA after immunoprecipitation shows if proteins interact and if the HA-tagged proteins were immunoprecipitated. Figure adapted from (93).

The IP and pre IP samples were tested with TACI, BCMA and anti-FLAG[®] ELISA as a control for the transfection and success of IP. The Anti-FLAG[®] ELISA was used to test the IP. The plate was coated with Anti-FLAG[®] M2 Antibody (dissolved in PBS at a concentration of 5 µg/ml) overnight at 4 °C (**Table 20**). The interaction was tested with anti-HA ELISA. The plates got coated with a HA antibody as capture antibody (5 µg/ml) and incubated over night at 4 °C (**Table 20**). Then the TACI DUO set or BCMA ELISA protocol was followed starting with the detection antibody step.

3.2.5. FUNCTIONAL TESTS

3.2.5.1. BINDING ELISA

A sandwich ELISA called binding ELISA was used to determine the affinity of the sTACI proteins to the Ligands BAFF and APRIL (**Figure 11**). The affinity of the proteins for BAFF and APRIL was compared by calculating the equilibrium dissociation constant (K_D) value. Generally, a small K_D indicates a high affinity of a protein to its ligand.

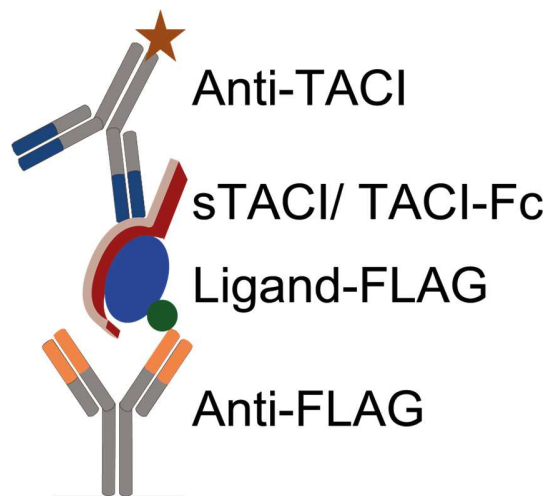


Figure 11: Principle of binding ELISA

The binding ELISA is a sandwich ELISA. The plate was coated with anti-FLAG antibody over night at 4 °C. The first incubation step is with a FLAG-tagged Ligand. The next step consists of application of sTACI-long, sTACI-short or TACI-Fc. To assess whether sTACI was able to bind to the FLAG-tagged Ligand the detection antibody of the TACI Duo set ELISA was used. The rest of the assay followed the normal TACI Duo set ELISA protocol. Figure was taken from (93).

For the Binding ELISA the plate was coated with Anti-FLAG[®] M2 Antibody (dissolved in PBS at a concentration of 5 µg/ml) overnight at 4 °C. After three washing steps the plate was blocked with Reagent Diluent (**Table 10**) for at least 1 h at room temperature. Then, BAFF-FLAG[®] (R&D Systems) or APRIL-FLAG[®] (mouse: AdipoGen or human: SIGMA-Aldrich[®] Co.LLC) were added in a concentration of 100 ng/ml and incubated for 2 h at room temperature. A dilution series of both sTACI isoforms was prepared, added to the plate and then incubated for 2 h at room temperature. After application of the dilution series, the TACI Duo set ELISA protocol was followed.

3.2.5.2. TEST OF DECOY FUNCTION WITH NFκB ASSAY

Ligand-receptor interactions can be assessed with reporter cell assays, like the NFκB assay. In NFκB assay activation of a receptor leads to intracellular NFκB pathway induction which can be detected, in this case with luciferase (151) (**Figure 12**).

The ability of a soluble receptor to decrease luciferase activation by disabling the ligand from binding to the cell can be measured in the form of an inhibition assay. The half maximal inhibitory concentration (IC_{50}), a value indicating the potency of a decoy receptor, was determined. Small IC_{50} values indicate good inhibition function of the substrate. The IC_{50} gives the concentration of a substrate that leads to a 50% decrease of the normal activation signal.

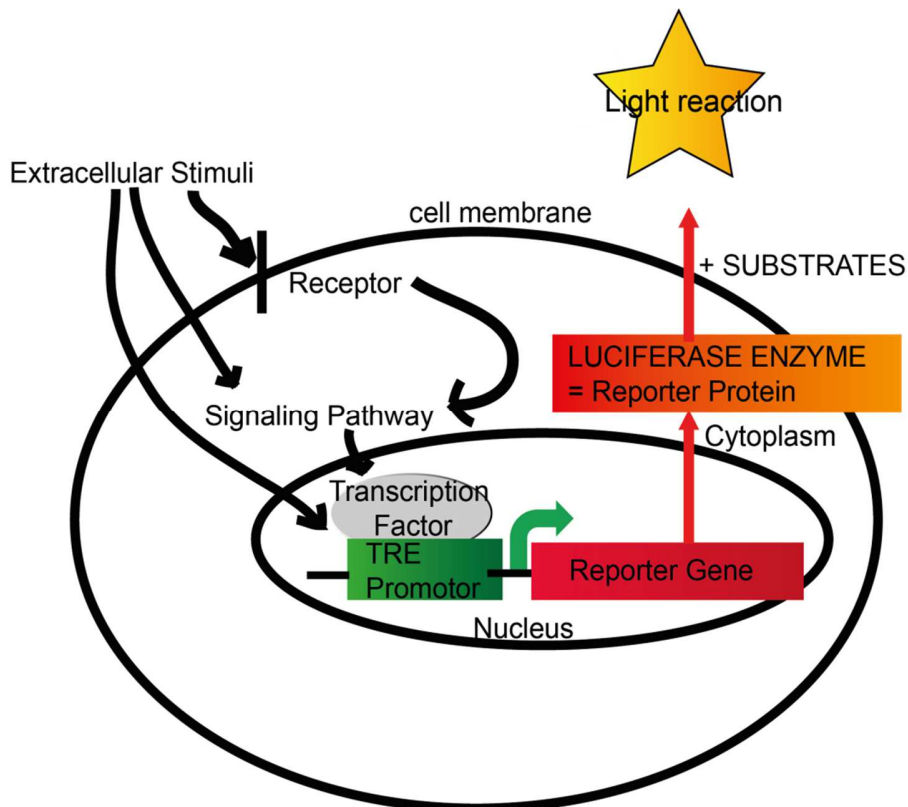


Figure 12: Principle of NFκB assay

After extracellular stimulation an intracellular cascade leads to synthesis of a TRE promoter dependent reporter protein. The reporter protein can be visualized by adding for example Luciferin and ATP if the reporter protein is luciferase. Adapted from (152).

In this assay NFκB activation was detected with the Firefly-Luciferase which is under control of NFκB transcriptional response element (TRE). In order to control for varying cell numbers, active Renilla-Luciferase was co-transfected constitutively, which is under control of the CMV promoter. To detect the reporter proteins a substrate mix of Luciferin and ATP (Biozym Scientific GmbH) was used for Firefly-Luciferase and coelenterazine (Promega) for Renilla-Luciferase. Full-length BCMA was used as a receptor for the ligands.

A dilutions series of sTACI was prepared 8 h after transfection of HEK293T cells with BCMA, Renilla-luciferase and Firefly-luciferase. APRIL (AdipoGen) or BAFF (R&D Systems) were added to the dilution series in a concentration of 100 ng/ml. The sTACI/ligand mixture was incubated in a heat shaker at 37 °C at 300 rpm for 15-30 min and then added to the transfected cells while discarding the old medium. Finally, 17 h later the NFκB activation was measured after lysing the cells. The lysed cells were pipetted into Corning™ 96-Well Solid White Polystyrene Microplates and the substrate mix for either Firefly-Luciferase or Renilla-Luciferase was added. Afterwards, luminescence was detected and read out with Perkin Elmer Victor2 1420 Multilabel Counter.

3.2.5.3. FLOW CYTOMETRY ASSAYS

Flow cytometry can be used to quantify and characterize the phenotype of cells. Cells are run cell by cell in a liquid medium by a laser to generate information about the size and complexity of the cells by assessing the scattering of light around them. The forward scatter generates information about the size and volume of the cell. The sideward scatter generates information about the granularity. Furthermore, the cells were characterized with fluorescence labeled antibodies. These antibodies recognize either a specific surface structure (direct detection) or an already bound antibody (indirect detection). The surface structures in this thesis were indirectly labeled with Anti-TACI or Anti-FLAG® antibodies, before detection with a PE labeled antibody (**Table 21**). When hit with a laser, a fluorescence signal is emitted after excitation of the fluorochrome of the antibody and can be detected by the flow cytometer. Several fluorochromes can be chosen for one measurement if the wavelength spectra of the emission differ. For this

thesis, only one fluorochrome was used for the characterization of all cells (PE) together with an indicator (TO-PRO[®]-3 Iodide (Invitrogen)) of dead cells (**Table 22**). The BD FACSVerser[™] flow cytometer (BD Biosciences) was used to generate the data in combination with the FlowJo software (BD Biosciences) which was used to analyze all data. Flow cytometry was used to assess the expression of membrane-bound TACI proteins after transfection of HEK293T cells and to test the membrane-bound binding properties of TACI isoforms to BAFF and APRIL (**Figure 13**).

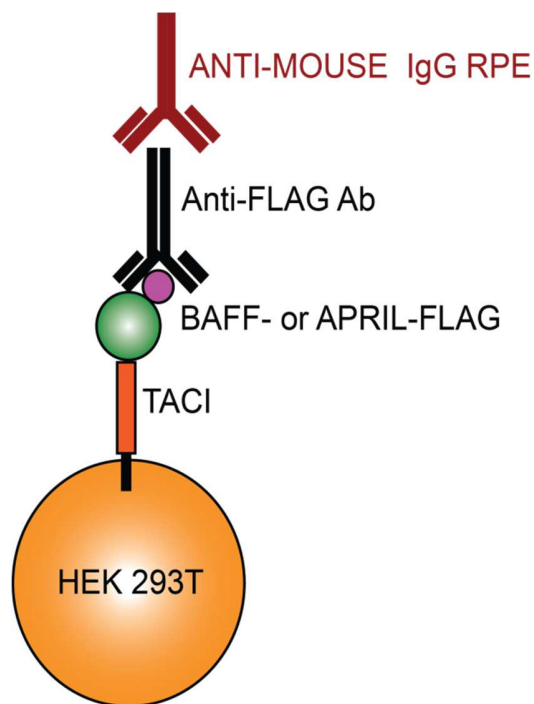


Figure 13: Principle of Binding flow cytometry

24 h after transfection with TACI-long or TACI-short the cells were either directly tested for surface expression or incubated for 3 h with BAFF- or APRIL-FLAG[®] to analyze the binding of the surface TACI isoforms to BAFF and APRIL. BAFF- or APRIL-FLAG[®] was added at a concentration of 100 ng/ml. The cells were transferred onto flow cytometry plates. All centrifugation steps were executed at 400 g for 5 min at 4 °C. The cells were centrifuged and the supernatants discarded. To remove the medium, two further washing steps with PBS containing 1% BSA were applied. The primary antibody was added and

incubated for 30 min on ice protected from light at a concentration of 1 $\mu\text{g/ml}$ (for both primary antibodies) (**Table 21**). Three further washing steps were executed to wash the primary antibody off and the secondary antibody (**Table 21**) was added and incubated for 30 min at 4 °C at a concentration of 5 $\mu\text{g/ml}$ while protected from light. The secondary Ab was then removed with three washing steps. TO-PRO®-3 Iodide (Invitrogen) (diluted 1/4000 in PBS) was used to assess the amount of dead cells.

3.2.6. STATISTICAL ANALYSIS

Prism Software (GraphPad) was used for all statistical and analytical analysis in this thesis with the only exception of the determination of MW by SEC. There, Excel was used to determine the calibration graph and MW values resulting from the K_{av} of the eluted proteins. Statistical significance for the expression assay, binding ELISA, and NF κ B reporter assay was assessed using unpaired two-tailed t-test with or without Welch's correction or normal one way ANOVA. The K_D and IC_{50} were calculated using specific programs that are already designed for these applications as part of the Prism Software. For multiple results as part of an experiment the arithmetic mean was calculated and is shown in the graphs as the main value. To show the varying distribution of values around the arithmetic mean in the graphs, the standard error of the mean (SEM) was determined.

4. RESULTS

4.1. CHARACTERIZATION OF SOLUBLE TACI ISOFORMS

4.1.1. CLONING AND RECOMBINANT PRODUCTION OF sTACI-LONG, sTACI-SHORT AND sTACI-SHORT (W-68-154)

First, the plasmids for sTACI-long and sTACI-short were cloned (**Figure 15**). The sequence was chosen according to two different studies (93, 146). sTACI-long has two cysteine rich domains (CRDs) (CRD1+CRD2), while sTACI-short has only one (CRD2) (**Figure 14**).

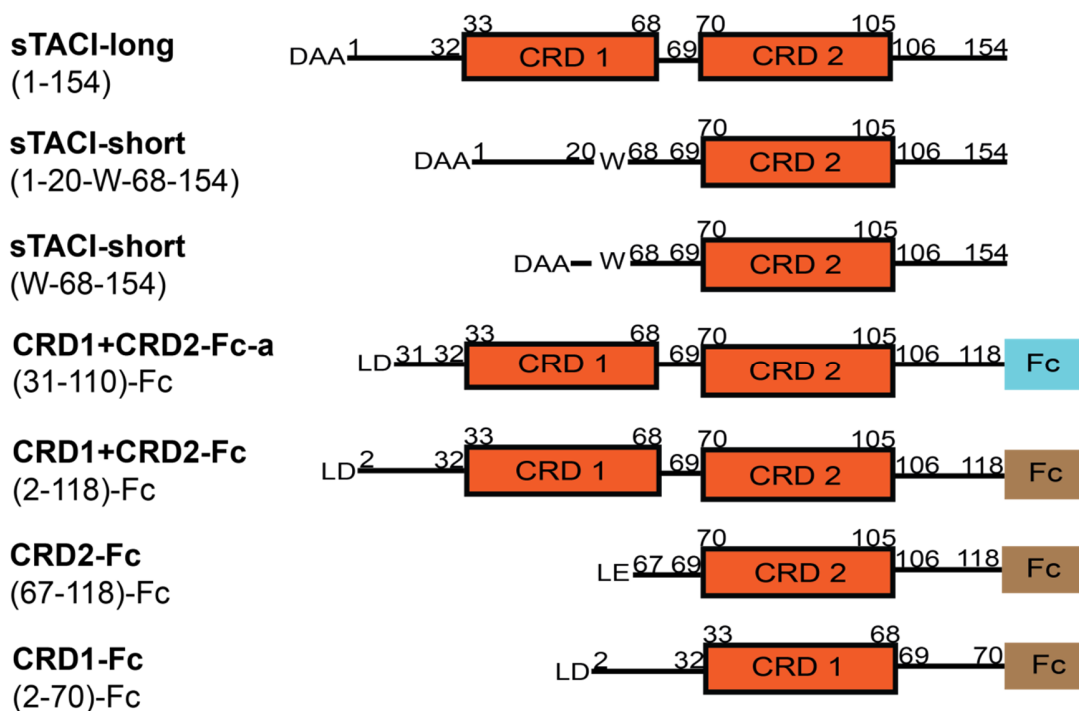


Figure 14: Illustration of different TACI constructs

sTACI-long, sTACI-short and sTACI-short (W-68-154) were produced recombinantly. The Fc constructs were provided by Pascal Schneider (University of Lausanne, Switzerland). The numbers below the name of the construct indicate the amino acid sequence of each construct. The illustration next to it shows the CRDs of each construct, the amino acid sequence and the addition of Fc if present. CRD1+CRD2-Fc-a, which is an atacept analog, was designed to have mutations in its Fc part so that FcγR binding and complement activation is prevented. The difference is illustrated by a light blue layered Fc for CRD1+CRD2-Fc-a in comparison to the brown layered Fc of the other TACI-Fc. The illustrations are adapted from (122, 146).

Previous constructs of TACI from other groups were missing the first 20 to 30 amino acids of the sequence on the N-terminal side and started directly at the CRDs (140). An ataccept analog variant (CRD1+CRD2-Fc-a) and other TACI-Fc constructs were provided by Pascal Schneider for this thesis (University of Lausanne, Switzerland). sTACI-short (W-68-154) which was designed to miss the first 20 amino acids on the N-terminal was developed to test if these 20 amino acids influence the binding affinity. The resulting protein sequences of sTACI-long, sTACI-short, and sTACI-short (W-68-154) are illustrated in **Figure 14**. The sequences of the TACI-Fc constructs are shown in comparison.

During the cloning process a His6-tag was added C-terminal for later affinity purification. The constructs contained the signal peptide of Ig-kappa N-terminal to ensure protein secretion. The resulting plasmids for sTACI-long and sTACI-short are depicted in **Figure 15**.

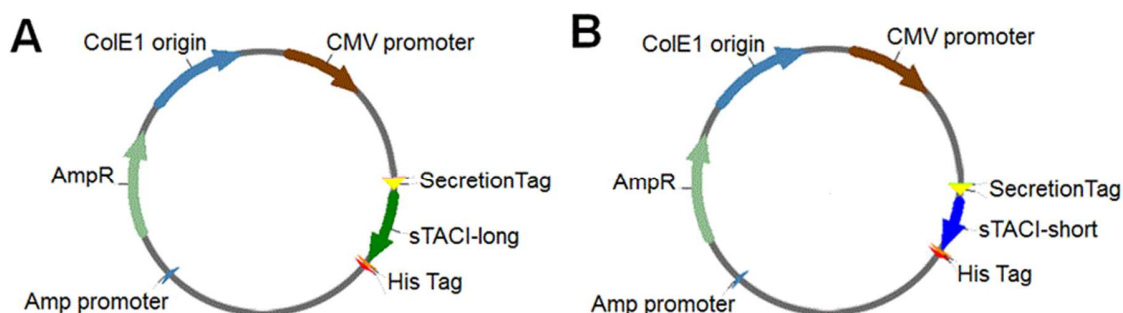


Figure 15: Plasmids of sTACI-long (A) and sTACI-short (B)

All three sTACI constructs were expressed in eukaryotic HEK293.EBNA cells and then affinity purified with HisTrap columns and a gradient using Imidazole essentially as published (153). The signal peptide of Ig kappa chain was cleaved intracellularly before secretion. The different steps of protein purification are indicated in small letters above the UV chromatogram in **Figure 16 A**. After purification, the eluted protein fractions were analyzed by Coomassie stained SDS-PAGE. Examples of after purification screenings of sTACI-long, sTACI-short, and sTACI-short (W-68-154) are shown in **Figure 16 B, C**, and

D. Fractions from fourteen purifications were pooled together for sTACI-long, fractions from five purifications for sTACI-short and fractions from three purifications for sTACI-short (W-68-154). The results from functional tests are not dependent on a single purification. The pooled samples were dialyzed against storage buffer and stored at -80 °C.

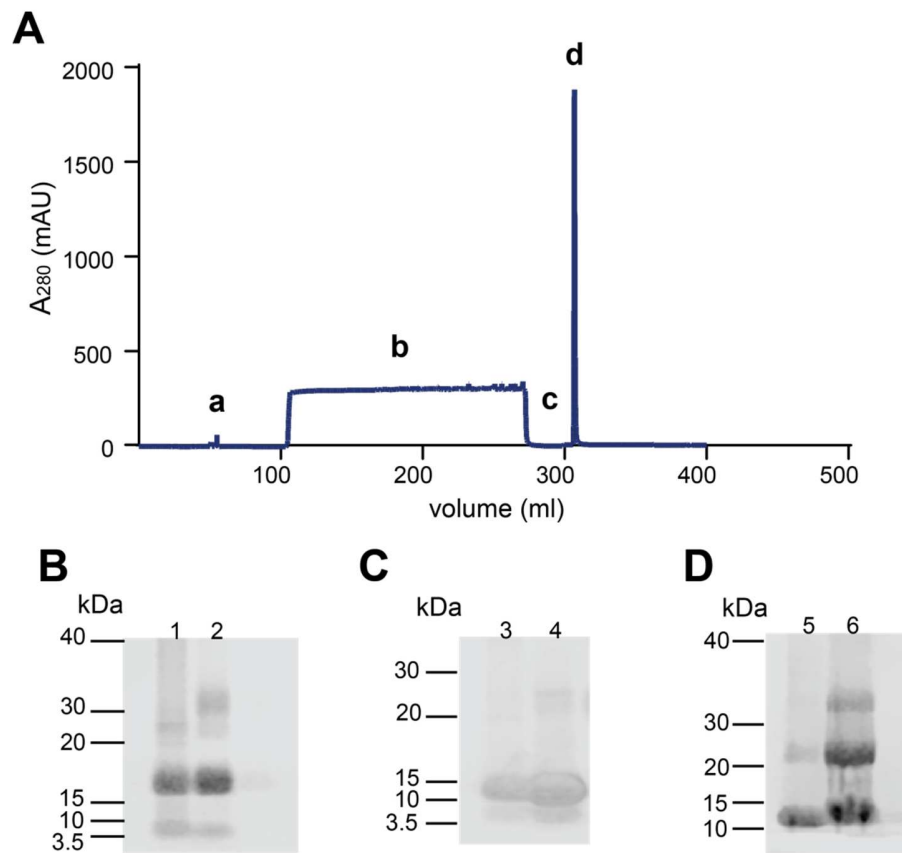


Figure 16: Affinity purification of sTACI variants

(A) UV chromatogram of a purification of sTACI-short (W-68-154). The different steps of affinity purification consist of the washing and equilibration of the column (a), the loading of the protein (b), an additional washing step to remove unspecifically bound proteins (c) and a final elution of the protein from the column (d). (B-D) Coomassie staining of SDS-PAGE of eluted fractions from affinity purification from 1L Hek293.EBNA cells (B) for sTACI-long, (C) sTACI-short and (D) sTACI-short (W-68-154). The numbers 1-6 indicate different fractions of the eluted proteins.

4.1.2. OLIGOMERIZATION OF sTACI

sTACI-long (**Figure 16 B**) and sTACI-short (W-68-154) (**Figure 16 D**) appeared at molecular weights suggesting that the preparations contain in addition to the monomeric form also oligomers. sTACI-short (**Figure 16 C**) showed these signs of oligomerization only in high amount of purified protein. For sTACI-long, the reducing agent DTT, but not heat denaturation for 5 min at 95 °C, was able to break the bond or denature the protein so that it appeared in its monomeric state (**Figure 17 A**). Furthermore, DTT was added to sTACI-short to study whether the amount of sTACI-short would increase as possible higher molecular oligomers would break. sTACI-long was used as positive control for DTT treatment and as a test if reduced and non-reduced sTACI-long could be detected by the same antibody in Western blot (**Figure 17 B**). DTT treatment had no effect on sTACI-short (**Figure 17 B**), while the dimers of sTACI-long turned onto monomers. Both sTACI-long monomers and dimers could be detected by our Western blot detection antibody. sTACI-long and sTACI-short detection decreased after DTT treatment (**Figure 17 B**).

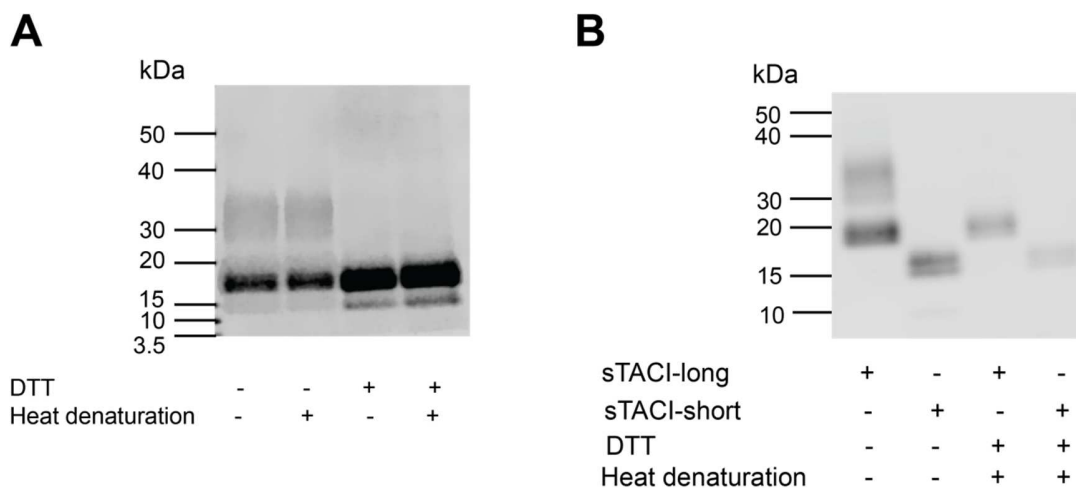


Figure 17: Analysis of stability of oligomerization of sTACI-long and sTACI-short

(A) sTACI-long was treated with heat-denaturation at 95 °C for 5 min, DTT or both, and compared to non-treated sTACI-long. Coomassie stained SDS-PAGE was used for analysis. (B) sTACI-long and sTACI-short were either analyzed without any treatment or with heat denaturation and DTT by Western blot using the mAb anti-TACI TACI/TNFRSF13B (Clone 165609).

It was previously proposed that divalent-ion/His6-tag interactions may cause oligomerization in recombinant purified proteins (84). Nickel ions that dissolved from the

purification column and passed to the eluted fragment, could cause artificial aggregates. EDTA is highly potent at forming chelates with divalent ions. To further investigate these findings, an interaction between the His6-tag of the purified sTACI-short (W-68-154) and possible eluted Nickel ions from the purification column was tested by EDTA assay. This assay was performed with sTACI-short (W-68-154) because we observed several higher oligomers for sTACI-short (W-68-154) (**Figure 16 C**) in Coomassie stained SDS-PAGE. sTACI-short (W-68-154) did not form new aggregates after higher molecular weight bonds were broken by DTT (**Figure 18**). There was no effect of EDTA on oligomerization in non-reducing conditions. After reduction with DTT the protein stayed in its monomeric state. Heat denaturation alone had no impact on oligomerization similar to sTACI-long.

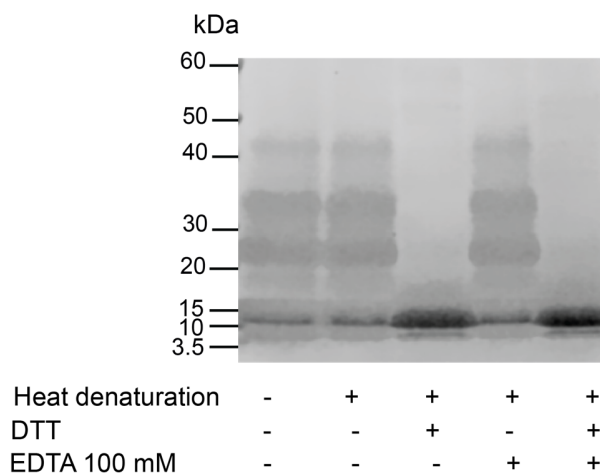


Figure 18: Analysis for possible artificial oligomerization of sTACI-short (W-68-154)
 Coomassie stained SDS-PAGE of sTACI-short (W-68-154). DTT was added to put sTACI-short (W-68-154) into its monomeric state. EDTA was then applied to sequester possible Nickel ions that were eluted from the HisTrap column. sTACI was incubated with DTT and/or EDTA for 1-2 h at room temperature to give Nickel ions the time to rebuild high molecular aggregates with the His6-tags of sTACI-short (W-68-154).

4.1.3. N-LINKED GLYCOSYLATION OF sTACI-LONG AND sTACI-SHORT

N-linked glycosylation was predicted for both sTACI isoforms at amino acid 128 (N) by Uniprot (28). The sequence pattern N-X-T/S indicates N-linked glycosylation sites which are glycosylated with a probability around 50% (154-157). This sequence is one time present within the sTACI sequence for both isoforms as illustrated in **(Figure 20)**. Posttranslational modifications such as sugars can disturb later evaluation of the proteins by mass spectrometry. Therefore and additionally to test the nature of the secreted proteins, a PNGase F assay was performed. PNGase F is an amidase that can cleave N-linked oligosaccharides from proteins (148). As a positive control, hMOG, which is known to be N-linked glycosylated, was used (158). PNGase F reduced the MW of hMOG, but not of TACI-long or TACI-short **(Figure 19)**. Thus, our sTACI-long and sTACI-short were not N-linked glycosylated.

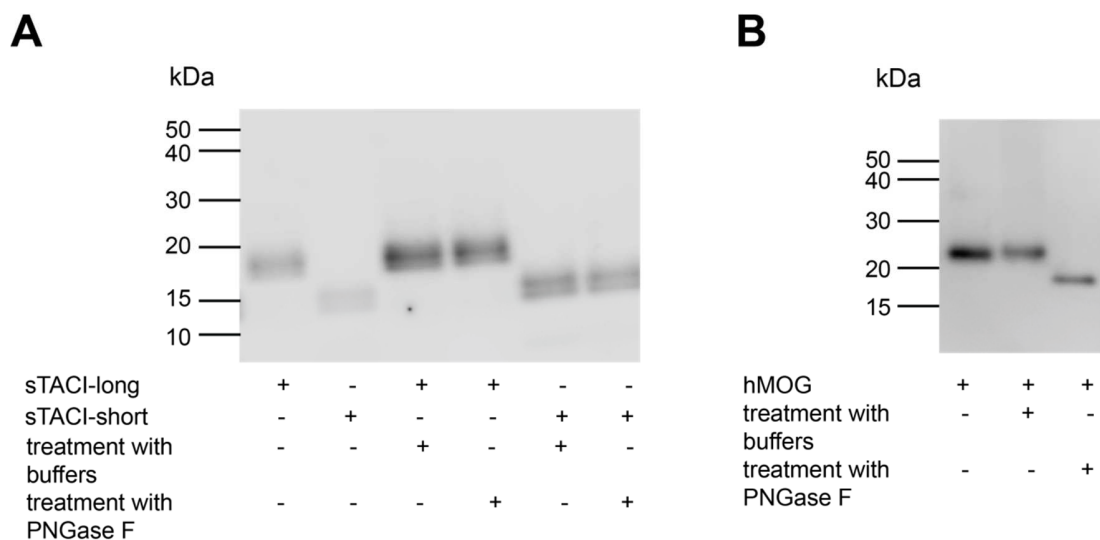


Figure 19: Analysis of glycosylation of sTACI-long, sTACI-short and hMOG
sTACI-long and sTACI-short (A) and as a control hMOG (B) were treated with the enzyme PNGase F as indicated. Subsequently, the proteins were separated by SDS-PAGE and detected by Western blot using the mAb anti-TACI TACI/TNFRSF13B (Clone 165609) for TACI (A) and murine anti-MOG antibody 8.18.c5 (B).

4.1.4. MASS SPECTROMETRY AND N-TERMINAL SEQUENCING OF sTACI-LONG AND sTACI-SHORT

Analysis of the recombinant proteins sTACI-long and sTACI-short by gel electrophoresis showed that both recombinant proteins appeared at the expected molecular weight (**Figure 20 A**). We noted that they did not appear as a single band, but rather as a double band. Additionally a smaller band appeared in sTACI-short preparations that could only be detected in Coomassie staining (**Figure 20 A, right part**). To clarify the identity of the different bands in our sTACI preparations mass-spectrometry and N-terminal sequencing were applied (**Figure 20 B-D**). This showed that all closely related bands were TACI.

The upper bands of both isoforms (sTACI-long (a) and sTACI-short (c)) largely consisted of the whole protein (**Figure 20 B-C**). The lower bands missed the first 15 amino acids of the sequence on the N-terminal side. The 7 kDa form of sTACI-short was missing the first 15 amino acids of the sequence on the N-terminal side and additionally 19 amino acids on the C-terminal side (**Figure 20 D**). This suggests that the 7 kDa form might represent a degradation-product. Full length sTACI-short is later on referred to as sTACI-short (1-20-W-68-154) and the 7 kDa variant as sTACI-short (16-20-W-68-135). The changes of sequence in sTACI-short (16-20-W-68-135) did not affect the CRD2 which is responsible for high affinity binding to the ligands BAFF and APRIL. Thus, these changes were not predicted to have an effect on the functionality of the protein within the BAFF/APRIL system.

Several additional sequences were found while analyzing the N-terminal side of sTACI-long and sTACI-short (**Figure 20 B-D**). These variants of the N-terminus could largely be attributed to Furin cleavage. Furin is a major protease of the secretory pathway primarily located at the Golgi apparatus. Furin cleaves proteins after basic residues in motifs such as Arg-X-X-Arg, Arg-X-Lys/Arg-Arg or Lys/Arg-X-X-X-Lys/Arg-Arg (159). Such motifs are also present two times within the first 20 amino acids of the sequence of TACI on the N-terminal side (**Figure 20**). The additional N-terminal sequence variant of sTACI-short could not be attributed to a specific protease yet.

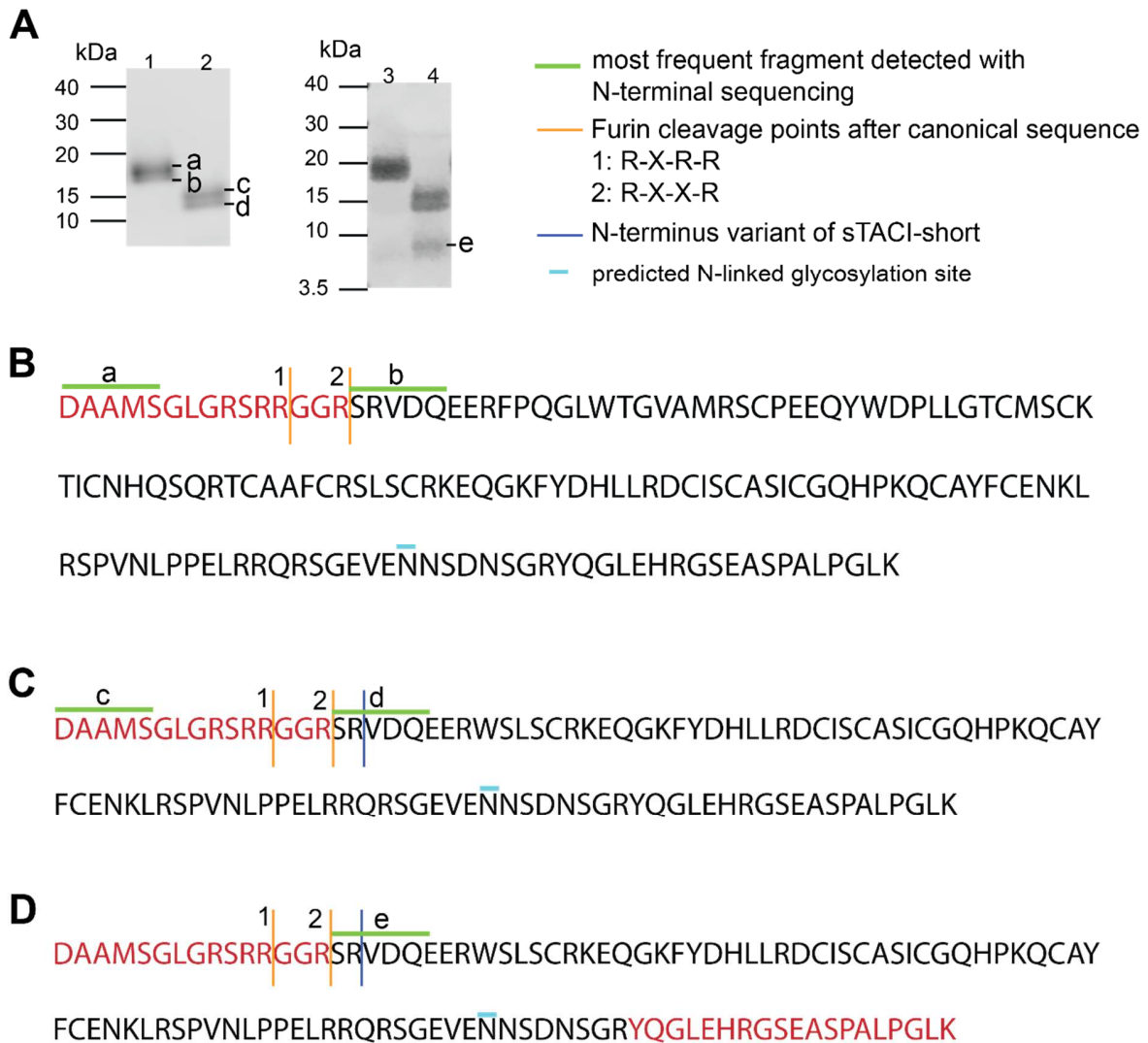


Figure 20: Analysis of recombinant sTACI-long and sTACI-short by Western blot, Coomassie staining, N-terminal sequencing and mass spectrometry

(A) sTACI-long (lane 1 and 3) and sTACI-short (lanes 2 and 4) were separated by SDS-PAGE and visualized by Western blot (left) or Coomassie staining (right). Band e could not be detected by Western blot (A). The bands indicated with a-e were cut and as displayed in (B-D), analyzed by N-terminal sequencing and after digestion with trypsin by mass-spectrometry (Reinhard Mentele). The amino acid sequence obtained by mass-spectrometry is given in black letters. The parts of TACI-long (A) and TACI-short (C, D) that were not detected by mass-spectrometry are given as red letters. The sequences most frequently obtained by N-terminal sequencing of the bands a-e are indicated with a green line. Cleavage points that can be attributed to Furin are indicated by an orange line and the number next to it shows the canonical sequence which is the basis for that particular cleavage. An additional N-terminus of a variant included in sTACI-short is indicated by a blue line. The light blue line indicates a predicted site for N-linked glycosylation.

4.1.5. SIZE EXCLUSION CHROMATOGRAPHY OF sTACI-LONG AND sTACI-SHORT

Size exclusion chromatography (SEC/gel-filtration) was performed to further assess the oligomerization of sTACI-long and sTACI-short. The proteins were run through a column that contained a specific matrix which led to separation of each fraction according to size. Directly after the column the different fractions were detected by a UV spectrometer (**Figure 21 A+B**) and analyzed for separation by Coomassie stained SDS-PAGE (**Figure 21 C+D**).

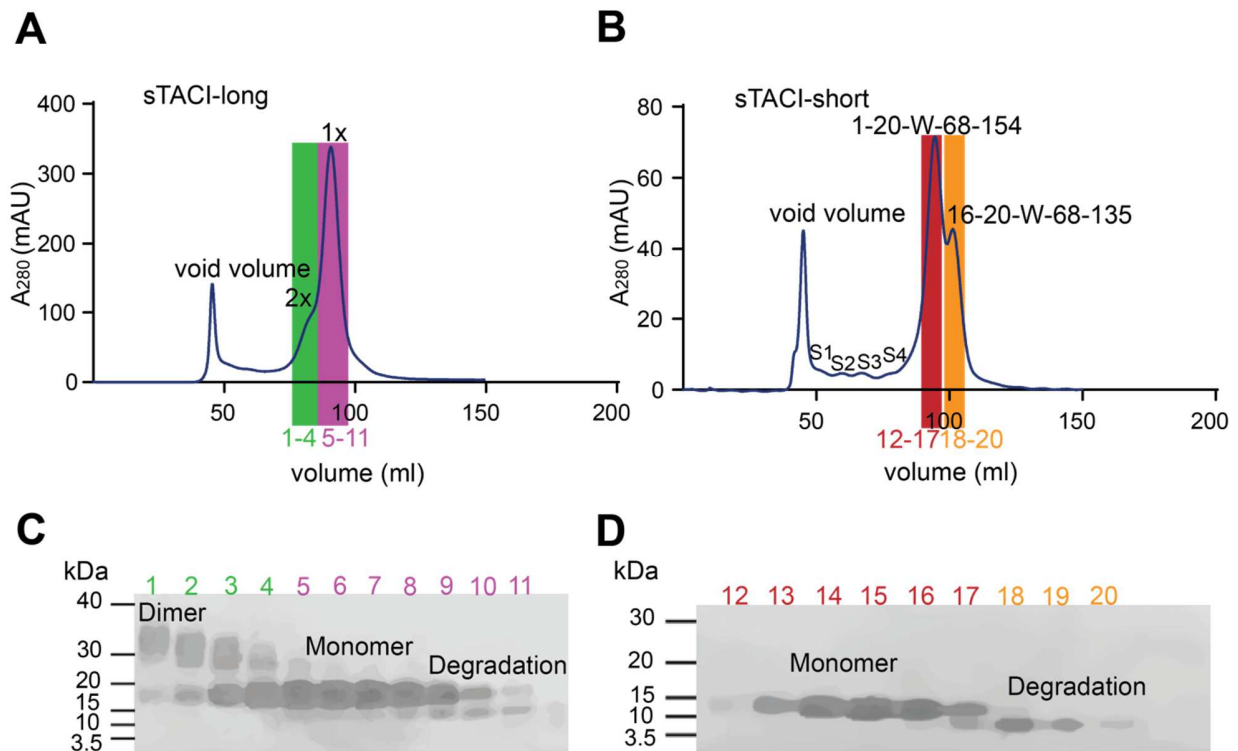


Figure 21: Analysis of Oligomerization of sTACI-long and sTACI-short by SEC

(A and B) sTACI-long (A) and sTACI-short (B) were analyzed by SEC and the resulting UV-chromatograms are shown. The sTACI-long monomer is indicated by the inscription 1x and a purple layer and the sTACI-long dimer by 2x and a green layer (A). The void volume is represented by the first peak in both UV-chromatograms (A and B). sTACI-short (1-20-W-68-154) is indicated by the inscription (1-20-W-68-154) and a red layer and sTACI-short (16-20-W-68-135) by (16-20-W-68-135) and an orange layer. The higher grade oligomers of sTACI-short are represented by S1-S4. (C and D) Coomassie stained SDS-PAGE of separated fractions after SEC of sTACI-long (C) and sTACI-short (D). The numbers below the x-axis in A and B indicate the fractions that were used for Coomassie staining in C and D.

sTACI-long appeared as a dimer and monomer in SEC (**Figure 21 A**). sTACI-short showed in addition to the monomeric sTACI-short (1-20-W-68-154) and sTACI-short (16-20-W-68-135) small amounts of higher oligomers (**Figure 21 B**). Furthermore, the dimer and the monomer of sTACI-long and sTACI-short (1-20-W-68-154), sTACI-short (16-20-W-68-135), and sTACI-short higher oligomers were separated of by SEC (**Figure 21 C+D**). Most fractions could be separated accurately except for the sTACI-long dimer. Pooled fractions of the sTACI-long dimer were a mixture of dimer and monomer with an enrichment of the dimer fraction. These fractions were pooled and stored at -80 °C for later used for functional evaluation.

Determination of the MW of the fractions S1-S4 of sTACI-short with SEC standard curve (data not shown) showed that these fractions most likely represent higher oligomers of sTACI-short (S4 = 3x sTACI-short, S3 = 6x sTACI-short, S2 = 9x, sTACI-short, S1 = 12x sTACI-short). This view is also supported by ELISA and Coomassie stained SDS-PAGE. The fractions were concentrated and shown to be TACI by hTACI ELISA (**Figure 22 A**). Additionally, the concentrated fraction of S3 could be detected at the expected MW weight of 6x sTACI-short (around 70 kDa) in Coomassie stained SDS-PAGE (**Figure 22 B**). These findings suggest that sTACI-short oligomerizes in small amounts. This is in concordance with our sTACI-short variant sTACI-short (W-68-154) that showed signs of higher molecular weight oligomers in Coomassie stained SDS-PAGE directly after affinity purification (**Figure 18**).

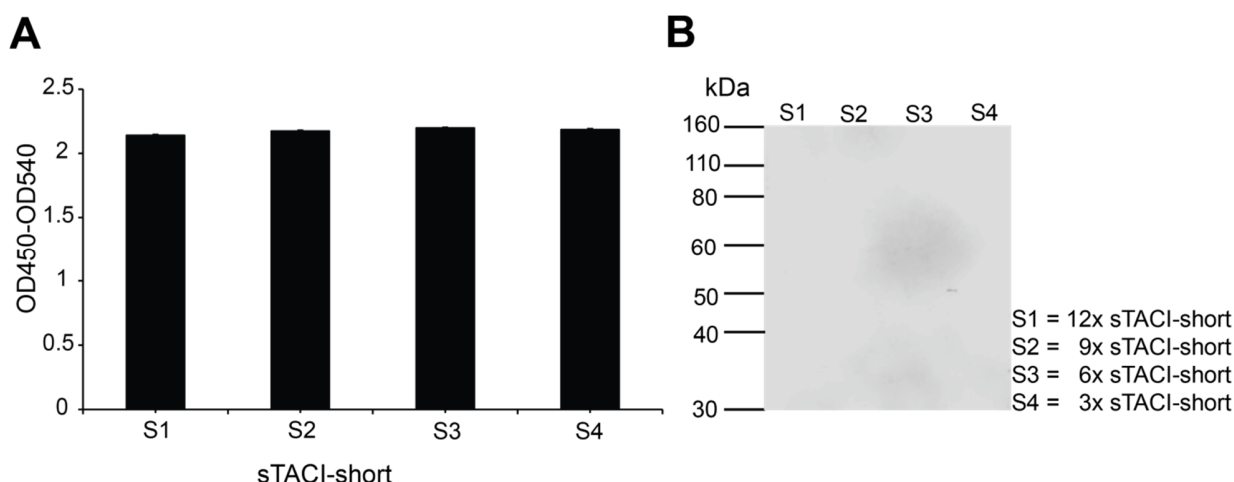


Figure 22: Analysis of small SEC peaks (S1-S4) of sTACI-short

(A) The fractions S1-S4 (see **Figure 21 (B)**) were concentrated and then measured by hTACI ELISA. (B) The concentrated samples were applied to Coomassie stained SDS-PAGE.

4.1.6. DETERMINATION OF MOLECULAR WEIGHT OF sTACI-LONG AND sTACI-SHORT

The MW of the monomer of sTACI-long was calculated at 17.4 kDa and sTACI-short (1-20-W-68-154) at 12.2 kDa by an online tool (ExPASy). The dimer of sTACI-long was approximated through Coomassie stained SDS-PAGE around 34 kDa and sTACI-short (16-20-W-68-135) at 7 kDa.

At first, we determined the MW of both sTACI isoforms by generating a SEC standard curve (**Figure 23**). With this method the sTACI-long monomer was calculated at 29.9 kDa and the sTACI-long dimer at 58.3 kDa. sTACI-short (1-20-W-68-154) was determined at 19.9 kDa and sTACI-short (16-20-W-68-135) at 9.2 kDa.

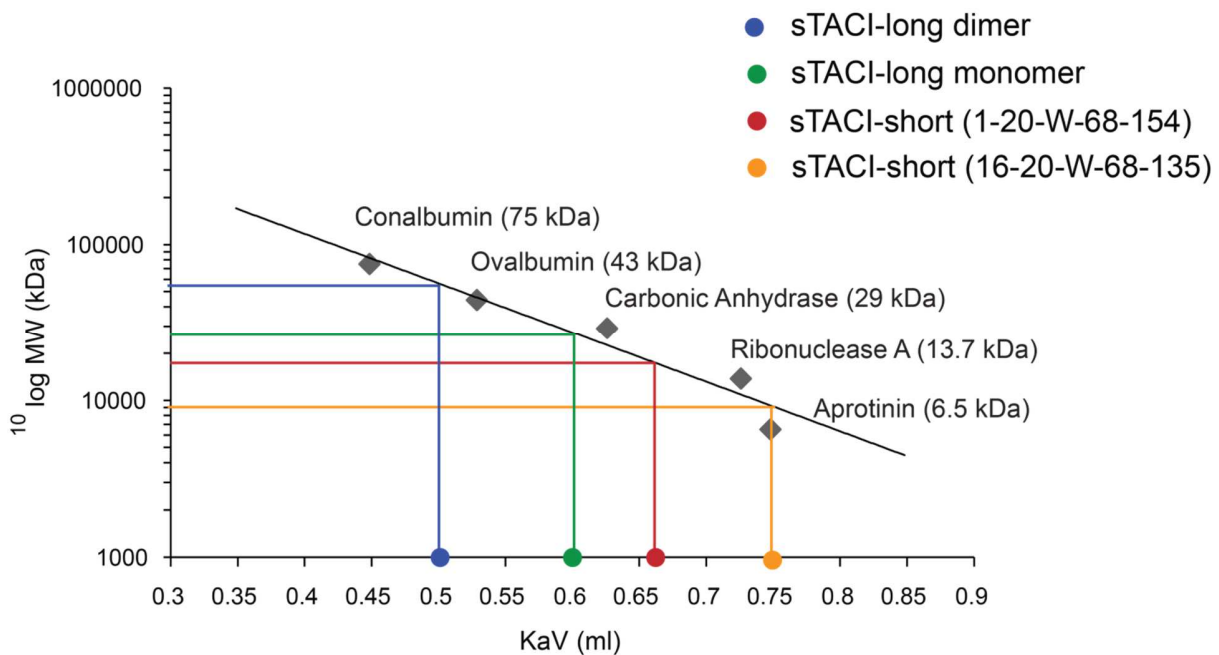


Figure 23: Molecular weight determination using SEC standard curve

Proteins of known molecular weights were used to generate a standard curve for the HiLoad 16/60 Superdex 75 pg column. The standard curve was generated by plotting the MW in logarithmic scale on the y-axis against the KaV on the x-axis. The KaV of the different sTACI fractions are indicated by dots on the x-axis.

The substantial differences between the results from MW determined by SEC (Figure 23) and the predicted and observed MW by Coomassie stained SDS-PAGE, led to the decision to analyze the proteins further with a SLS/SEC system (**Figure 24**). With

our SLS/SEC system we were able to analyze our proteins with size exclusion chromatography (SEC) coupled to static light scatter (SLS). Before application of our own samples the system had to be optimized and a dilution series with human albumin fraction V was applied to find out the proper amount of protein that needs to be used. We found out that 1-3 mg/ml of sample led to optimal results (data not shown). Some proteins from the standard curve were used as positive control. As an example Conalbumin with a given MW of 75 kDa and Ribonuclease A with a given MW of 13.7 kDa were chosen. SLS calculated Conalbumin at 76.3 kDa and Ribonuclease A at 14.3 kDa (**Figure 24**).

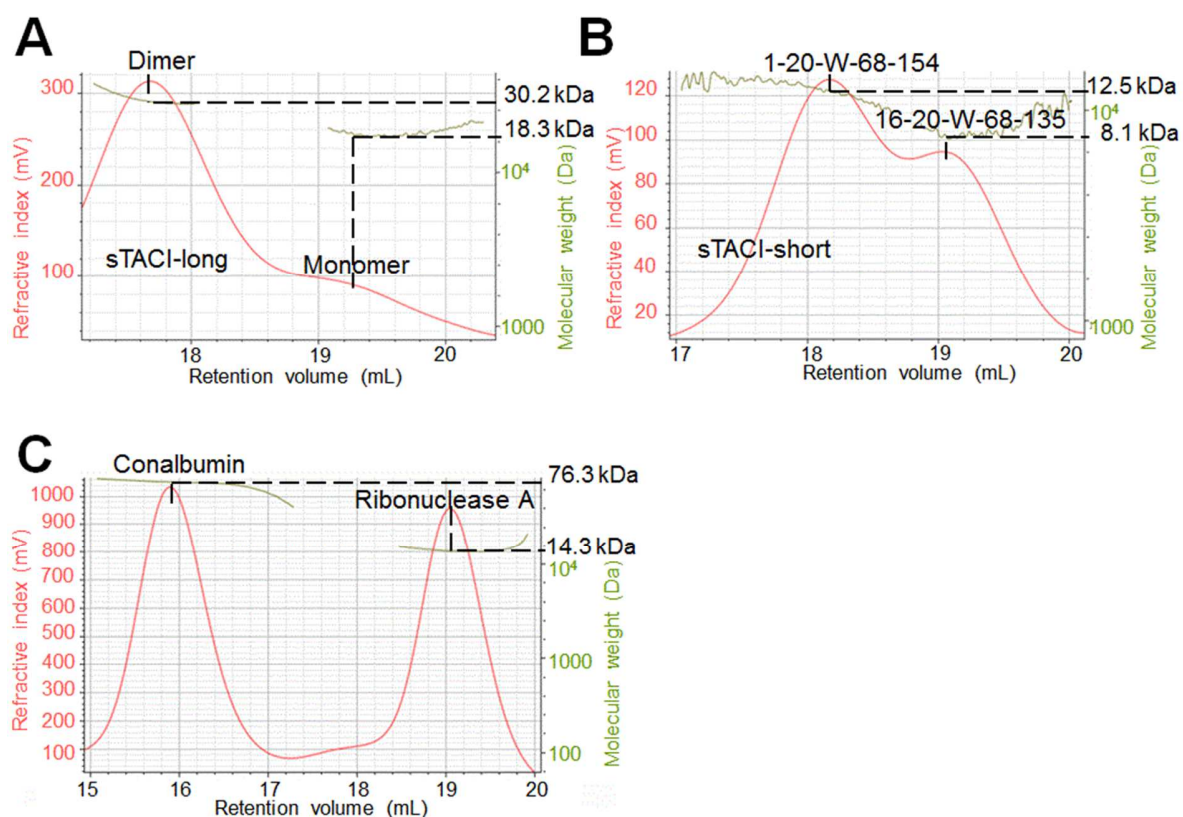


Figure 24: Molecular weight determination using SLS/SEC

After SEC the separated fractions were directly analyzed with SLS. (A-C) sTACI-long (A), sTACI-short (B) and Conalbumin together with Ribonuclease A (C) were run through the SLS/SEC system. The refractive index (concentration) is put on the y1-axis, the MW on the y2-axis and the retention volume on the x-axis.

The calculated MW values for sTACI-long and sTACI-short that were derived by SLS/SEC analysis were close to the predicted and observed MW values. The MW of the

sTACI-long dimer was calculated at 30.2 kDa and of the sTACI-long monomer at 18.3 kDa. For sTACI-short (1-20-W-68-154) the MW was determined at 12.5 kDa and for sTACI-short (16-20-W-68-135) at 8.1 kDa. Unexpectedly, sTACI-long dimer showed the highest peak/concentration in refractive index in SLS/SEC analysis indicating that sTACI-long appeared mainly as a dimer (**Figure 24 B**). sTACI-short in comparison presented itself as a mixture of sTACI-short (1-20-W-68-154) and sTACI-short (16-20-W-68-135) (**Figure 24 C**). Both sTACI-short variants that were separated by SEC needed to be pooled to have enough protein for analysis. Thus, the higher oligomers that were seen in SEC analysis could not be detected and analyzed with SLS/SEC. We focused on the two main variants of sTACI-short (sTACI-short (1-20-W-68-154) and sTACI-short (16-20-W-68-135)) as the amount of higher oligomers in sTACI-short observed by SEC made the detection of these oligomers with SLS/SEC rather unlikely. In summary, SLS/SEC led to more accurate estimations of the MW of the sTACI isoforms than SEC alone (**Table 25**).

Table 25: Comparison of MW determination of sTACI isoforms with SLS/SEC system and SEC standard curve

Construct	Expected MW (kDa)	SLS/SEC MW (kDa)	SEC MW (kDa)
sTACI-long dimer	34	30.2	58.3
sTACI-long monomer	17.4	18.3	29.9
sTACI-short (1-20-W-68-154)	12.2	12.5	19.9
sTACI-short (16-20-W-68-135)	7	8.1	9.2

4.1.7. STABILITY OF sTACI-LONG DIMER AND MONOMER

In an equilibrium, constructs are in a stable system. That means that the proportion of one element to the other element in the system is constant. If you remove one part of the system the equilibrium reinstates after some time. We tested if the dimer and monomer of sTACI-long form such a constant equilibrium by a provocation assay (**Figure 25**). During the incubation period, a development of an equilibrium state was not observed. The dimer (**Figure 25 A**) and monomer (**Figure 25 B**) of sTACI-long were stable. After 72 h a small degradation-like band was observed in the sTACI-long monomer (**Figure 25 B**).

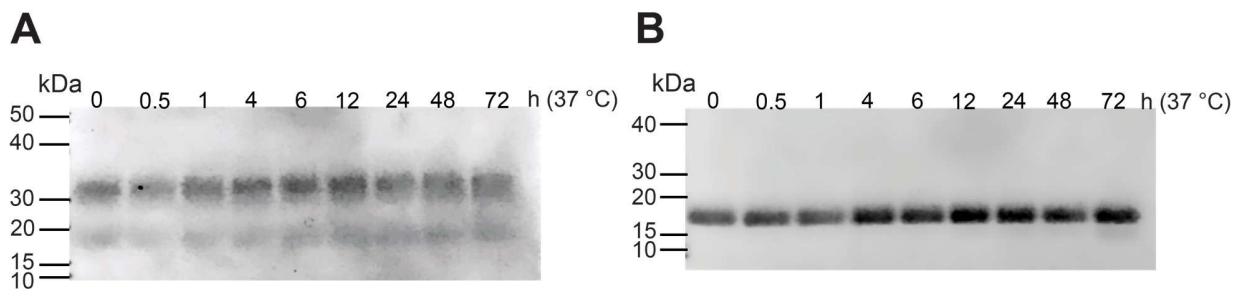


Figure 25: Stability test of sTACI-long dimer and monomer

The dimer and monomer of sTACI-long that were separated by SEC were tested in a provocation assay and analyzed by Coomassie staining. Above each band stands the timepoint at which the protein was taken during the experiment. sTACI-long dimer/monomer mix (A) and monomer (B) were incubated at 37 °C for 72 h.

4.1.8. SUMMARY OF PROTEIN CHARACTERIZATION

This part of the thesis showed that sTACI-long and sTACI-short were both produced recombinantly in HEK293.EBNA cells. First, we investigated both sTACI isoforms for N-linked glycosylation before mass spectrometry analysis. Neither of our sTACI proteins were N-linked glycosylated. Next, the identity of the recombinant TACI isoforms was confirmed by mass spectrometry and N-terminal sequencing. We observed closely located double bands for sTACI-long and sTACI-short in Western blot and Coomassie stained SDS-PAGE and a 5 kDa smaller band for sTACI-short. We were able

to characterize all bands by mass spectrometry and N-terminal sequencing. sTACI-short was revealed to be a mixture of sTACI-short (1-20-W-68-154) and sTACI-short (16-20-W-68-135). We were able to determine changes within the N-terminal sequence for the observed closely located double bands of both sTACI-short and sTACI-long. Two out of three sequences of the N-terminal variations are predicted to be the result of intracellular Furin cleavage. The additional sequence of sTACI-short could not be attributed to a protease yet. Next, we analyzed both isoforms for oligomerization. We found that sTACI-long presented itself mainly as a dimer as shown by Coomassie stained SDS-PAGE, Western blot, SEC and SLS/SEC. We also tested if the dimer and monomer of sTACI-long were in a constant equilibrium. We found that both the dimer and the monomer were in a stable state without any equilibrium. The dimer was not influenced by heat-denaturation or SDS-PAGE, whereas DTT could break its higher molecular bonds. sTACI-short exhibited small amounts of oligomers in SEC. The existence of these oligomers could be verified by the analysis of their MW by SEC standard curve, hTACI ELISA, and with Coomassie stained SDS-PAGE of the concentrated oligomers.

4.2. FUNCTIONAL ANALYSIS

4.2.1. EVALUATION OF THE AFFINITY BY BINDING ELISA

We used an ELISA based method to assess the binding affinity of sTACI-long and sTACI-short to their ligands BAFF and APRIL, similar to several previously described assays for affinity determination (136, 160-162). To compare the affinity of our different TACI variants we calculated a dissociation constant (K_d). The K_d represents the value of concentration at which the (binding-)reaction is in an equilibrium, that means half of the proteins are bound and the other half is free. Generally, a small K_d indicates a high affinity of a protein to its ligand. **Figure 14** shows an illustration of the different constructs that were evaluated by this method. sTACI-long and sTACI-short appeared in different variants based on N-terminal truncation, presumably mediated by Furin-convertase (**Figure 20**). These truncations are N-terminal of the CRD2 and are not predicted to have a major impact on decoy function and ligand binding. The resulting difference in size between

these different variants is too small to separate them by SEC and analyze them separately. Thus, sTACI-long and sTACI-short were tested including these variants.

First, we compared sTACI-long and sTACI-short with each other and tested different ligands (**Figure 26 A+B**). We found that sTACI-long and sTACI-short bound to BAFF with similar affinity (**Figure 26 C**). The affinity of both isoforms to APRIL was tested with mega- (mouse) (**Figure 26 B**) and human-APRIL (data not shown).

We found that sTACI-short and sTACI-long exhibited high affinities for APRIL, although sTACI-long displayed a significantly higher affinity for mega-APRIL in comparison to sTACI-short (**Figure 26 D**). Human-APRIL led to similar results (data not shown) concerning affinity differences between sTACI-long and sTACI-short, but showed less overall affinity to both TACI isoforms. Human-APRIL showed additionally high background binding in HEK293T cells without transfected TACI in flow cytometry (data not shown). Thus, we chose mega-APRIL for our binding studies.

We compared further CRD1-Fc, CRD2-Fc, CRD1+CRD2-Fc and CRD1+CRD2-Fc-a (**Figure 26 A+B**). The exact sequences of all compared constructs are depicted in **Figure 14**. sTACI-short (W-68-154), was additionally created to analyze whether the first 20 amino acids of the sequence affect binding to BAFF and mega-APRIL. All constructs including sTACI-short bound to BAFF significantly better than CRD1-Fc (**Figure 26 C**). When we looked at mega-APRIL affinity we found that sTACI-short, sTACI-short (W-68-154) and CRD1-Fc bound significantly worse to mega-APRIL when compared to the other constructs (**Figure 26 D**). The difference between sTACI-short and CRD1-Fc in APRIL affinity was not significant. Thus, CRD1-Fc bound both BAFF and APRIL only weakly. sTACI-short (W-68-154) bound too weakly to mega-APRIL to calculate any Kd.

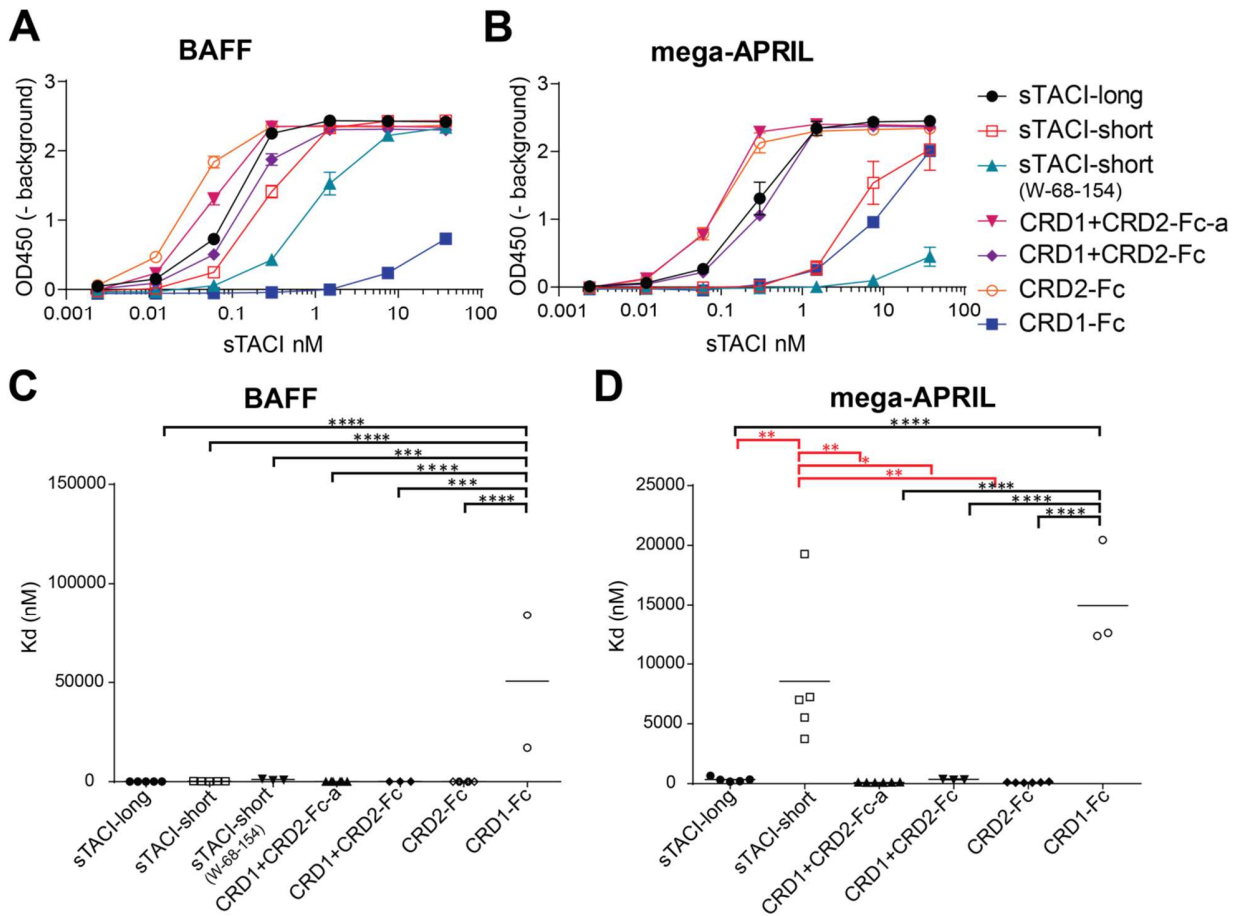


Figure 26 : Binding of various TACI constructs to BAFF and APRIL measured by ELISA
 (A+B) V-bottom plates were coated with anti-FLAG antibodies (5 $\mu\text{g}/\text{ml}$). FLAG-tagged BAFF- or mega-APRIL were added (100 ng/ml) and a dilution series of the different constructs were applied. On the x-axis stands the concentration of the used dilution series and on the y-axis the OD450 normalized against the background binding of the used ligand (normalized against BAFF (A) or mega-APRIL (B)). (C+D) Scatter blot of normal one way ANOVA (* $P < 0.05$, ** $P < 0.005$, *** $P < 0.0005$, **** $P < 0.00005$); Combined data of three (sTACI-short (W-68-154), CRD1+CRD2-Fc and CRD1-Fc), five (sTACI-long and sTACI-short) or six (atacept and CRD2-Fc) independent experiments (mean \pm SEM).

Next, we analyzed the different fractions of sTACI-long and sTACI-short that were separated by SEC (**Figure 27**). We did this comparison mainly because of the two following reasons. First, we wanted to see if dimerization led to an increased affinity in our proteins. Second, we wanted to rule out that sTACI-short (16-20-W-68-154) lost its functionality within the BAFF/APRIL system. Both effects could contribute and partly explain the decreased affinity of sTACI-short to mega-APRIL.

Coomassie stained SDS-PAGE was performed immediately prior to application of the proteins to the plates. We wanted verify that the different pooled fractions remained in the same state they were originally separated and stored at. It was found that the separated fractions remained in the same state that they were frozen in (**Figure 27 A**). The dimer fraction was comprised of a mixture of monomer and dimer. The amount of dimer was enriched in that fraction. All other fractions were separated completely.

The comparison of the dimer and monomer of sTACI-long revealed significant differences in their affinities for BAFF and mega-APRIL (**Figure 27 B+C**). The dimer of sTACI-long bound to BAFF and mega-APRIL significantly better than the monomer (**Figure 27 F+G**). When we compared sTACI-short (1-20-W-68-154) and sTACI-short (16-10-W-68-135) (**Figure 27 D+E**), we detected no difference in their binding properties for BAFF (**Figure 27 H**). When we analyzed the affinity for mega-APRIL, we found that the full-length sTACI-short (1-20-W-68-154) was able to bind to mega-APRIL significantly better than sTACI-short (16-20-W-68-135) (**Figure 27 I**).

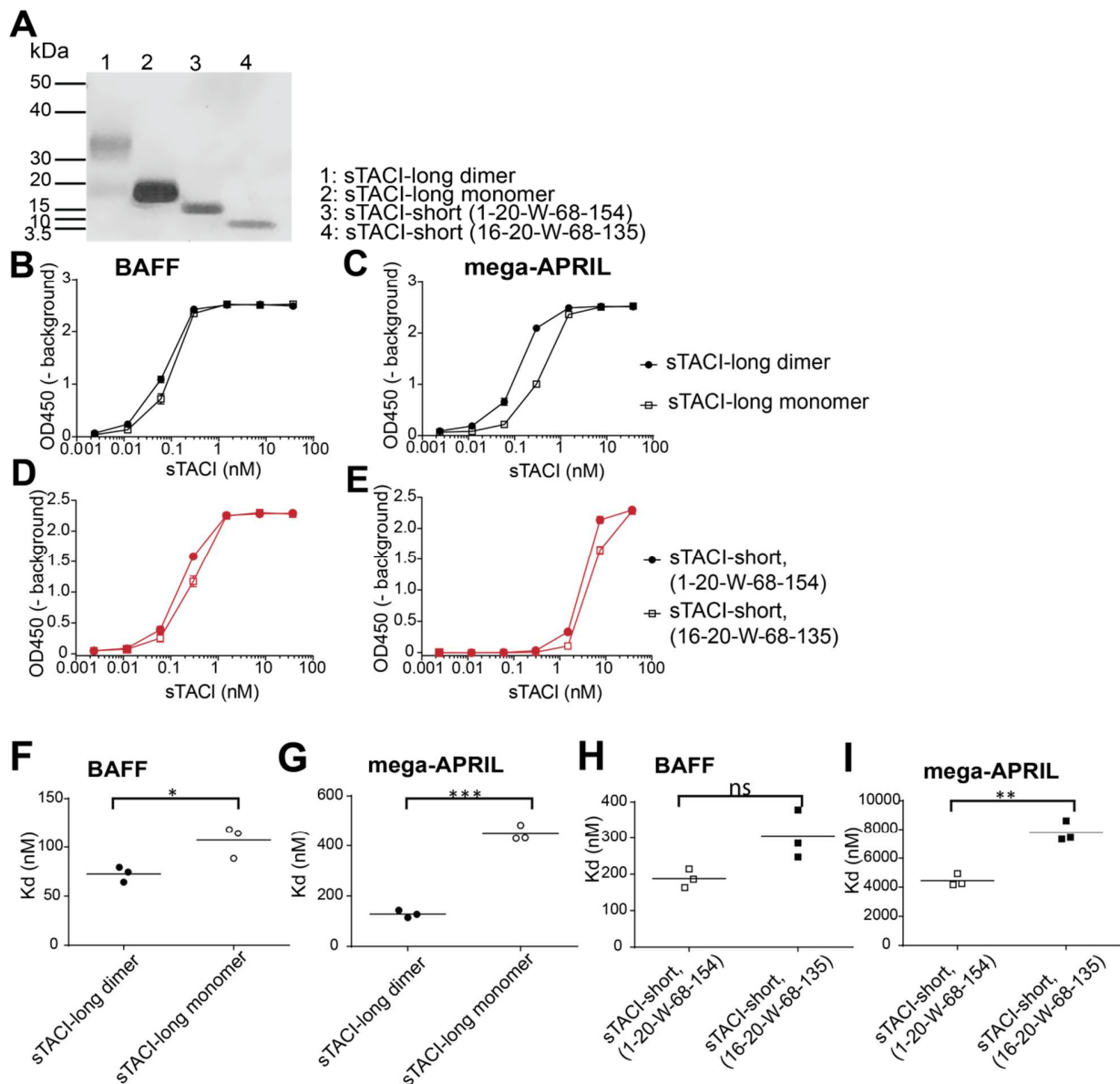


Figure 27: Binding of SEC-separated fractions of sTACI-long and sTACI-short to BAFF and APRIL measured by ELISA

(A) Coomassie stained SDS-PAGE of different sTACI fractions. (B-E) V-bottom plates were coated with anti-FLAG antibodies (5 $\mu\text{g/ml}$). FLAG-tagged BAFF- or mega-APRIL were added (100 ng/ml) and a dilution series of the different fractions was applied. On the x-axis stands the concentration of the dilution series and on the y-axis the OD450 normalized against the background binding of the used ligand (normalized against BAFF (B, D) or mega-APRIL (C, E)). (F-I) Scatter plot of unpaired two-tailed t-test with Welch's correction for B-D (ns: not significant; * $P < 0.05$, ** $P < 0.005$, *** $P < 0.0005$) Combined data of three independent experiments (mean \pm SEM).

Table 26 shows the summary of mean Kd values from each construct for BAFF and mega-APRIL.

Table 26: Binding affinity of BAFF and APRIL to TACI-constructs.*

TACI construct	BAFF Kd (pM)	mega-APRIL Kd (pM)
sTACI-long	100	292
sTACI-long dimer	72	127
sTACI-long monomer	106	447
sTACI-short	270	5960
sTACI-short (1-20-W-68-154)	187	4434
sTACI-short (16-20-W-68-135)	301	7741
sTACI-short (W-68-154)	1065	n.a.
CRD1+CRD2-Fc-a	54	93
CRD1+CRD2-Fc	139	346
CRD2-Fc	30	77
CRD1-Fc	54160	14470

*N.a. means that the interaction that was measured was too low to calculate the Kd. Means were calculated from 3-6 experiments. Both isoforms of sTACI were analyzed as mixtures. sTACI-long preparations contained a dimeric and a monomeric form, while sTACI-short was a mixture of the monomeric sTACI-short (1-20-W-68-154) and sTACI-short (16-20-W-68-135) and to a small extent higher oligomers of sTACI-short. The different fractions of the sTACI-long and sTACI-short preparations were separated by SEC (**Figure 21 + Figure 27**) and analyzed independently.

4.2.2. EVALUATION OF DECOY FUNCTION BY LUCIFERASE ASSAY (NFκB ASSAY)

A luciferase based assay (NFκB assay) was used as a second read out system, complementary to the Binding ELISA. The NFκB assay is a reporter cell assay that can be used to test the decoy function of soluble receptors. The IC50 was calculated to indicate the potency of soluble receptors in inhibiting NFκB activation. The IC50 means the concentration of a soluble receptor that is needed for the NFκB activation to be decreased for 50%.

First, we compared sTACI-long to sTACI-short for their decoy function (**Figure 28**). sTACI-long and sTACI-short displayed a similar decoy function for BAFF (**Figure 28 A+F**). Both receptors were able to act as decoy receptor for BAFF at high concentrations. In contrast, only sTACI-long was able to capture mega-APRIL (**Figure 28 B+E**) and human-APRIL (**Figure 28 C**) at high concentrations and thus prevent NFκB activation (**Figure 28 B+C**). sTACI-short was not able to act as decoy receptor for mega- or human-APRIL and thus showed no influence on NFκB activation. The monomer and dimer of sTACI-long were tested for their decoy function after a significant difference was detected in their ability to bind mega-APRIL by binding ELISA (**Figure 28 D,E,G,H**). In concordance with the findings of our binding ELISA, we were able to detect significant differences for the decoy function between the dimer and monomer of sTACI-long for BAFF and APRIL (**Figure 28 G+H**). **Table 27** shows the summary of mean IC50 values from each measured construct for BAFF and mega-APRIL.

Table 27: Decoy activity of sTACI-long, sTACI-long dimer, sTACI-long monomer and sTACI-short for BAFF and APRIL*

TACI	BAFF IC50 (nM)	mega-APRIL IC50 (nM)	Human-APRIL IC50 (nM)
sTACI-long	1.791	1.982	4.443
sTACI-long dimer	0.438	1.762	-
sTACI-long monomer	1.176	6.807	-
sTACI-short	1.679	n.a.	n.a.

*N.a. means that the interaction that was measured was too low to calculate the IC50 and the straight line (-) means that the receptors were not tested with that ligand. Means were calculated from 3-6 experiments.

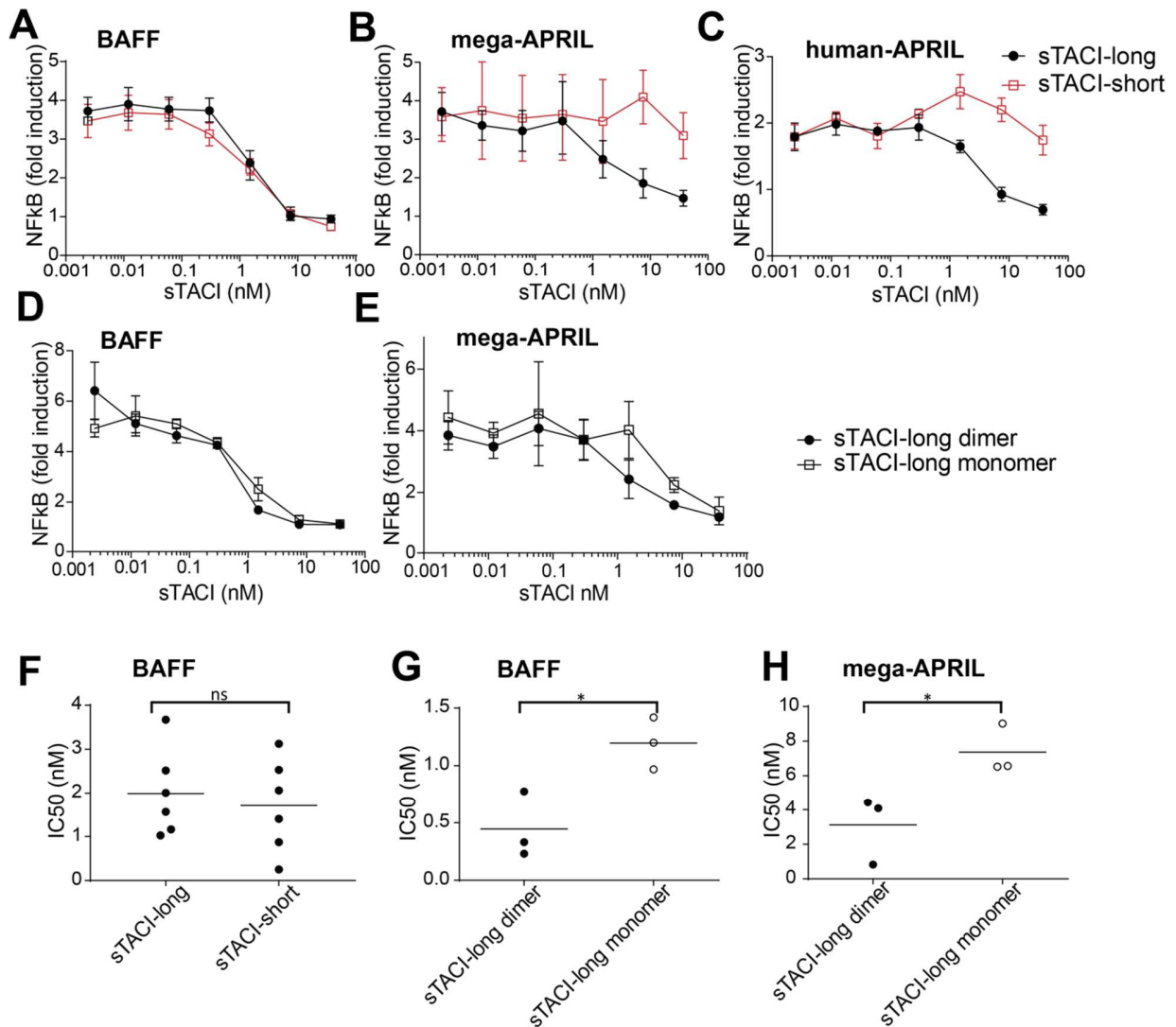


Figure 28: Decoy activity of TACI constructs for BAFF and APRIL measured by NFκB assay

(A-E) HEK293T cells were transfected with BCMA (2.5 ng), Renilla (40 ng) and Firefly (40 ng). FLAG-tagged BAFF, mega- or human-APRIL (100 ng/ml) were added together with a dilutions series of sTACI-long or sTACI-short. The concentration of the sTACI-isoforms is represented on the x-axis, the NFκB fold induction on the y axis (F-H) Scatter blot of unpaired two-tailed t-test with Welch's correction for A, D, and E (ns: not significant; *P < 0.05). Combined data of six (A and B) or three (C,D,E) independent experiments (mean +/- SEM).

4.2.3. SUMMARY OF FUNCTIONAL TESTS

In the second part of this thesis, we analyzed sTACI-long and sTACI-short for their ligand-binding and functionality with two different read-out systems, binding ELISA and NFκB reporter assay. We found that both isoforms of TACI showed a similar affinity for BAFF, while sTACI-long bound to APRIL with significantly higher affinity than sTACI-short. In a second read-out system, an NFκB reporter assay, similar results were obtained. Using SEC separated fractions, we found that the dimer of sTACI-long showed significantly higher affinity to BAFF and APRIL than the monomer. Three constructs of sTACI-short that differed in the sequence in the N-terminal side outside of CRD2 were available and tested for ligand binding. sTACI-short (1-20-W-68-154), sTACI-short (16-20-W-68-135), and sTACI-short (W-68-154) displayed similar binding affinities for BAFF, while sTACI-short (1-20-W-68-154) bound significantly better to APRIL than sTACI-short (16-20-W-68-135) and sTACI-short (W-68-154). sTACI-short (16-20-W-68-135) lacks 19 amino acids at the C-terminus outside of the CRD2 which are present in the other two versions of sTACI-short. This could contribute to the reduced binding affinity to APRIL. The abolished APRIL binding of sTACI-short (W-68-154) indicates, however, that the N-terminal part is crucial for binding to APRIL. Thus, these amino acids N-terminal outside of CRD2 have little effect on BAFF-binding, but seem to contribute to the (weak) APRIL binding of sTACI-short. The two isoforms of sTACI were compared to TACI-Fc constructs, comprising CRD1 and CRD2 individually or together and to an atacept analog (CRD1+CRD2-Fc-a). We found that CRD1+CRD2-Fc, CRD2-Fc and CRD1+CRD2-Fc-a exhibited similar high affinities for BAFF and APRIL, while CRD1-Fc showed little ligand binding. Surprisingly, CDR2-Fc appeared different from sTACI-short with respect to APRIL binding.

4.3. MEMBRANE-BOUND TACI ISOFORMS

4.3.1. ASSESSMENT OF THE EXPRESSION, SHEDDING AND LIGAND INTERACTION OF TACI-LONG AND TACI-SHORT FROM HEK293T CELLS

We tested transfected HEK293T cells for their expression, ligand binding and shedding of TACI-long and TACI-short. HEK293T cells were chosen because they do not express TACI endogenously. Flow cytometry was used to assess surface expression (membrane-bound TACI) and binding of ligands. ELISA was applied to test for shedding (sTACI).

Both TACI-long and TACI-short were expressed and constitutively shed from transfected HEK293T cells. TACI-short was shed in significantly higher amount from the cell surface than TACI-long (**Figure 29 A**). In concordance, TACI-short expression was higher on HEK293T cells than TACI-long expression (**Figure 29 B**), when equal amount of plasmids were used for transfection. At the highest amount of transfected plasmid (100 ng) TACI-short was expressed significantly higher than TACI-long.

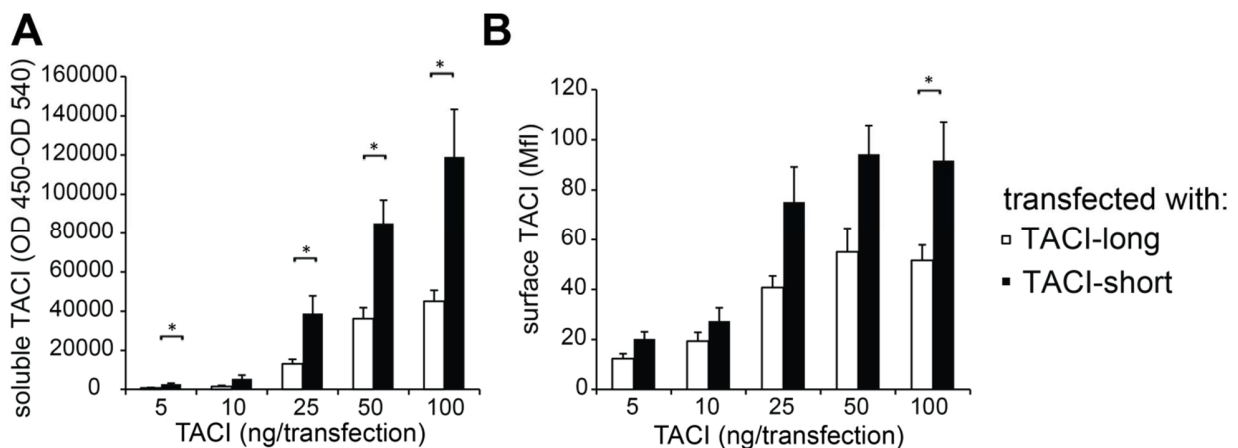


Figure 29: Expression and shedding of TACI-long and TACI-short by transfected HEK293T cells

(A-D) HEK293T cells were transfected with increasing amounts of TACI-long or TACI-short. (A) The amount of shed TACI was determined by ELISA. (B) Surface expression was analyzed by flow-cytometry. The MFI was calculated by subtracting the signal from non-transfected cells from the signal of transfected cells. (Combined data of five independent experiments (mean +/- SEM), unpaired two-tailed t-test (*P<0.05).

The binding capacity of the membrane-bound TACI isoforms for BAFF and mega-APRIL was analyzed with our cell based assay as well. HEK293T cells were transfected with different amount of TACI-long or TACI-short similar to the expression assay. In an additional step, FLAG[®]-tagged BAFF or mega-APRIL was added in a constant concentration and ligand binding was assessed by flow cytometry. We could replicate in concordance with our previous findings, that TACI-short is expressed significantly more on transfected HEK293T cells than TACI-long. We found that both membrane-bound isoforms can bind to BAFF and mega-APRIL. Both TACI isoforms bound to BAFF and APRIL similarly (**Figure 30 A+B**). In a different assay setup we tried constant amounts of transfected plasmid and varied the concentration of BAFF and mega-APRIL. Unspecific binding of mega-APRIL, when higher amount than 100 ng/ml were added, limited this approach. Human-APRIL could not be used at all for this assay as it displayed already in small amounts unspecific binding (data not shown).

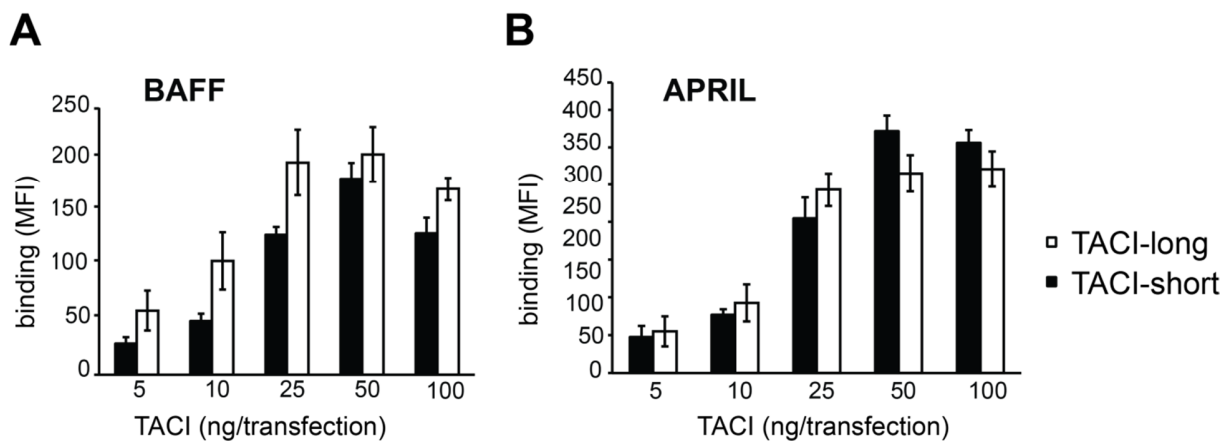


Figure 30: Analysis of membrane-bound TACI-long and TACI-short BAFF and APRIL interaction

(A and B) HEK293T cells were transfected with increasing amounts of TACI-long or TACI-short. BAFF- (A) or mega-APRIL-FLAG (B) (100 ng/ml) were added. The binding of BAFF and mega-APRIL was analyzed by flow-cytometry. The MFI was calculated by subtracting the isotype signal of non-transfected cells with BAFF or APRIL-FLAG from the signal of transfected cells. Combined data of three independent experiments (mean +/- SEM).

4.3.2. CO-IMMUNOPRECIPITATION OF TACI-LONG AND TACI-SHORT IN SOLUBLE AND MEMBRANE-BOUND FORM

Co-IP was used to analyze for homo- or heterotypic interaction of both TACI isoforms in soluble and membrane-bound form in one single assay. Therefore, TACI-short was cloned with a N-terminal FLAG[®]-tag or HA-tag. No interaction between BCMA and TACI has been reported so far. BCMA with a FLAG[®]-tag was used for comparison.

The efficiency of the IP was tested by anti-FLAG[®] ELISA (**Figure 31**). The FLAG[®]-tag was used to immunoprecipitate proteins with anti-FLAG[®]-tagged beads. Each condition was tested for TACI and BCMA occurrence with pre and post IP samples by ELISA. Conditions with FLAG[®]-tagged proteins could be detected pre IP and post IP for both soluble (**Figure 31 A**) and membrane-bound proteins (**Figure 31 B**). Exclusively HA-tagged conditions could not be detected after IP. The existence of TACI in solely HA-tagged conditions pre IP was verified by hTACI ELISA (**Figure 31 C+D**). Therefore, the IP was able to specifically extract FLAG[®]-tagged proteins from our samples.

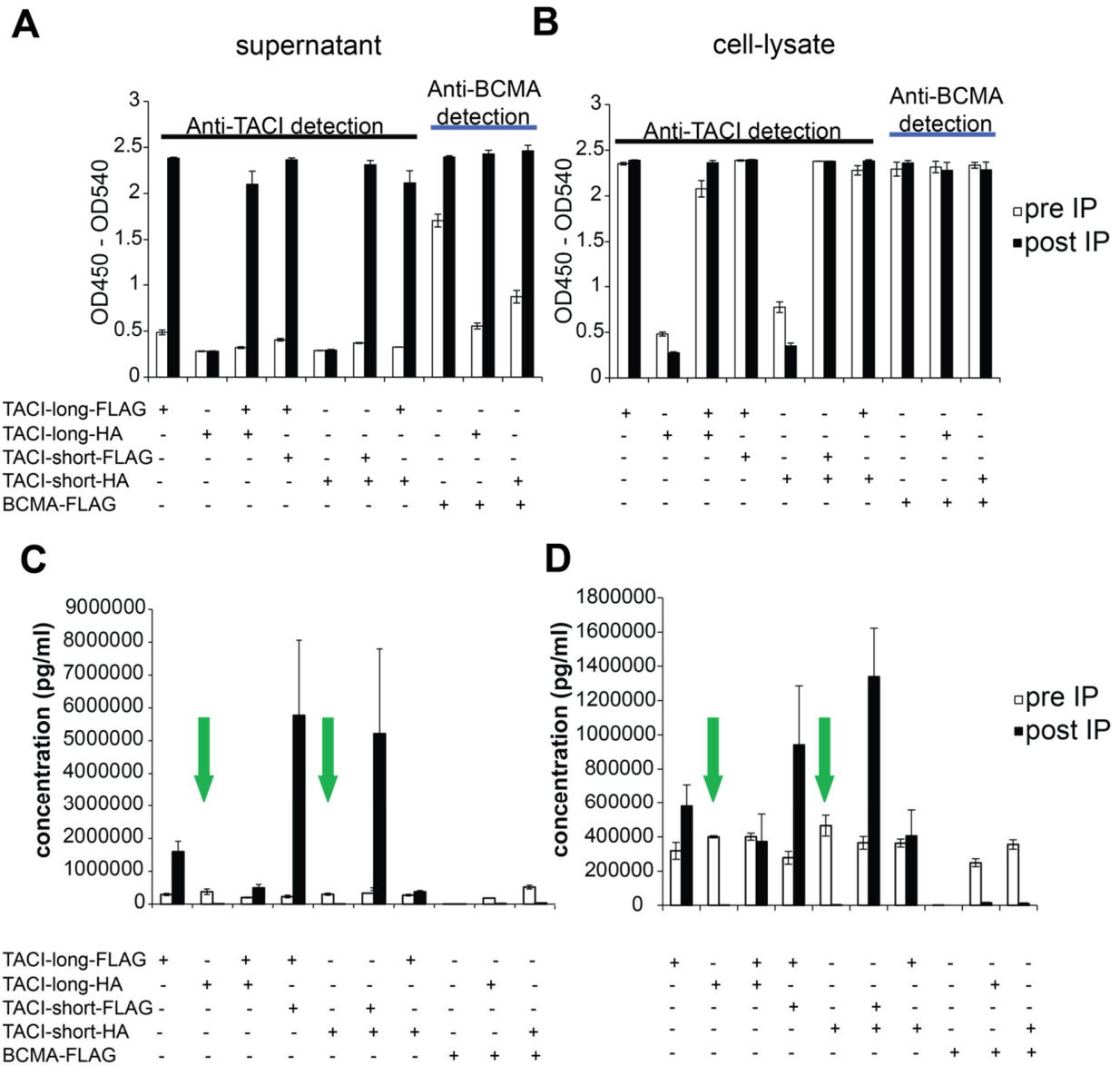


Figure 31: Test of efficiency of IP

(A - D) HEK293T cells were transfected with the indicated plasmids. The supernatants (A,C) and cell-lysates (B,D) were harvested 48-72h after transfection. Small fractions of each condition were saved before FLAG[®]-IP. The pre- and post IP samples were then measured by anti-FLAG[®] ELISA (A and B) or hTACI ELISA (C and D) on ELISA plates. The proteins were either detected by an anti-TACI detection antibody or anti-BCMA detection antibody (for BCMA-FLAG in anti-FLAG[®] ELISA). The green arrow indicates pre IP and HA-tag only conditions in hTACI ELISA. Combined data of three independent experiments (mean +/- SEM).

In principle, HA-tagged proteins could only be detected post IP if these proteins formed an interaction with FLAG[®]-tagged proteins. Thus, the HA-tagged proteins were not lost during IP. The anti-HA ELISA was used to distinguish if our proteins formed such an interaction with each other in a homotypic or heterotypic way. We tested this for both soluble (supernatant) (**Figure 32 A**) and membrane-bound (cell-lysate) proteins (**Figure 32 B**). No difference could be detected between soluble and membrane-bound conditions. We found that TACI-long interacted homotypically with itself, as previously described (93). Similarly, TACI-short showed the same homotypic interaction and both TACI-short and TACI-long interacted heterotypically with each other. No interaction of BCMA with either of the TACI isoforms could be detected.

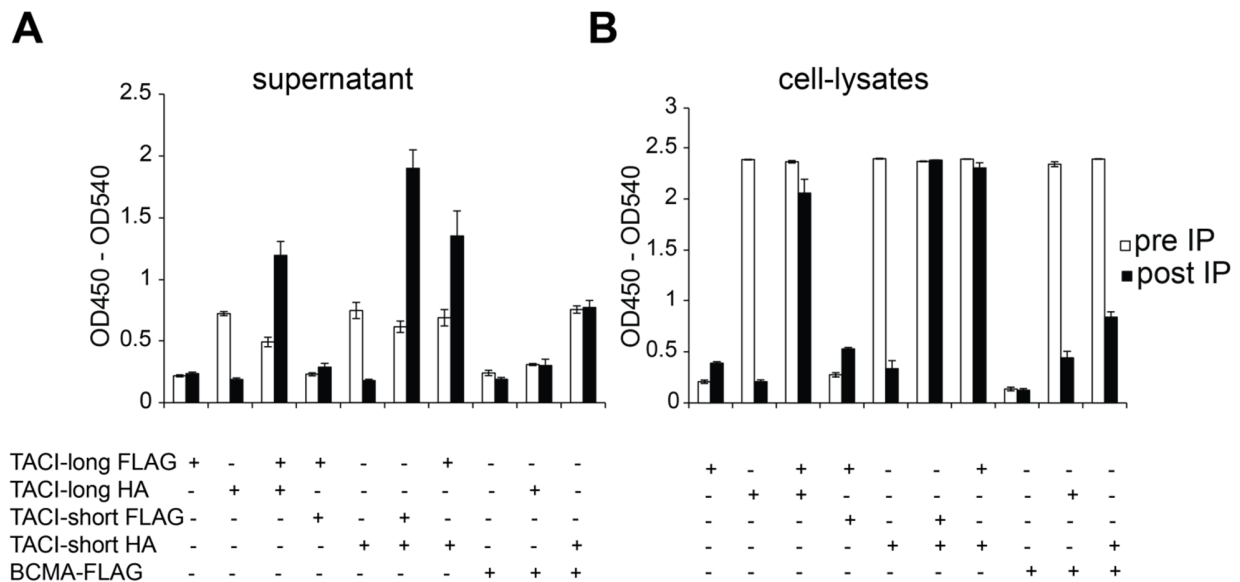


Figure 32: Analysis of homo- and heterotypic interaction of TACI isoforms in soluble and membrane-bound form

(A and B) HEK293T cells were co-transfected with plasmids that contained either a HA- or FLAG[®]-tag. The different conditions are indicated in the legend below the graph. The supernatants and cell-lysates were harvested 48-72 h after transfection. Small fractions of each condition were saved before FLAG[®]-IP. The pre- and post IP samples were then measured by anti-HA ELISA. The proteins were detected by an anti-TACI detection antibody. Combined data of three independent experiments (mean +/- SEM).

4.3.3. SUMMARY OF THE ANALYSIS OF MEMBRANE-BOUND ISOFORMS OF TACI

In this last part of this thesis we found that both TACI-long and TACI-short were expressed on and spontaneously shed into the cell culture medium from the membrane of transiently transfected HEK293T cells. TACI-short levels were significantly higher on the cell membrane and in the cell culture medium. Both membrane-bound isoforms of TACI bound to BAFF and mega-APRIL similarly. The homotypic interaction of the soluble and membrane-bound TACI isoforms was further evaluated by Co-IP. We have shown that both TACI-long and TACI-short form homotypic interactions and that TACI-short and TACI-long exhibited a heterotypic interaction with each other in soluble and membrane-bound form. No interaction of TACI isoforms and BCMA was detected.

5. DISCUSSION

5.1. BASIC CHARACTERIZATION OF sTACI-LONG AND sTACI-SHORT

In this project, we aimed to investigate the molecular characteristics and functions of two different TACI isoforms (sTACI-long and sTACI-short) by generating proteins that have the identical sequence with the endogenously shed TACI that our lab had recently identified (93). Our previous studies found so far that (i) TACI gets shed by the protease ADAM10 from activated B-cells, (ii) TACI interacts homotypic in soluble and membrane-bound form and (iii) sTACI exists in vivo in B-cell pathologies (93, 163). sTACI-long and sTACI-short differ from each other on the extracellular domain. sTACI-long expresses both CRDs (CRD1 and CRD2), while TACI-short only the CRD2 as a consequence of alternative splicing (**Figure 6**) (140). Both isoforms of TACI were analyzed in membrane-bound form by a previous study that reported that TACI-short is more potent inducing plasma cell differentiation (146).

5.1.1. PURITY

We produced the two isoforms of sTACI recombinantly, secreted from HEK293.EBNA cells (153). Combined analysis of Coomassie stained SDS-PAGE, Western blot, mass-spectrometry and N-terminal sequencing yielded only TACI indicating the purity of the recombinantly produced proteins. The purity of our proteins was the result of on the one hand usage of serum-free medium during expression and on the other hand purifying them with an affinity based method.

5.1.2. DIFFERENT VARIANTS OF sTACI-LONG AND sTACI-SHORT OUTSIDE OF THE CYSTEINE RICH DOMAINS

We noticed that both of our TACI isoforms did not appear as a single band in Coomassie stained SDS-PAGE and Western blot. Both isoforms were rather comprised of double bands, while sTACI-short showed an additional 5 kDa smaller variant. We analyzed all variants by mass spectrometry and N-terminal sequencing. The 5 kDa smaller variant of sTACI-short was revealed to be missing parts on both the C- and N-terminal side. Thus, our sTACI-short preparations were a mixture of full-length sTACI-short (1-20-W-68-154) and sTACI-short (16-20-W-68-135). N-terminal sequencing revealed further heterogeneity within the sequence of sTACI-long and sTACI-short on the N-terminal side, which we could largely attribute to Furin cleavage. Furin is a protease primarily located at the Golgi apparatus (159). The cleavage points that we observed for our sTACI-long and sTACI-short are depicted in **Figure 20** together with the canonical sequences of the Furin protease. Cleavage by Furin often leads to activation of proteins like for example observed for shiga toxin, Influenza virus hemagglutinin, and the hepcidin regulator hemojuvelin (159, 164-166). We found an additional variant of the N-terminus for sTACI-short that we could not attribute to a protease yet.

5.1.3. OLIGOMERIZATION OF sTACI ISOFORMS

Coomassie stained SDS-PAGE and Western blot revealed possible oligomers of our sTACI isoforms. We found that our recombinantly produced sTACI-long built mainly dimers and to a smaller extent monomers, whereas sTACI-short appeared mainly as monomer and in small amounts as higher oligomers. SEC and SLS/SEC analysis confirmed our previous observations that sTACI-short appeared mainly as a mixture of the monomers sTACI-short (1-20-W-68-154) and sTACI-short (16-20-W-68-135).

Thus, both isoforms of sTACI are able to form oligomers. It was previously described that the CRD1 is needed for oligomerization of surface TACI (145). Nevertheless, our sTACI-short which lacks the CRD1 built oligomers indicating that

oligomerization seems to not solely depend on the CRD1. The differing ways of oligomerization of both sTACI isoforms could, however, be the result of different interactions. Earlier studies support the role of the CRD1 in dimerization of TACI-long (145). In general, additional CRDs are reported to bring extra abilities to other TNF receptors. The additional CRDs stabilized the receptors and increased the affinity and specificity of the receptors to their ligands (140, 167-170). Moreover, another study proposed that the CRD1 of TACI was an evolutionary relict by reporting that it cannot contribute to ligand/receptor interactions with BAFF and APRIL (140). Taken together, the main role and function for the CRD1 could be the dimerization and stabilization of TACI-long, while the cause of oligomerization in sTACI-short remains unknown.

Concerning the observed dimerization of sTACI-long, we assessed its stability with several different conditions. We found that heat denaturation did not disrupt the dimers and that there was no state of equilibrium between the dimer and monomer, at physiological conditions. This observation suggested that the dimer was formed by a highly stable bond. Only DTT, which is a reducing agent, was able to break the bond, further supporting our hypothesis.

This highly stable covalent interaction could be caused by disulfide bonds (171). Disulfide bonds are important posttranslational modifications that contribute to proper folding, stabilization and functionality of proteins (172). The redox reaction that generates these bonds takes part in the ER (173). Cleavage of disulfide bonds can exert regulatory effects (172). This effect was shown for several receptors like the scavenger receptor class B, type 1 (SR-B1), vasopressin V2 receptor (V2-R), and Thyrotropin-releasing Hormone Receptor (TRH-R) (174-177) . Several disulfide bonds are predicted for the CRDs of TACI on the extracellular domain (**Figure 33**) (140).

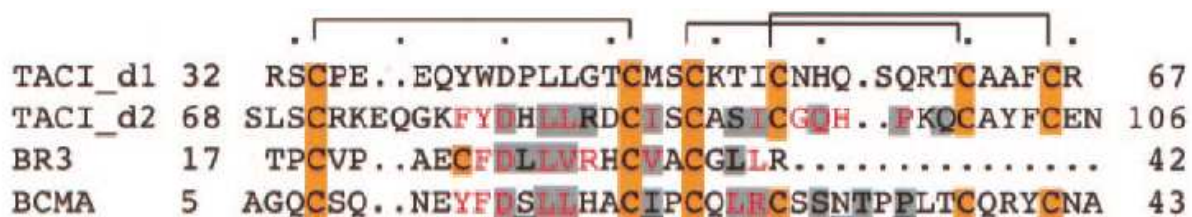


Figure 33: Sequence alignment of the CRD1 (TACI_d1), CRD2 (TACI_d2), BAFF-R (BR3) and BCMA

CRD1, CRD2 and BCMA share the identical arrangement of their cysteine residues. The proposed interaction between these residues is indicated by the connecting brackets above the sequence. The residues are all connected in inner-molecular disulfide bonds. Figure taken from (140).

Disulfide bonds could either directly be involved in generating a disulfide-linked dimer, or as intramolecular bonds that induce proper formation and folding for protein interaction. Interestingly, the mutation C104R within the extracellular domain of TACI - a mutation associated with the diseases common variable immune deficiency (CVID) and IgA deficiency (IgAD) (120-122, 127, 145, 178, 179) - is located at the cysteine at position 104 which is predicted to form an intramolecular disulfide bond with the cysteine at position 93 (140). A mutation at that position abolishes the proposed disulfide bond which could explain the changed properties of C104R mutated TACI, although no effect could be observed at receptor preassociation (145). The mutation was shown to annihilate ligand binding and intracellular signaling (120, 121, 178) and is discussed to increase susceptibility to disease outbreak (127).

Whether disulfide bonds are the cause of oligomerizations of TACI could not be shown yet. Previous studies detected oligomerization of soluble TACI-long by Co-IP (93) and of membrane-bound TACI by crosslinked cell surface molecules in murine B-cells (145), Förster resonance energy transfer (FRET) analysis independent of a ligand (145) and Co-IP (93, 145). Sequential nondenaturing IP revealed that TACI assembled at least as trimer in the ER (145). In that study DTT was able to break higher oligomers of cross-linked TACI in cell lysates, but without any explanation. In other TNF receptors extracellular disulfide bonds were shown to attribute to native dimerization such as for the death receptor 5 (180) and CD40 (181-183). Both receptors exhibited extracellular disulfide-linked dimers. The addition of a reducing agent broke both dimers (180, 181).

The dimerization of CD40 is controversially discussed, since another study attributes dimerization to the CRD1 of CD40 (184).

Another N-terminal variant of sTACI-short that was cloned, namely sTACI-short-(W-68-154) showed the tendency to build several high grade oligomers already quite prominent in Coomassie stained SDS-PAGE. In contrast to our recombinantly produced sTACI-short, we did not find an additional degraded sTACI (16-20-W-68-135)-like variant in our sTACI-short (W-68-154) preparation. Therefore, the terminal stalk right before the transmembrane region (amino acids 135-154) of sTACI-short could contribute to the low level of oligomers formed by sTACI-short. An additional assay was performed with sTACI-short (W-68-154) to further assess its oligomerization. It was tested, whether the simple addition of EDTA, which is potent at forming chelates with divalent ions, abrogates oligomerization by capturing Nickel ions. Therefore, the formation of a chelate between eluted Nickel ions from HisTrap columns and the His6-tag of sTACI-short (W-68-154) would be prevented. This phenomenon was suggested previously to explain the formation of the BAFF60mer, although it was found that the BAFF60mer was not the consequence of such an interaction (84, 85). Accordingly to the BAFF60mer, addition of EDTA had no effect on oligomerization of sTACI-short (W-68-154). Following studies could further evaluate the disulfide bonds of TACI. An urea gel could be run to determine whether our oligomers are linked by intermolecular disulfide bonds. In principle, urea denaturizes proteins by destruction of their tertiary structure (177, 185-187).

5.1.4. GLYCOLSYLATION OF TACI ISOFORMS

Last, we investigated the glycosylation of our proteins. Glycosylation was shown to have effects on ligand/receptor interactions and membrane assembly of receptors in previous studies (188, 189). N-linked glycosylation was predicted at amino acid 128 (N) for TACI by Uniprot. We found that both of our recombinantly produced isoforms were missing the predicted N-linked glycosylation as proven by PNGase F (**Figure 20**).

N-linked glycosylation was shown to have an important regulatory effect on BCMA (190). BCMA expresses a single N-linked glycosylation site on the extracellular domain at asparagine 42. In BCMA small changes and different parts of the glycosylation pattern affected the function by improving ligand binding and causing either cell surface retention or removal of BCMA (190).

It remains to be clarified whether the sTACI shed from B-cells also lacks N-linked glycosylation, since glycosylation could be different in HEK293T- and B-cells. Future studies should investigate the glycosylation of B-cell derived TACI and sTACI. Therefore, supernatants of the Raji cell line (191-193) – a lymphoblast cell line that expresses TACI- could be concentrated, followed by separation of sTACI-long and sTACI-short by SEC and analysis for glycosylation by PNGase F.

5.2. LIGAND BINDING AND DECOY FUNCTION OF sTACI-LONG AND sTACI-SHORT

To analyze interactions of TACI-variants and their ligands, we used two different read out systems, namely ELISA and NF κ B assay. In general, ELISA or surface plasmon resonance (SPR) based methods can be used to determine affinity and calculate K_d values (136, 160, 161, 194, 195). Both methods detect different reactions and consequently differ in exact values, but the general conclusions are mostly uniform and equivalent between both methods (196). In our binding ELISA we immobilized FLAG[®]-tagged BAFF and APRIL to pre-coated anti-FLAG[®] antibodies on the plate and added a dilutions series of sTACI in molar concentration which we then detected by colorimetry. Another previously described ELISA based method which was used to evaluate the binding affinity of BCMA-Fc and TACI-Fc (basically TACI-long) to BAFF and APRIL showed that BCMA-Fc and TACI-Fc exhibit similar affinities to BAFF and APRIL (136). In that study BCMA and TACI were used as Fc fused homodimers. BCMA-Fc and TACI-Fc were immobilized to plates and BAFF or APRIL were added in a dilution series (136). For our second read out system - the NF κ B assay- we used an inhibition based method and determined the IC₅₀ essentially as published (93). We transfected HEK293T cells with BCMA and added a mixture of BAFF or APRIL with a dilution series of TACI and checked for NF κ B activation.

We found that sTACI-long and sTACI-short exhibited similar affinity and decoy function for BAFF. In contrast, sTACI-long bound with significantly higher affinity to APRIL than sTACI-short. In harmony with this observation, only sTACI-long was able to act as a decoy receptor for APRIL. A previous study from our lab showed that sTACI can bind to BAFF and APRIL and that it acts as a decoy receptor for both ligands (93), which is confirmed in this study. That study did not compare the different isoforms of TACI, it only analyzed the full-length isoform which represents sTACI-long.

Another study analyzing the contributions of CRD1 and CRD2 of TACI to binding of BAFF and APRIL concluded that only CRD2 is needed for high affinity-binding to both ligands (140). CRD1 alone bound only weakly; when CRD1+CRD2 (basically sTACI-long) was compared to CRD2 only (basically sTACI-short), the CRD1 did not contribute

substantially to ligand binding (140). While many of these results are similar to the ones obtained here with the sTACI variants, one difference appeared. In that study (140), CRD2 showed a strong APRIL binding, while in our study sTACI-short showed only a weak APRIL binding.

Possible reasons for the different results could be (a) different methods to determine the affinity, (b) sequence differences beyond the CRDs, (c) differences in the used protein expression systems, (d) differences in state of oligomerization, (e) and differences in the applied variant of APRIL.

(a) That study used different methods to determine the affinity (140). First, an inhibition assay was used which measured binding kinetics by SPR (194, 195). In that assay BCMA-Fc was coupled to a chip and different amounts of TACI were added together with constant amounts of BAFF and APRIL (140). The aim of that assay was to calculate the ability of TACI to inhibit the binding of BAFF and APRIL to BCMA-Fc (IC₅₀). Second, a competitive ELISA assay was used as an additional read out system. The competitive ELISA assay was designed as an inhibition assay as well (IC₅₀). BAFF and APRIL were coupled to plates and a mixture of each TACI construct with a dilution series of soluble BAFF and APRIL was added. The concentration of the receptors was not used in molarity in contrast to our study if the indicated protocol was followed (140, 141). As previously described, all methods for the determination of affinity mostly lead to the same conclusions (196). Therefore, other effects are most likely to cause the differences we observed between our sTACI isoforms and that study.

(b) The constructs of that study were designed to start directly at the CRDs of TACI and not as full-length proteins like ours (**Figure 34**). Indeed, we observed that the N-terminal part of sTACI-short outside of the CRD2 have an effect on APRIL binding as described below. Our observation that sTACI-short (W-68-154) showed almost no APRIL interaction shows that the N-terminus outside of CRD2 is not the reason for the discrepant results. Nevertheless, our sTACI-short extended to amino acid 154 or 135, while the CRD2 used in that study stops at amino acid 109. The C-terminal part outside of CRD2 would not be expected to contribute to APRIL binding, although this has not been analyzed specifically.

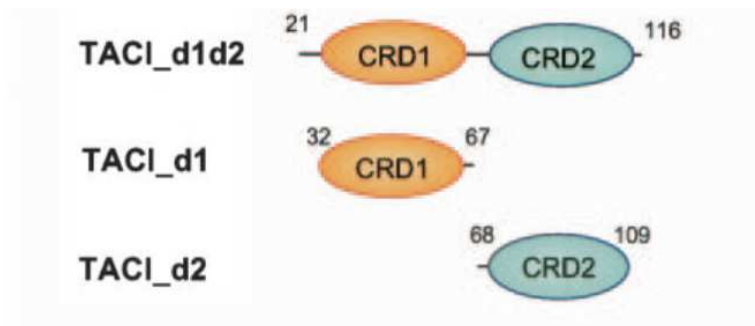


Figure 34: Sequence of the TACI constructs from Hymowitz et al (Figure taken from (140))

(c) The proteins of that study (140) were produced in *E. coli* and insect cells, while we produced in eukaryotic HEK.293 cells. In detail, the CRD2-version was produced in *E. coli*. In general, recombinant protein production in *E. coli* gives high yields of protein and is fast, but it can lead to misfolded, aggregated, and degraded proteins that lack the posttranslational modifications of native human proteins (197, 198). Regardless, the CRD2 construct of that study (140) was shown to be fully functional concerning BAFF and APRIL binding. The constructs that were comprised of the CRD1 and CRD1+CRD2 were produced differently by using baculovirus expression system with Hi5 cells. This method enables the generation of active proteins that highly depend on posttranslational modifications, proper folding and disulfide bonds (199). Expression in insect cells was reported to yield functional CRD1 and CRD1+CRD2 constructs likewise to the *E. coli* expressed variant of CRD2 (140). Our eukaryotic expressed isoforms of sTACI were fully functional within the BAFF/APRIL system. Therefore, the choice of different expression systems is most likely not the reason for the different results.

(d) We noted a difference in oligomerization between the sTACI isoforms in our preparations. sTACI-long was mainly formed as a dimer, whereas sTACI-short was primarily in monomeric form. In that study (140), it was not reported whether the applied CRD domains were monomeric or oligomeric. To further assess the effect of oligomerization and to address the seemingly discrepant results, we analyzed TACI-Fc constructs, which are dimers due to the Fc-tag. Using these constructs, we basically obtained similar results as in that study (140). Specifically, we found that CRD1+CRD2-Fc, CRD2-Fc and an atacept analog (CRD1+CRD2-Fc-a) showed no difference in their capability to bind to BAFF and APRIL, whereas CRD1-Fc exhibited little BAFF and APRIL

interaction. Thus, a different state of oligomerization of sTACI-short versus CRD2-Fc could be an explanation for the different observations in this study and in (140).

(e) This and the previous study (140) observed consistently that murine APRIL bound human TACI better than human APRIL. In that study trimeric murine APRIL (76) was used, while we used APRIL as an ARCP fused hexamer. It is unclear whether this contributes to the different results.

Hence, the most plausible explanation for our observed differences of affinity is the state of oligomerization of sTACI-short versus CRD2-Fc. The importance of dimerization for ligand binding has been observed in several previous studies (94, 200-203). For example, it was shown that different binding properties exist between sBCMA and BCMA-Fc (94). sBCMA is like sTACI shed from the cell surface and exists as a soluble receptor (94). sBCMA was produced with the same expression assay as our sTACI isoforms (94, 153). It was demonstrated that sBCMA was able to bind APRIL, while BCMA-Fc was able to bind BAFF and APRIL (94). This finding is in concordance with another study which observed similar findings when they compared BCMA-Fc which is a homodimer with a monomeric version of BCMA (203). The dimerization increased the binding affinity of BCMA (203).

To further validate our theory, we compared the dimer to the monomer of sTACI-long. We were able to separate the dimer from the monomer by SEC. We could detect a significant improvement of binding to BAFF and APRIL for the dimer, which we could also replicate by NF κ B assay. We could confirm that oligomerization improves ligand/receptor interaction.

We noted that our sTACI-preparations contained variants that differ in the length of the stretches outside of the CRDs. This allowed us to analyze the contributions of these stretches to ligand binding. Specifically, our sTACI-short preparation contained the full-length sTACI-short (1-20-W-68-154) and sTACI-short (16-20-W-68-135) which we separated by SEC. Additionally, we cloned sTACI-short (W-68-154) as another N-terminal variant. We compared the three N-terminal variants for their binding properties to analyze a possible contribution of the N-terminal amino acids to ligand binding. We found that all N-terminal variants showed no difference in binding to BAFF. In contrast, sTACI-short (1-20-W-68-154) bound with significantly higher affinity to APRIL than sTACI-short (16-20-W-68-135) and sTACI-short (W-58-154). sTACI-short (16-20-W-68-135) lacks 19 amino

acids at the C-terminus outside of the CRD2 which are present in the other two versions of sTACI-short. This could contribute to the reduced binding affinity to APRIL. The abolished APRIL binding of sTACI-short (W-68-154) indicates, however, that the N-terminal part is crucial for binding to APRIL. Hence, these amino acids N-terminal outside of CRD2 have little effect on BAFF-binding, but seem to contribute to the (weak) APRIL binding of sTACI-short.

The BAFF/APRIL system is very diverse. Further analysis of our proteins with all different variations of ligands like the BAFF60mer (83) or the heterotrimers of BAFF and APRIL (74, 88, 89) could improve the understanding of this complex system.

5.3. EXPRESSION, SHEDDING, LIGAND BINDING AND OLIGOMERIZATION OF MEMBRANE-BOUND TACI-LONG AND TACI-SHORT

5.3.1. EXPRESSION, SHEDDING AND LIGAND BINDING

We found that TACI-short was expressed and also constitutively shed in higher amount from transiently transfected HEK293T cells than TACI-long. Both TACI-long and TACI-short could bind to BAFF and APRIL.

TACI had already been tested by cell based assay for its binding ability to BAFF and APRIL after identifying TACI as a possible receptor for BAFF (137, 146, 204). It was shown that TACI could bind to BAFF and APRIL in a similar assay set up as ours and that binding of the ligands lead to NF κ B activation (137). Another study compared membrane-bound TACI-long and TACI-short (146). That study found that (i) both isoforms are equally expressed when transfected on a murine B-cell line, (ii) both isoforms can bind to BAFF and APRIL and (iii) the shorter isoform seems to be more potent at inducing plasma cell differentiation independent of a ligand (146).

Concerning membrane-bound studies, several different possibilities should be taken under consideration for future studies. Higher expression of TACI-short in comparison to TACI-long could lead to higher amount of BAFF and APRIL bound to TACI-short transfected cells. In general, cell surface oligomerization is known to be important for interaction of ligands with transmembrane receptors (205, 206), which most likely correlates to membrane-expression. First, the difference of expression of our isoforms could be compensated by co-transfecting the constructs with an EGFP tracer for expression (151, 207). The EGFP tracer would be used to indicate the general transfection and expression efficiency. Second, in another set of experiments we could see that different proteases seem to cause the shedding of TACI from HEK293T in comparison to B-cells (data not shown). Although HEK293T cells do not endogenously express TACI (208), the usage of human B-cells subtypes that do not express TACI should be discussed as a more physiological solution. Therefore, EBV immortalized B-cells from TACI deficient CVID patients could be used and checked for different expression and binding abilities for BAFF and APRIL after being transduced with either TACI-long or TACI-short. Finally, the

ability of our sTACI isoforms to bind to membrane-bound BAFF should be analyzed. APRIL cannot be assessed as it is not expressed on the cell surface. The U373 MG cell line which is known to express BAFF (and APRIL) could be used and tested for binding of both sTACI isoforms (209, 210). It could be evaluated if shedding of BAFF is inhibited by sTACI binding which would indicate another negative effect of TACI on immunity. Several previous studies examined the possibility of reverse signaling through soluble versions of TACI, although no general consensus has been found (59, 211-217).

5.3.2. HOMOTYPIC AND HETEROTYPIC INTERACTION

After assessing oligomerization of our soluble recombinant proteins extensively, we wanted to see whether we could extend our findings to membrane-bound TACI. Both TACI-long and TACI-short interacted homotypically and heterotypically with each other in soluble and membrane-bound form as seen by Co-IP from cells simultaneously transfected with TACI-long and TACI-short. This is the first time that a homotypic interaction has been described for TACI-short and a heterotypic interaction between both receptors. Neither of the TACI isoforms interacted in any way with BCMA.

Co-Immunoprecipitation is a commonly employed method to analyze protein-protein interactions (218, 219). This method had already been used before to analyze TACI-ligand (136-138, 145) and TACI-TACI interactions (93). One limitation of this approach is that we do not know and cannot say whether the proteins form dimers or higher oligomers. We can only prove the existence of an interaction. Therefore, FRET analysis (220, 221) and Fluorescence Correlation Spectroscopy (FCS) (222-224) could be used to give more insight into oligomerization. FRET analysis is based on donor acceptor energy transfer (220) and FCS on changes in fluorescence intensity (225). Last, the TACI-long/TACI-short heteromers could be analyzed for their functionality within the BAFF/APRIL system and existence in vivo, similar to the BAFF and APRIL heteromers (88-90).

6. CONCLUSION AND OUTLOOK

We observed differences in the binding affinity, decoy function and oligomerization between sTACI-long and sTACI-short. This increases our knowledge about the complexity of the BAFF/APRIL system. Next, antibodies should be developed that distinguish both isoforms and to quantify the relative abundance of both isoforms in human body fluids. In previous studies from our lab sTACI was found to be a potentially useful biomarker in MS and SLE (93) and also in primary CNS lymphoma (96). The development of ELISAs distinguishing the two isoforms of TACI might improve its use as a biomarker.

Concerning membrane-bound TACI isoforms, further studies with the isoform specific antibodies could determine the distribution of both isoforms on different B-cell subsets and show which isoform is predominating at which step of B-cell differentiation. Next, an association of B-cell pathologies to isoform specific B-cell subsets could be analyzed. If an association is found, the isoform specific antibodies could be used therapeutically to target directly identified subsets. Moreover, a general effect of B-cell depletion therapy such as rituximab on the B-cell repertoire, especially TACI expression, could be analyzed to assess whether B-cell depletion changes the population.

7. REFERENCES

1. Milo R, Kahana E. Multiple sclerosis: geoepidemiology, genetics and the environment. *Autoimmunity reviews*. 2010;9(5):A387-94.
2. Pietrangelo A, Higuera V. *Multiple Sclerosis by the Numbers: Facts, Statistics, and You* New York, San Francisco: Healthline; 2015 [cited 2018 31.01.2018]. Available from: <https://www.healthline.com/health/multiple-sclerosis/facts-statistics-infographic>.
3. Alonso A, Hernan MA. Temporal trends in the incidence of multiple sclerosis: a systematic review. *Neurology*. 2008;71(2):129-35.
4. Pugliatti M, Rosati G, Carton H, Riise T, Drulovic J, Vecsei L, et al. The epidemiology of multiple sclerosis in Europe. *European journal of neurology*. 2006;13(7):700-22.
5. Flachenecker P, Zettl UK, Gotze U, Haas J, Schimrigk S, Elias W, et al. [MS registry in Germany-- design and first results of the pilot phase]. *Der Nervenarzt*. 2005;76(8):967-75.
6. Bronnum-Hansen H, Koch-Henriksen N, Stenager E. Trends in survival and cause of death in Danish patients with multiple sclerosis. *Brain : a journal of neurology*. 2004;127(Pt 4):844-50.
7. McDonald WI, Compston A, Edan G, Goodkin D, Hartung HP, Lublin FD, et al. Recommended diagnostic criteria for multiple sclerosis: guidelines from the International Panel on the diagnosis of multiple sclerosis. *Annals of neurology*. 2001;50(1):121-7.
8. Polman CH, Reingold SC, Banwell B, Clanet M, Cohen JA, Filippi M, et al. Diagnostic criteria for multiple sclerosis: 2010 revisions to the McDonald criteria. *Annals of neurology*. 2011;69(2):292-302.
9. Lublin FD, Reingold SC. Defining the clinical course of multiple sclerosis: results of an international survey. *National Multiple Sclerosis Society (USA) Advisory Committee on Clinical Trials of New Agents in Multiple Sclerosis*. *Neurology*. 1996;46(4):907-11.
10. Lublin FD, Reingold SC, Cohen JA, Cutter GR, Sorensen PS, Thompson AJ, et al. Defining the clinical course of multiple sclerosis: the 2013 revisions. *Neurology*. 2014;83(3):278-86.
11. Hoffmann F, Meinl E. B cells in multiple sclerosis: good or bad guys?: An article for 28 May 2014 - World MS Day 2014. *European journal of immunology*. 2014;44(5):1247-50.
12. McKay KA, Kwan V, Duggan T, Tremlett H. Risk factors associated with the onset of relapsing-remitting and primary progressive multiple sclerosis: a systematic review. *BioMed research international*. 2015;2015:817238.
13. Dendrou CA, Fugger L, Friese MA. Immunopathology of multiple sclerosis. *Nature reviews Immunology*. 2015;15(9):545-58.
14. Robertson NP, Clayton D, Fraser M, Deans J, Compston DA. Clinical concordance in sibling pairs with multiple sclerosis. *Neurology*. 1996;47(2):347-52.
15. Sadovnick AD, Baird PA. The familial nature of multiple sclerosis: age-corrected empiric recurrence risks for children and siblings of patients. *Neurology*. 1988;38(6):990-1.
16. Jersild C, Svejgaard A, Fog T. HL-A antigens and multiple sclerosis. *Lancet (London, England)*. 1972;1(7762):1240-1.
17. Naito S, Namerow N, Mickey MR, Terasaki PI. Multiple sclerosis: association with HL-A3. *Tissue antigens*. 1972;2(1):1-4.
18. Cree BA. Multiple sclerosis genetics. *Handbook of clinical neurology*. 2014;122:193-209.
19. Beecham AH, Patsopoulos NA, Xifara DK, Davis MF, Kempainen A, Cotsapas C, et al. Analysis of immune-related loci identifies 48 new susceptibility variants for multiple sclerosis. *Nature genetics*. 2013;45(11):1353-60.
20. Kurtzke JF. A reassessment of the distribution of multiple sclerosis. Part one. *Acta neurologica Scandinavica*. 1975;51(2):110-36.

21. Elian M, Nightingale S, Dean G. Multiple sclerosis among United Kingdom-born children of immigrants from the Indian subcontinent, Africa and the West Indies. *Journal of neurology, neurosurgery, and psychiatry*. 1990;53(10):906-11.
22. Kurtzke JF. Epidemiologic evidence for multiple sclerosis as an infection. *Clinical microbiology reviews*. 1993;6(4):382-427.
23. Marrie RA. Environmental risk factors in multiple sclerosis aetiology. *The Lancet Neurology*. 2004;3(12):709-18.
24. Mark BL, Carson JA. Vitamin D and autoimmune disease--implications for practice from the multiple sclerosis literature. *Journal of the American Dietetic Association*. 2006;106(3):418-24.
25. Ramagopalan SV, Dobson R, Meier UC, Giovannoni G. Multiple sclerosis: risk factors, prodromes, and potential causal pathways. *The Lancet Neurology*. 2010;9(7):727-39.
26. Rudolf Manfred Schmidt FH, Jürgen H. Faiss, Wolfgang Köhler, Uwe K. Zettl. *Multiple Sklerose*. 7 ed. München: Urban & Fischer Verlag/Elsevier GmbH; 2017.
27. Charcot J. Histologie de la sclérose en plaques. *Gazette Hôpitaux* 1868;41: 554, 7–8, 66.
28. Popescu BF, Pirko I, Lucchinetti CF. Pathology of multiple sclerosis: where do we stand? *Continuum (Minneapolis, Minn)*. 2013;19(4 Multiple Sclerosis):901-21.
29. Hacke W. *Neurologie*. 14. ed. Hacke W, editor: Springer Verlag; 2015.
30. Popescu BF, Lucchinetti CF. Pathology of demyelinating diseases. *Annual review of pathology*. 2012;7:185-217.
31. Martino G, Adorini L, Rieckmann P, Hillert J, Kallmann B, Comi G, et al. Inflammation in multiple sclerosis: the good, the bad, and the complex. *The Lancet Neurology*. 2002;1(8):499-509.
32. Bruck W. The pathology of multiple sclerosis is the result of focal inflammatory demyelination with axonal damage. *Journal of neurology*. 2005;252 Suppl 5:v3-9.
33. Lucchinetti C, Bruck W, Parisi J, Scheithauer B, Rodriguez M, Lassmann H. Heterogeneity of multiple sclerosis lesions: implications for the pathogenesis of demyelination. *Annals of neurology*. 2000;47(6):707-17.
34. Henderson AP, Barnett MH, Parratt JD, Prineas JW. Multiple sclerosis: distribution of inflammatory cells in newly forming lesions. *Annals of neurology*. 2009;66(6):739-53.
35. Gildeen DH. Infectious causes of multiple sclerosis. *The Lancet Neurology*. 2005;4(3):195-202.
36. Derfuss T, Gurkov R, Then Bergh F, Goebels N, Hartmann M, Barz C, et al. Intrathecal antibody production against *Chlamydia pneumoniae* in multiple sclerosis is part of a polyspecific immune response. *Brain : a journal of neurology*. 2001;124(Pt 7):1325-35.
37. Derfuss T, Hohlfeld R, Meinl E. Intrathecal antibody (IgG) production against human herpesvirus type 6 occurs in about 20% of multiple sclerosis patients and might be linked to a polyspecific B-cell response. *Journal of neurology*. 2005;252(8):968-71.
38. Derfuss T, Hohlfeld R, Meinl E. [Multiple sclerosis. Chlamydia hypothesis in debate]. *Der Nervenarzt*. 2001;72(10):820-3.
39. Otto C, Oltmann A, Stein A, Frenzel K, Schroeter J, Habel P, et al. Intrathecal EBV antibodies are part of the polyspecific immune response in multiple sclerosis. *Neurology*. 2011;76(15):1316-21.
40. Serafini B, Rosicarelli B, Franciotta D, Magliozzi R, Reynolds R, Cinque P, et al. Dysregulated Epstein-Barr virus infection in the multiple sclerosis brain. *The Journal of experimental medicine*. 2007;204(12):2899-912.
41. Willis SN, Stadelmann C, Rodig SJ, Caron T, Gattenloehner S, Mallozzi SS, et al. Epstein-Barr virus infection is not a characteristic feature of multiple sclerosis brain. *Brain : a journal of neurology*. 2009;132(Pt 12):3318-28.
42. Sargsyan SA, Shearer AJ, Ritchie AM, Burgoon MP, Anderson S, Hemmer B, et al. Absence of Epstein-Barr virus in the brain and CSF of patients with multiple sclerosis. *Neurology*. 2010;74(14):1127-35.

43. Lassmann H, Niedobitek G, Aloisi F, Middelorp JM. Epstein-Barr virus in the multiple sclerosis brain: a controversial issue--report on a focused workshop held in the Centre for Brain Research of the Medical University of Vienna, Austria. *Brain : a journal of neurology*. 2011;134(Pt 9):2772-86.
44. Balashov KE, Aung LL, Dhib-Jalbut S, Keller IA. Acute multiple sclerosis lesion: conversion of restricted diffusion due to vasogenic edema. *Journal of neuroimaging : official journal of the American Society of Neuroimaging*. 2011;21(2):202-4.
45. Hohlfeld R, Dornmair K, Meinl E, Wekerle H. The search for the target antigens of multiple sclerosis, part 1: autoreactive CD4+ T lymphocytes as pathogenic effectors and therapeutic targets. *The Lancet Neurology*. 2015. 15(2):198-209
46. Hohlfeld R, Dornmair K, Meinl E, Wekerle H. The search for the target antigens of multiple sclerosis, part 2: CD8+ T cells, B cells, and antibodies in the focus of reverse-translational research. *The Lancet Neurology*. 2016;15(3):317-31.
47. Mirshafiey A, Kianiaslani M. Autoantigens and autoantibodies in multiple sclerosis. *Iranian journal of allergy, asthma, and immunology*. 2013;12(4):292-303.
48. Vojdani A, Vojdani E, Cooper E. Antibodies to myelin basic protein, myelin oligodendrocytes peptides, alpha-beta-crystallin, lymphocyte activation and cytokine production in patients with multiple sclerosis. *Journal of internal medicine*. 2003;254(4):363-74.
49. Bruno R, Sabater L, Sospedra M, Ferrer-Francesch X, Escudero D, Martinez-Caceres E, et al. Multiple sclerosis candidate autoantigens except myelin oligodendrocyte glycoprotein are transcribed in human thymus. *European journal of immunology*. 2002;32(10):2737-47.
50. Barkhof F, van Walderveen M. Characterization of tissue damage in multiple sclerosis by nuclear magnetic resonance. *Philosophical transactions of the Royal Society of London Series B, Biological sciences*. 1999;354(1390):1675-86.
51. Wekerle H. B cells in multiple sclerosis. *Autoimmunity*. 2017;50(1):57-60.
52. Krumbholz M, Derfuss T, Hohlfeld R, Meinl E. B cells and antibodies in multiple sclerosis pathogenesis and therapy. *Nature reviews Neurology*. 2012;8(11):613-23.
53. Serafini B, Rosicarelli B, Magliozzi R, Stigliano E, Aloisi F. Detection of ectopic B-cell follicles with germinal centers in the meninges of patients with secondary progressive multiple sclerosis. *Brain pathology (Zurich, Switzerland)*. 2004;14(2):164-74.
54. Esiri MM. Multiple sclerosis: a quantitative and qualitative study of immunoglobulin-containing cells in the central nervous system. *Neuropathology and applied neurobiology*. 1980;6(1):9-21.
55. Lucchinetti CF, Popescu BF, Bunyan RF, Moll NM, Roemer SF, Lassmann H, et al. Inflammatory cortical demyelination in early multiple sclerosis. *The New England journal of medicine*. 2011;365(23):2188-97.
56. Zettervall O, Link H. Electrophoretic distribution of kappa and lambda immunoglobulin light chain determinants in serum and cerebrospinal fluid in multiple sclerosis. *Clinical and experimental immunology*. 1970;7(3):365-72.
57. Obermeier B, Mentele R, Malotka J, Kellermann J, Kumpfel T, Wekerle H, et al. Matching of oligoclonal immunoglobulin transcriptomes and proteomes of cerebrospinal fluid in multiple sclerosis. *Nature medicine*. 2008;14(6):688-93.
58. Brandle SM, Obermeier B, Senel M, Bruder J, Mentele R, Khademi M, et al. Distinct oligoclonal band antibodies in multiple sclerosis recognize ubiquitous self-proteins. *Proceedings of the National Academy of Sciences of the United States of America*. 2016;113(28):7864-9.
59. Nys J, Smulski CR, Tardivel A, Willen L, Kowalczyk C, Donze O, et al. No evidence that soluble TACI induces signalling via membrane-expressed BAFF and APRIL in myeloid cells. *PloS one*. 2013;8(4):e61350.
60. Stangel M, Fredrikson S, Meinl E, Petzold A, Stuve O, Tumani H. The utility of cerebrospinal fluid analysis in patients with multiple sclerosis. *Nature reviews Neurology*. 2013;9(5):267-76.
61. Höftberger R, Mader SA, Reindl M. Cerebrospinal Fluid in Clinical Neurology 2015. 143-58 p.

62. Walsh MJ, Tourtellotte WW. Temporal invariance and clonal uniformity of brain and cerebrospinal IgG, IgA, and IgM in multiple sclerosis. *The Journal of experimental medicine*. 1986;163(1):41-53.
63. Krumbholz M, Theil D, Derfuss T, Rosenwald A, Schrader F, Monoranu CM, et al. BAFF is produced by astrocytes and up-regulated in multiple sclerosis lesions and primary central nervous system lymphoma. *The Journal of experimental medicine*. 2005;201(2):195-200.
64. Krumbholz M, Theil D, Cepok S, Hemmer B, Kivisakk P, Ransohoff RM, et al. Chemokines in multiple sclerosis: CXCL12 and CXCL13 up-regulation is differentially linked to CNS immune cell recruitment. *Brain : a journal of neurology*. 2006;129(Pt 1):200-11.
65. von Budingen HC, Kuo TC, Sirota M, van Belle CJ, Apeltsin L, Glanville J, et al. B cell exchange across the blood-brain barrier in multiple sclerosis. *The Journal of clinical investigation*. 2012;122(12):4533-43.
66. Stern JN, Yaari G, Vander Heiden JA, Church G, Donahue WF, Hintzen RQ, et al. B cells populating the multiple sclerosis brain mature in the draining cervical lymph nodes. *Science translational medicine*. 2014;6(248):248ra107.
67. Krishnamoorthy G, Lassmann H, Wekerle H, Holz A. Spontaneous opticospinal encephalomyelitis in a double-transgenic mouse model of autoimmune T cell/B cell cooperation. *The Journal of clinical investigation*. 2006;116(9):2385-92.
68. Krishnamoorthy G, Saxena A, Mars LT, Domingues HS, Mentele R, Ben-Nun A, et al. Myelin-specific T cells also recognize neuronal autoantigen in a transgenic mouse model of multiple sclerosis. *Nature medicine*. 2009;15(6):626-32.
69. Pollinger B, Krishnamoorthy G, Berer K, Lassmann H, Bosl MR, Dunn R, et al. Spontaneous relapsing-remitting EAE in the SJL/J mouse: MOG-reactive transgenic T cells recruit endogenous MOG-specific B cells. *The Journal of experimental medicine*. 2009;206(6):1303-16.
70. Hauser SL, Waubant E, Arnold DL, Vollmer T, Antel J, Fox RJ, et al. B-cell depletion with rituximab in relapsing-remitting multiple sclerosis. *The New England journal of medicine*. 2008;358(7):676-88.
71. Kappos L, Li D, Calabresi PA, O'Connor P, Bar-Or A, Barkhof F, et al. Ocrelizumab in relapsing-remitting multiple sclerosis: a phase 2, randomised, placebo-controlled, multicentre trial. *Lancet (London, England)*. 2011;378(9805):1779-87.
72. Sabatino JJ, Jr., Zamvil SS, Hauser SL. B-Cell Therapies in Multiple Sclerosis. *Cold Spring Harbor perspectives in medicine*. 2018. a032037.
73. Frampton JE. Ocrelizumab: First Global Approval. *Drugs*. 2017;77(9):1035-41.
74. Samy E, Wax S, Huard B, Hess H, Schneider P. Targeting BAFF and APRIL in systemic lupus erythematosus and other antibody-associated diseases. *International reviews of immunology*. 2017;36(1):3-19.
75. Cancro MP. BLYS Ligands and Receptors. 1 ed. Totowa, NJ: Humana Press; 2010.
76. Wallweber HJ, Compaan DM, Starovasnik MA, Hymowitz SG. The crystal structure of a proliferation-inducing ligand, APRIL. *Journal of molecular biology*. 2004;343(2):283-90.
77. Oren DA, Li Y, Volovik Y, Morris TS, Dharia C, Das K, et al. Structural basis of BLYS receptor recognition. *Nature structural biology*. 2002;9(4):288-92.
78. Karpusas M, Cachero TG, Qian F, Boriack-Sjodin A, Mullen C, Strauch K, et al. Crystal structure of extracellular human BAFF, a TNF family member that stimulates B lymphocytes. *Journal of molecular biology*. 2002;315(5):1145-54.
79. Bodmer JL, Schneider P, Tschopp J. The molecular architecture of the TNF superfamily. *Trends in biochemical sciences*. 2002;27(1):19-26.
80. Schneider P, MacKay F, Steiner V, Hofmann K, Bodmer JL, Holler N, et al. BAFF, a novel ligand of the tumor necrosis factor family, stimulates B cell growth. *The Journal of experimental medicine*. 1999;189(11):1747-56.

81. Moore PA, Belvedere O, Orr A, Pieri K, LaFleur DW, Feng P, et al. BlyS: member of the tumor necrosis factor family and B lymphocyte stimulator. *Science*. 1999;285(5425):260-3.
82. Lopez-Fraga M, Fernandez R, Albar JP, Hahne M. Biologically active APRIL is secreted following intracellular processing in the Golgi apparatus by furin convertase. *EMBO reports*. 2001;2(10):945-51.
83. Liu Y, Xu L, Opalka N, Kappler J, Shu HB, Zhang G. Crystal structure of sTALL-1 reveals a virus-like assembly of TNF family ligands. *Cell*. 2002;108(3):383-94.
84. Zhukovsky EA, Lee JO, Villegas M, Chan C, Chu S, Mroske C. TNF ligands: is TALL-1 a trimer or a virus-like cluster? *Nature*. 2004;427(6973):413-4; discussion 4.
85. Cachero TG, Schwartz IM, Qian F, Day ES, Bossen C, Ingold K, et al. Formation of virus-like clusters is an intrinsic property of the tumor necrosis factor family member BAFF (B cell activating factor). *Biochemistry*. 2006;45(7):2006-13.
86. Ingold K, Zumsteg A, Tardivel A, Huard B, Steiner QG, Cachero TG, et al. Identification of proteoglycans as the APRIL-specific binding partners. *The Journal of experimental medicine*. 2005;201(9):1375-83.
87. Hendriks J, Planelles L, de Jong-Odding J, Hardenberg G, Pals ST, Hahne M, et al. Heparan sulfate proteoglycan binding promotes APRIL-induced tumor cell proliferation. *Cell death and differentiation*. 2005;12(6):637-48.
88. Schuepbach-Mallepell S, Das D, Willen L, Vigolo M, Tardivel A, Lebon L, et al. Stoichiometry of Heteromeric BAFF and APRIL Cytokines Dictates Their Receptor Binding and Signaling Properties. *J Biol Chem*. 2015;290(26):16330-42.
89. Maskos K, Lammens A, Tan SL, Hess H, Palinsky W, Schneider P, et al. Data for the crystal structure of APRIL-BAFF-BAFF heterotrimer. *Data in brief*. 2016;6:438-44.
90. Roschke V, Sosnovtseva S, Ward CD, Hong JS, Smith R, Albert V, et al. BlyS and APRIL form biologically active heterotrimers that are expressed in patients with systemic immune-based rheumatic diseases. *J Immunol*. 2002;169(8):4314-21.
91. Bossen C, Cachero TG, Tardivel A, Ingold K, Willen L, Dobles M, et al. TACI, unlike BAFF-R, is solely activated by oligomeric BAFF and APRIL to support survival of activated B cells and plasmablasts. *Blood*. 2008;111(3):1004-12.
92. Zhang Y, Li J, Zhang YM, Zhang XM, Tao J. Effect of TACI signaling on humoral immunity and autoimmune diseases. *Journal of immunology research*. 2015;2015:247426.
93. Hoffmann FS, Kuhn PH, Laurent SA, Hauck SM, Berer K, Wendlinger SA, et al. The immunoregulator soluble TACI is released by ADAM10 and reflects B cell activation in autoimmunity. *J Immunol*. 2015;194(2):542-52.
94. Laurent SA, Hoffmann FS, Kuhn PH, Cheng Q, Chu Y, Schmidt-Supprian M, et al. gamma-Secretase directly sheds the survival receptor BCMA from plasma cells. *Nature communications*. 2015;6:7333.
95. Kyrtsolis MC, Sarris K, Koulteris E, Maltezas D, Nikolaou E, Angelopoulou MK, et al. Serum soluble TACI, a BlyS receptor, is a powerful prognostic marker of outcome in chronic lymphocytic leukemia. *BioMed research international*. 2014;2014:159632.
96. Thaler FS, Laurent SA, Huber M, Mulazzani M, Dreyling M, Kodel U, et al. Soluble TACI and soluble BCMA as biomarkers in primary central nervous system lymphoma. *Neuro Oncol*. 2017.
97. Mackay F, Schneider P. Cracking the BAFF code. *Nature reviews Immunology*. 2009;9(7):491-502.
98. Steri M, Orru V, Idda ML, Pitzalis M, Pala M, Zara I, et al. Overexpression of the Cytokine BAFF and Autoimmunity Risk. *The New England journal of medicine*. 2017;376(17):1615-26.
99. Stohl W, Metyas S, Tan SM, Cheema GS, Oamar B, Xu D, et al. B lymphocyte stimulator overexpression in patients with systemic lupus erythematosus: longitudinal observations. *Arthritis and rheumatism*. 2003;48(12):3475-86.
100. Sabahi R, Anolik JH. B-cell-targeted therapy for systemic lupus erythematosus. *Drugs*. 2006;66(15):1933-48.

101. Dorner T. Crossroads of B cell activation in autoimmunity: rationale of targeting B cells. *The Journal of rheumatology Supplement*. 2006;77:3-11.
102. Ding C, Jones G. Belimumab Human Genome Sciences/Cambridge Antibody Technology/GlaxoSmithKline. *Current opinion in investigational drugs* (London, England : 2000). 2006;7(5):464-72.
103. Stohl W, Hilbert DM. The discovery and development of belimumab: the anti-BLyS-lupus connection. *Nature biotechnology*. 2012;30(1):69-77.
104. Gross JA, Johnston J, Mudri S, Enselman R, Dillon SR, Madden K, et al. TACI and BCMA are receptors for a TNF homologue implicated in B-cell autoimmune disease. *Nature*. 2000;404(6781):995-9.
105. Gross JA, Dillon SR, Mudri S, Johnston J, Littau A, Roque R, et al. TACI-Ig neutralizes molecules critical for B cell development and autoimmune disease. impaired B cell maturation in mice lacking BLyS. *Immunity*. 2001;15(2):289-302.
106. Yaccoby S, Pennisi A, Li X, Dillon SR, Zhan F, Barlogie B, et al. Atacicept (TACI-Ig) inhibits growth of TACI(high) primary myeloma cells in SCID-hu mice and in coculture with osteoclasts. *Leukemia*. 2008;22(2):406-13.
107. Canfield SM, Morrison SL. The binding affinity of human IgG for its high affinity Fc receptor is determined by multiple amino acids in the CH2 domain and is modulated by the hinge region. *The Journal of experimental medicine*. 1991;173(6):1483-91.
108. Tao MH, Smith RI, Morrison SL. Structural features of human immunoglobulin G that determine isotype-specific differences in complement activation. *The Journal of experimental medicine*. 1993;178(2):661-7.
109. Dall'Era M, Chakravarty E, Wallace D, Genovese M, Weisman M, Kavanaugh A, et al. Reduced B lymphocyte and immunoglobulin levels after atacicept treatment in patients with systemic lupus erythematosus: results of a multicenter, phase Ib, double-blind, placebo-controlled, dose-escalating trial. *Arthritis and rheumatism*. 2007;56(12):4142-50.
110. Tak PP, Thurlings RM, Rossier C, Nestorov I, Dimic A, Mircetic V, et al. Atacicept in patients with rheumatoid arthritis: results of a multicenter, phase Ib, double-blind, placebo-controlled, dose-escalating, single- and repeated-dose study. *Arthritis and rheumatism*. 2008;58(1):61-72.
111. Stohl W. Inhibition of B cell activating factor (BAFF) in the management of systemic lupus erythematosus (SLE). *Expert review of clinical immunology*. 2017. 13(6):623-633.
112. Cogollo E, Silva MA, Isenberg D. Profile of atacicept and its potential in the treatment of systemic lupus erythematosus. *Drug design, development and therapy*. 2015;9:1331-9.
113. Isenberg D, Gordon C, Licu D, Copt S, Rossi CP, Wofsy D. Efficacy and safety of atacicept for prevention of flares in patients with moderate-to-severe systemic lupus erythematosus (SLE): 52-week data (APRIL-SLE randomised trial). *Annals of the rheumatic diseases*. 2015;74(11):2006-15.
114. Hartung HP. [Atacicept: a new B lymphocyte-targeted therapy for multiple sclerosis]. *Der Nervenarzt*. 2009;80(12):1462-72.
115. Hartung HP, Kieseier BC. Atacicept: targeting B cells in multiple sclerosis. *Therapeutic advances in neurological disorders*. 2010;3(4):205-16.
116. Kappos L, Hartung HP, Freedman MS, Boyko A, Radu EW, Mikol DD, et al. Atacicept in multiple sclerosis (ATAMS): a randomised, placebo-controlled, double-blind, phase 2 trial. *The Lancet Neurology*. 2014;13(4):353-63.
117. Seshasayee D, Valdez P, Yan M, Dixit VM, Tumas D, Grewal IS. Loss of TACI causes fatal lymphoproliferation and autoimmunity, establishing TACI as an inhibitory BLyS receptor. *Immunity*. 2003;18(2):279-88.
118. Yan M, Wang H, Chan B, Roose-Girma M, Erickson S, Baker T, et al. Activation and accumulation of B cells in TACI-deficient mice. *Nat Immunol*. 2001;2(7):638-43.
119. von Bulow GU, van Deursen JM, Bram RJ. Regulation of the T-independent humoral response by TACI. *Immunity*. 2001;14(5):573-82.

120. Castigli E, Wilson SA, Garibyan L, Rachid R, Bonilla F, Schneider L, et al. TACI is mutant in common variable immunodeficiency and IgA deficiency. *Nature genetics*. 2005;37(8):829-34.
121. Castigli E, Wilson S, Garibyan L, Rachid R, Bonilla F, Schneider L, et al. Reexamining the role of TACI coding variants in common variable immunodeficiency and selective IgA deficiency. *Nature genetics*. 2007;39(4):430-1.
122. Salzer U, Chapel HM, Webster AD, Pan-Hammarstrom Q, Schmitt-Graeff A, Schlesier M, et al. Mutations in TNFRSF13B encoding TACI are associated with common variable immunodeficiency in humans. *Nature genetics*. 2005;37(8):820-8.
123. Salzer U, Bacchelli C, Buckridge S, Pan-Hammarstrom Q, Jennings S, Lougaris V, et al. Relevance of biallelic versus monoallelic TNFRSF13B mutations in distinguishing disease-causing from risk-increasing TNFRSF13B variants in antibody deficiency syndromes. *Blood*. 2009;113(9):1967-76.
124. Darce JR, Arendt BK, Wu X, Jelinek DF. Regulated expression of BAFF-binding receptors during human B cell differentiation. *J Immunol*. 2007;179(11):7276-86.
125. von Bulow GU, Bram RJ. NF-AT activation induced by a CAML-interacting member of the tumor necrosis factor receptor superfamily. *Science*. 1997;278(5335):138-41.
126. Castigli E, Wilson SA, Scott S, Dedeoglu F, Xu S, Lam KP, et al. TACI and BAFF-R mediate isotype switching in B cells. *The Journal of experimental medicine*. 2005;201(1):35-9.
127. Poodt AE, Driessen GJ, de Klein A, van Dongen JJ, van der Burg M, de Vries E. TACI mutations and disease susceptibility in patients with common variable immunodeficiency. *Clinical and experimental immunology*. 2009;156(1):35-9.
128. He B, Santamaria R, Xu W, Cols M, Chen K, Puga I, et al. The transmembrane activator TACI triggers immunoglobulin class switching by activating B cells through the adaptor MyD88. *Nat Immunol*. 2010;11(9):836-45.
129. Tsuji S, Cortesao C, Bram RJ, Platt JL, Cascalho M. TACI deficiency impairs sustained Blimp-1 expression in B cells decreasing long-lived plasma cells in the bone marrow. *Blood*. 2011;118(22):5832-9.
130. Ou X, Xu S, Lam KP. Deficiency in TNFRSF13B (TACI) expands T-follicular helper and germinal center B cells via increased ICOS-ligand expression but impairs plasma cell survival. *Proceedings of the National Academy of Sciences of the United States of America*. 2012;109(38):15401-6.
131. Tsuji S, Stein L, Kamada N, Nunez G, Bram R, Vallance BA, et al. TACI deficiency enhances antibody avidity and clearance of an intestinal pathogen. *The Journal of clinical investigation*. 2014;124(11):4857-66.
132. Kanno Y, Sakurai D, Hase H, Kojima H, Kobata T. TACI induces cIAP1-mediated ubiquitination of NIK by TRAF2 and TANK to limit non-canonical NF-kappaB signaling. *Journal of receptor and signal transduction research*. 2010;30(2):121-32.
133. Figgitt WA, Fairfax K, Vincent FB, Le Page MA, Katik I, Deliyanti D, et al. The TACI receptor regulates T-cell-independent marginal zone B cell responses through innate activation-induced cell death. *Immunity*. 2013;39(3):573-83.
134. Goenka R, Matthews AH, Zhang B, O'Neill PJ, Scholz JL, Migone TS, et al. Local BlyS production by T follicular cells mediates retention of high affinity B cells during affinity maturation. *The Journal of experimental medicine*. 2014;211(1):45-56.
135. Kreuzaler M, Rauch M, Salzer U, Birmelin J, Rizzi M, Grimbacher B, et al. Soluble BAFF levels inversely correlate with peripheral B cell numbers and the expression of BAFF receptors. *Journal of immunology (Baltimore, Md : 1950)*. 2012;188(1):497-503.
136. Marsters SA, Yan M, Pitti RM, Haas PE, Dixit VM, Ashkenazi A. Interaction of the TNF homologues BlyS and APRIL with the TNF receptor homologues BCMA and TACI. *Current biology : CB*. 2000;10(13):785-8.
137. Wu Y, Bressette D, Carrell JA, Kaufman T, Feng P, Taylor K, et al. Tumor necrosis factor (TNF) receptor superfamily member TACI is a high affinity receptor for TNF family members APRIL and BlyS. *J Biol Chem*. 2000;275(45):35478-85.

138. Yan M, Marsters SA, Grewal IS, Wang H, Ashkenazi A, Dixit VM. Identification of a receptor for BlyS demonstrates a crucial role in humoral immunity. *Nat Immunol.* 2000;1(1):37-41.
139. Yu G, Boone T, Delaney J, Hawkins N, Kelley M, Ramakrishnan M, et al. APRIL and TALL-I and receptors BCMA and TACI: system for regulating humoral immunity. *Nat Immunol.* 2000;1(3):252-6.
140. Hymowitz SG, Patel DR, Wallweber HJ, Runyon S, Yan M, Yin J, et al. Structures of APRIL-receptor complexes: like BCMA, TACI employs only a single cysteine-rich domain for high affinity ligand binding. *J Biol Chem.* 2005;280(8):7218-27.
141. Patel DR, Wallweber HJ, Yin J, Shriver SK, Marsters SA, Gordon NC, et al. Engineering an APRIL-specific B cell maturation antigen. *J Biol Chem.* 2004;279(16):16727-35.
142. Gordon NC, Pan B, Hymowitz SG, Yin J, Kelley RF, Cochran AG, et al. BAFF/BlyS receptor 3 comprises a minimal TNF receptor-like module that encodes a highly focused ligand-binding site. *Biochemistry.* 2003;42(20):5977-83.
143. Kim HM, Yu KS, Lee ME, Shin DR, Kim YS, Paik SG, et al. Crystal structure of the BAFF-BAFF-R complex and its implications for receptor activation. *Nature structural biology.* 2003;10(5):342-8.
144. Kayagaki N, Yan M, Seshasayee D, Wang H, Lee W, French DM, et al. BAFF/BlyS receptor 3 binds the B cell survival factor BAFF ligand through a discrete surface loop and promotes processing of NF-kappaB2. *Immunity.* 2002;17(4):515-24.
145. Garibyan L, Lobito AA, Siegel RM, Call ME, Wucherpennig KW, Geha RS. Dominant-negative effect of the heterozygous C104R TACI mutation in common variable immunodeficiency (CVID). *The Journal of clinical investigation.* 2007;117(6):1550-7.
146. Garcia-Carmona Y, Cols M, Ting AT, Radigan L, Yuk FJ, Zhang L, et al. Differential induction of plasma cells by isoforms of human TACI. *Blood.* 2015;125(11):1749-58.
147. Chaiet L, Wolf FJ. THE PROPERTIES OF STREPTAVIDIN, A BIOTIN-BINDING PROTEIN PRODUCED BY STREPTOMYCETES. *Archives of biochemistry and biophysics.* 1964;106:1-5.
148. Maley F, Trimble RB, Tarentino AL, Plummer TH, Jr. Characterization of glycoproteins and their associated oligosaccharides through the use of endoglycosidases. *Analytical biochemistry.* 1989;180(2):195-204.
149. Voet D, Voet JG. *Biochemistry.* 4. ed. New York, NY: John Wiley & Sons; 2011.
150. Malvern. Static Light Scattering technologies for GPC - SEC explained [Internet]: Malvern Instruments limited; 2015. Podcast
151. Schneider P, Willen L, Smulski CR. Tools and techniques to study ligand-receptor interactions and receptor activation by TNF superfamily members. *Methods in enzymology.* 2014;545:103-25.
152. Allard STM, Kopish K. Luciferase Reporter Assays: Powerful, Adaptable Tools for Cell Biology Research. *Cell Notes.* 2008;21:23-26.
153. Perera NC, Wiesmuller KH, Larsen MT, Schacher B, Eickholz P, Borregaard N, et al. NSP4 is stored in azurophil granules and released by activated neutrophils as active endoprotease with restricted specificity. *J Immunol.* 2013;191(5):2700-7.
154. Gavel Y, von Heijne G. Sequence differences between glycosylated and non-glycosylated Asn-X-Thr/Ser acceptor sites: implications for protein engineering. *Protein engineering.* 1990;3(5):433-42.
155. Chuang GY, Boyington JC, Joyce MG, Zhu J, Nabel GJ, Kwong PD, et al. Computational prediction of N-linked glycosylation incorporating structural properties and patterns. *Bioinformatics (Oxford, England).* 2012;28(17):2249-55.
156. Petrescu AJ, Milac AL, Petrescu SM, Dwek RA, Wormald MR. Statistical analysis of the protein environment of N-glycosylation sites: implications for occupancy, structure, and folding. *Glycobiology.* 2004;14(2):103-14.
157. Zielinska DF, Gnad F, Wisniewski JR, Mann M. Precision mapping of an in vivo N-glycoproteome reveals rigid topological and sequence constraints. *Cell.* 2010;141(5):897-907.
158. Mayer MC, Breithaupt C, Reindl M, Schanda K, Rostasy K, Berger T, et al. Distinction and temporal stability of conformational epitopes on myelin oligodendrocyte glycoprotein recognized by

- patients with different inflammatory central nervous system diseases. *Journal of immunology* (Baltimore, Md : 1950). 2013;191(7):3594-604.
159. Thomas G. Furin at the cutting edge: from protein traffic to embryogenesis and disease. *Nat Rev Mol Cell Biol*. 2002;3(10):753-66.
160. Bobrovnik SA. Determination of antibody affinity by ELISA. Theory. *Journal of biochemical and biophysical methods*. 2003;57(3):213-36.
161. Raghava GP, Agrewala JN. Method for determining the affinity of monoclonal antibody using non-competitive ELISA: a computer program. *Journal of immunoassay*. 1994;15(2):115-28.
162. Rosenbluh J, Kapelnikov A, Shalev DE, Rusnati M, Bugatti A, Loyter A. Positively charged peptides can interact with each other, as revealed by solid phase binding assays. *Analytical biochemistry*. 2006;352(2):157-68.
163. Thaler FS, Laurent SA, Huber M, Mulazzani M, Dreyling M, Kodel U, et al. Soluble TACI and soluble BCMA as biomarkers in primary central nervous system lymphoma. *Neuro-oncology*. 2017;19(12):1618-27.
164. Garred O, van Deurs B, Sandvig K. Furin-induced cleavage and activation of Shiga toxin. *J Biol Chem*. 1995;270(18):10817-21.
165. Stieneke-Grober A, Vey M, Angliker H, Shaw E, Thomas G, Roberts C, et al. Influenza virus hemagglutinin with multibasic cleavage site is activated by furin, a subtilisin-like endoprotease. *The EMBO journal*. 1992;11(7):2407-14.
166. Lin L, Nemeth E, Goodnough JB, Thapa DR, Gabayan V, Ganz T. Soluble hemojuvelin is released by proprotein convertase-mediated cleavage at a conserved polybasic RNRR site. *Blood cells, molecules & diseases*. 2008;40(1):122-31.
167. Hymowitz SG, Christinger HW, Fuh G, Ultsch M, O'Connell M, Kelley RF, et al. Triggering cell death: the crystal structure of Apo2L/TRAIL in a complex with death receptor 5. *Molecular cell*. 1999;4(4):563-71.
168. Banner DW, D'Arcy A, Janes W, Gentz R, Schoenfeld HJ, Broger C, et al. Crystal structure of the soluble human 55 kd TNF receptor-human TNF beta complex: implications for TNF receptor activation. *Cell*. 1993;73(3):431-45.
169. Cha SS, Sung BJ, Kim YA, Song YL, Kim HJ, Kim S, et al. Crystal structure of TRAIL-DR5 complex identifies a critical role of the unique frame insertion in conferring recognition specificity. *J Biol Chem*. 2000;275(40):31171-7.
170. Mongkolsapaya J, Grimes JM, Chen N, Xu XN, Stuart DI, Jones EY, et al. Structure of the TRAIL-DR5 complex reveals mechanisms conferring specificity in apoptotic initiation. *Nature structural biology*. 1999;6(11):1048-53.
171. Trivedi MV, Laurence JS, Siahaan TJ. The role of thiols and disulfides on protein stability. *Current protein & peptide science*. 2009;10(6):614-25.
172. Cook KM, Hogg PJ. Post-translational control of protein function by disulfide bond cleavage. *Antioxidants & redox signaling*. 2013;18(15):1987-2015.
173. Feige MJ, Hendershot LM. Disulfide bonds in ER protein folding and homeostasis. *Current opinion in cell biology*. 2011;23(2):167-75.
174. Papale GA, Hanson PJ, Sahoo D. Extracellular disulfide bonds support scavenger receptor class B type I-mediated cholesterol transport. *Biochemistry*. 2011;50(28):6245-54.
175. Schulein R, Zuhlke K, Oksche A, Hermosilla R, Furkert J, Rosenthal W. The role of conserved extracellular cysteine residues in vasopressin V2 receptor function and properties of two naturally occurring mutant receptors with additional extracellular cysteine residues. *FEBS letters*. 2000;466(1):101-6.
176. Perlman JH, Wang W, Nussenzveig DR, Gershengorn MC. A disulfide bond between conserved extracellular cysteines in the thyrotropin-releasing hormone receptor is critical for binding. *J Biol Chem*. 1995;270(42):24682-5.

177. Graslund S, Nordlund P, Weigelt J, Hallberg BM, Bray J, Gileadi O, et al. Protein production and purification. *Nature methods*. 2008;5(2):135-46.
178. Lee JJ, Jabara HH, Garibyan L, Rauter I, Sannikova T, Dillon SR, et al. The C104R mutant impairs the function of transmembrane activator and calcium modulator and cyclophilin ligand interactor (TACI) through haploinsufficiency. *J Allergy Clin Immunol*. 2010;126(6):1234-41.e2.
179. Romberg N, Virdee M, Chamberlain N, Oe T, Schickel JN, Perkins T, et al. TNF receptor superfamily member 13b (TNFRSF13B) hemizyosity reveals transmembrane activator and CAML interactor haploinsufficiency at later stages of B-cell development. *J Allergy Clin Immunol*. 2015. 136(5):1315-25.
180. Valley CC, Lewis AK, Mudaliar DJ, Perlmutter JD, Braun AR, Karim CB, et al. Tumor necrosis factor-related apoptosis-inducing ligand (TRAIL) induces death receptor 5 networks that are highly organized. *J Biol Chem*. 2012;287(25):21265-78.
181. Reyes-Moreno C, Girouard J, Lapointe R, Darveau A, Mourad W. CD40/CD40 homodimers are required for CD40-induced phosphatidylinositol 3-kinase-dependent expression of B7.2 by human B lymphocytes. *J Biol Chem*. 2004;279(9):7799-806.
182. Girouard J, Reyes-Moreno C, Darveau A, Akoum A, Mourad W. Requirement of the extracellular cysteine at position six for CD40/CD40 dimer formation and CD40-induced IL-8 expression. *Molecular immunology*. 2005;42(7):773-80.
183. Reyes-Moreno C, Sharif-Askari E, Girouard J, Leveille C, Jundi M, Akoum A, et al. Requirement of oxidation-dependent CD40 homodimers for CD154/CD40 bidirectional signaling. *J Biol Chem*. 2007;282(27):19473-80.
184. Smulski CR, Beyrath J, Decossas M, Chekkat N, Wolff P, Estieu-Gionnet K, et al. Cysteine-rich domain 1 of CD40 mediates receptor self-assembly. *J Biol Chem*. 2013;288(15):10914-22.
185. Nozaki Y, Tanford C. The solubility of amino acids and related compounds in aqueous urea solutions. *J Biol Chem*. 1963;238:4074-81.
186. Zhou R, Li J, Hua L, Yang Z, Berne BJ. Comment on "urea-mediated protein denaturation: a consensus view". *The journal of physical chemistry B*. 2011;115(5):1323-6; discussion 7-8.
187. Bennion BJ, Daggett V. The molecular basis for the chemical denaturation of proteins by urea. *Proceedings of the National Academy of Sciences of the United States of America*. 2003;100(9):5142-7.
188. Varki A. Biological roles of oligosaccharides: all of the theories are correct. *Glycobiology*. 1993;3(2):97-130.
189. Partridge EA, Le Roy C, Di Guglielmo GM, Pawling J, Cheung P, Granovsky M, et al. Regulation of cytokine receptors by Golgi N-glycan processing and endocytosis. *Science*. 2004;306(5693):120-4.
190. Huang HW, Chen CH, Lin CH, Wong CH, Lin KI. B-cell maturation antigen is modified by a single N-glycan chain that modulates ligand binding and surface retention. *Proceedings of the National Academy of Sciences of the United States of America*. 2013;110(27):10928-33.
191. Pulvertaft JV. Cytology of burkitt's tumour (african lymphoma). *Lancet*. 1964;1(7327):238-40.
192. Epstein MA, Achong BG, Barr YM. Virus particles in cultured lymphoblasts from burkitt's lymphoma. *Lancet*. 1964;1(7335):702-3.
193. Karpova MB, Schoumans J, Ernberg I, Henter JI, Nordenskjold M, Fadeel B. Raji revisited: cytogenetics of the original Burkitt's lymphoma cell line. *Leukemia*. 2005;19(1):159-61.
194. Karlsson R, Michaelsson A, Mattsson L. Kinetic analysis of monoclonal antibody-antigen interactions with a new biosensor based analytical system. *Journal of immunological methods*. 1991;145(1-2):229-40.
195. Karlsson R. SPR for molecular interaction analysis: a review of emerging application areas. *Journal of molecular recognition : JMR*. 2004;17(3):151-61.
196. Heinrich L, Tissot N, Hartmann DJ, Cohen R. Comparison of the results obtained by ELISA and surface plasmon resonance for the determination of antibody affinity. *Journal of immunological methods*. 2010;352(1-2):13-22.

197. Hannig G, Makrides SC. Strategies for optimizing heterologous protein expression in *Escherichia coli*. *Trends in biotechnology*. 1998;16(2):54-60.
198. Rogl H, Kosemund K, Kuhlbrandt W, Collinson I. Refolding of *Escherichia coli* produced membrane protein inclusion bodies immobilised by nickel chelating chromatography. *FEBS letters*. 1998;432(1-2):21-6.
199. Unger T, Peleg Y. Recombinant protein expression in the baculovirus-infected insect cell system. *Methods in molecular biology*. 2012;800:187-99.
200. Pabbisetty KB, Yue X, Li C, Himanen JP, Zhou R, Nikolov DB, et al. Kinetic analysis of the binding of monomeric and dimeric ephrins to Eph receptors: correlation to function in a growth cone collapse assay. *Protein science : a publication of the Protein Society*. 2007;16(3):355-61.
201. Miura Y, Takahashi T, Jung SM, Moroi M. Analysis of the interaction of platelet collagen receptor glycoprotein VI (GPVI) with collagen. A dimeric form of GPVI, but not the monomeric form, shows affinity to fibrous collagen. *J Biol Chem*. 2002;277(48):46197-204.
202. Zhou M, Felder S, Rubinstein M, Hurwitz DR, Ullrich A, Lax I, et al. Real-time measurements of kinetics of EGF binding to soluble EGF receptor monomers and dimers support the dimerization model for receptor activation. *Biochemistry*. 1993;32(32):8193-8.
203. Day ES, Cachero TG, Qian F, Sun Y, Wen D, Pelletier M, et al. Selectivity of BAFF/BLyS and APRIL for binding to the TNF family receptors BAFFR/BR3 and BCMA. *Biochemistry*. 2005;44(6):1919-31.
204. Xia XZ, Treanor J, Senaldi G, Khare SD, Boone T, Kelley M, et al. TACI is a TRAF-interacting receptor for TALL-1, a tumor necrosis factor family member involved in B cell regulation. *The Journal of experimental medicine*. 2000;192(1):137-43.
205. Tetsch L, Jung K. How are signals transduced across the cytoplasmic membrane? Transport proteins as transmitter of information. *Amino acids*. 2009;37(3):467-77.
206. Heldin CH. Dimerization of cell surface receptors in signal transduction. *Cell*. 1995;80(2):213-23.
207. Bossen C, Ingold K, Tardivel A, Bodmer JL, Gaide O, Hertig S, et al. Interactions of tumor necrosis factor (TNF) and TNF receptor family members in the mouse and human. *J Biol Chem*. 2006;281(20):13964-71.
208. Lin YC, Boone M, Meuris L, Lemmens I, Van Roy N, Soete A, et al. Genome dynamics of the human embryonic kidney 293 lineage in response to cell biology manipulations. *Nature communications*. 2014;5:4767.
209. Ponten J, Macintyre EH. Long term culture of normal and neoplastic human glia. *Acta pathologica et microbiologica Scandinavica*. 1968;74(4):465-86.
210. Thangarajh M, Masterman T, Hillert J, Moerk S, Jonsson R. A proliferation-inducing ligand (APRIL) is expressed by astrocytes and is increased in multiple sclerosis. *Scandinavian journal of immunology*. 2007;65(1):92-8.
211. Jeon ST, Kim WJ, Lee SM, Lee MY, Park SB, Lee SH, et al. Reverse signaling through BAFF differentially regulates the expression of inflammatory mediators and cytoskeletal movements in THP-1 cells. *Immunology and cell biology*. 2010;88(2):148-56.
212. Lee SM, Jeon ST, Suk K, Lee WH. Macrophages express membrane bound form of APRIL that can generate immunomodulatory signals. *Immunology*. 2010;131(3):350-6.
213. Lee SM, Kim WJ, Suk K, Lee WH. Cell to Cell Interaction Can Activate Membrane-bound APRIL Which Are Expressed on Inflammatory Macrophages. *Immune network*. 2010;10(5):173-80.
214. Diaz-de-Durana Y, Mantchev GT, Bram RJ, Franco A. TACI-BLyS signaling via B-cell-dendritic cell cooperation is required for naive CD8+ T-cell priming in vivo. *Blood*. 2006;107(2):594-601.
215. Bischof D, Elswa SF, Mantchev G, Yoon J, Michels GE, Nilson A, et al. Selective activation of TACI by syndecan-2. *Blood*. 2006;107(8):3235-42.
216. Johnson GB, Brunn GJ, Platt JL. Cutting edge: an endogenous pathway to systemic inflammatory response syndrome (SIRS)-like reactions through Toll-like receptor 4. *J Immunol*. 2004;172(1):20-4.

217. Johnson GB, Brunn GJ, Kodaira Y, Platt JL. Receptor-mediated monitoring of tissue well-being via detection of soluble heparan sulfate by Toll-like receptor 4. *J Immunol.* 2002;168(10):5233-9.
218. Phizicky EM, Fields S. Protein-protein interactions: methods for detection and analysis. *Microbiological reviews.* 1995;59(1):94-123.
219. Avila JR, Lee JS, Torii KU. Co-Immunoprecipitation of Membrane-Bound Receptors. *The arabidopsis book.* 2015;13:e0180.
220. Förster T. Zwischenmolekulare Energiewanderung und Fluoreszenz. *Annalen der Physik.* 1948;437(1-2):55-75.
221. Ma L, Yang F, Zheng J. Application of fluorescence resonance energy transfer in protein studies. *Journal of molecular structure.* 2014;1077:87-100.
222. Sahoo B, Drombosky KW, Wetzel R. Fluorescence Correlation Spectroscopy: A Tool to Study Protein Oligomerization and Aggregation In Vitro and In Vivo. *Methods in molecular biology.* 2016;1345:67-87.
223. Elson EL, Magde D. Fluorescence correlation spectroscopy. I. Conceptual basis and theory. *Biopolymers.* 1974;13(1):1-27.
224. Magde D, Elson EL, Webb WW. Fluorescence correlation spectroscopy. II. An experimental realization. *Biopolymers.* 1974;13(1):29-61.
225. Magde D, Elson E, Webb WW. Thermodynamic Fluctuations in a Reacting System\char22{}Measurement by Fluorescence Correlation Spectroscopy. *Physical Review Letters.* 1972;29(11):705-8.

